

---

# Conceptual Design Review of an Orbital Transfer Vehicle

---

*June 8<sup>th</sup>, 2015*

Prepared For:

The American Institute of Aeronautics and Astronautics  
Undergraduate Team Space Transportation Design Competition



Prepared By:

David Brandyberry

Jake Dluhy

Peter Grega

Kevin Kim

David Knourek

Matt Kosky

Evan White



## Design Team:

**David Brandyberry**

*ADCS/Communications Engineer, Pg. 50-67*



**Jake Dluhy**

*Power/Thermal Systems Engineer, Pg. 67-79*



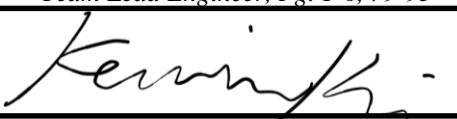
**Peter Grega**

*Orbital Mechanics Engineer, Pg. 14-24*



**Kevin Kim**

*Team Lead Engineer, Pg. 1-6, 79-93*



**David Knourek**

*Propulsion Systems Engineer Pg. 38-50*



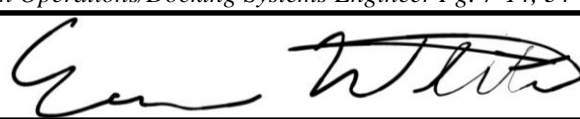
**Matt Kosky**

*Structural Engineer Pg. 24-34*



**Evan White**

*Launch Operations/Docking Systems Engineer Pg. 7-14, 34-38*



**David Carroll**

*Faculty Advisor*

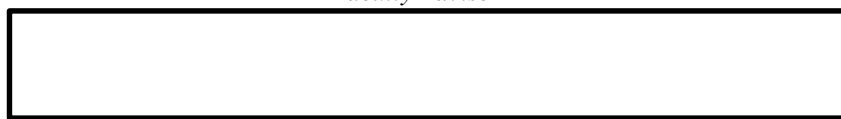


## Table of Contents

<b>1. EXECUTIVE SUMMARY .....</b>	<b>1</b>
<b>2. OVERALL MISSION ARCHITECTURE.....</b>	<b>5</b>
2.1. VEHICLE OVERVIEW .....	5
2.2. PROGRAM SCHEDULE.....	5
<b>3. LAUNCH OPERATIONS .....</b>	<b>7</b>
3.1. LAUNCH VEHICLE .....	7
3.2. LAUNCH SITE .....	10
3.3. LOGISTICS AND LAUNCH TIMELINE.....	11
<b>4. ORBITAL TRAJECTORY AND DETERMINATION.....</b>	<b>14</b>
4.1. DESIGN APPROACH .....	14
4.2. CONCEPT DEVELOPMENT.....	15
4.3. ORBITAL SEQUENCE SUMMARY .....	21
4.4. AEROBRAKING TRAJECTORY CONSIDERATION .....	23
<b>5. STRUCTURAL DEFINITION .....</b>	<b>23</b>
5.1. DESIGN APPROACH .....	23
5.2. DESIGN CONSIDERATION .....	24
5.3. CONCEPT DEVELOPMENT.....	25
<b>6. DOCKING SYSTEMS .....</b>	<b>33</b>
6.1. DOCKING INTERFACES .....	33
6.2. REFUELING.....	35
<b>7. PROPULSION SYSTEMS .....</b>	<b>37</b>
7.1. MAIN ENGINES.....	37
7.2. PROPELLANT TANKS .....	41
7.3. RCS AND MANEUVERING SYSTEM.....	46
<b>8. ATTITUDE DETERMINATION AND CONTROL SYSTEMS .....</b>	<b>48</b>
8.1. CONTROL ACTUATORS.....	48
8.2. ATTITUDE SENSORS .....	51
8.3. ON-BOARD PROCESSING .....	54
8.4. ASSEMBLY MANEUVERING SYSTEM .....	56
8.5. NAVIGATION .....	57
<b>9. COMMUNICATIONS .....</b>	<b>58</b>
9.1. DESIGN APPROACH .....	58
9.2. GROUND STATION.....	58
9.3. ANTENNA SELECTION .....	63
9.4. OTHER DESIGN CONSIDERATIONS.....	65
<b>10. POWER AND THERMAL SYSTEMS .....</b>	<b>65</b>

10.1. SUBSYSTEM REQUIREMENTS .....	65
10.2. POWER GENERATION SELECTION AND SIZING .....	67
10.3. BATTERY SELECTION AND SIZING.....	68
10.4. POWER DISTRIBUTION AND REGULATION .....	70
10.5. MAIN BUS DESIGN AND THERMAL ANALYSIS.....	71
10.6. FUEL TANK THERMAL PROTECTION.....	75
<b>11. COST ANALYSIS .....</b>	<b>77</b>
11.1. NON-RECURRING COSTS .....	78
11.2. RECURRING COSTS.....	83
11.3. COST SCHEDULE .....	87
<b>12. RISK ANALYSIS AND MITIGATION .....</b>	<b>87</b>
<b>13. CONCLUSION .....</b>	<b>91</b>
<b>14. REFERENCES .....</b>	<b>92</b>

## 1. Executive Summary

Earth-Moon Lagrange Points (EML) have great potential to widen the scope of modern space exploration. As of yet, no technology that can safely deliver manned and unmanned payloads between Low Earth Orbit (LEO) and Lagrange Points exists. WayPoint seeks to fill that gap and help the space industry take the next step. As a direct response to the American Institute for Aeronautics and Astronautics' (AIAA) Request for Proposal (RFP), WayPoint introduces Hermes (Figure 1.1 and Figure 1.2): a reusable Orbital Transfer Vehicle (OTV) capable of transporting both manned and unmanned payloads between LEO and EMLs 1 and 2. Hermes increases feasibility of missions beyond the Moon by easily shuttling resources, equipment, and both human and non-human cargo the Lagrange Points. The OTV enables concepts such as stations near the Moon that can support extended missions and provide new capabilities for trans-lunar exploration.

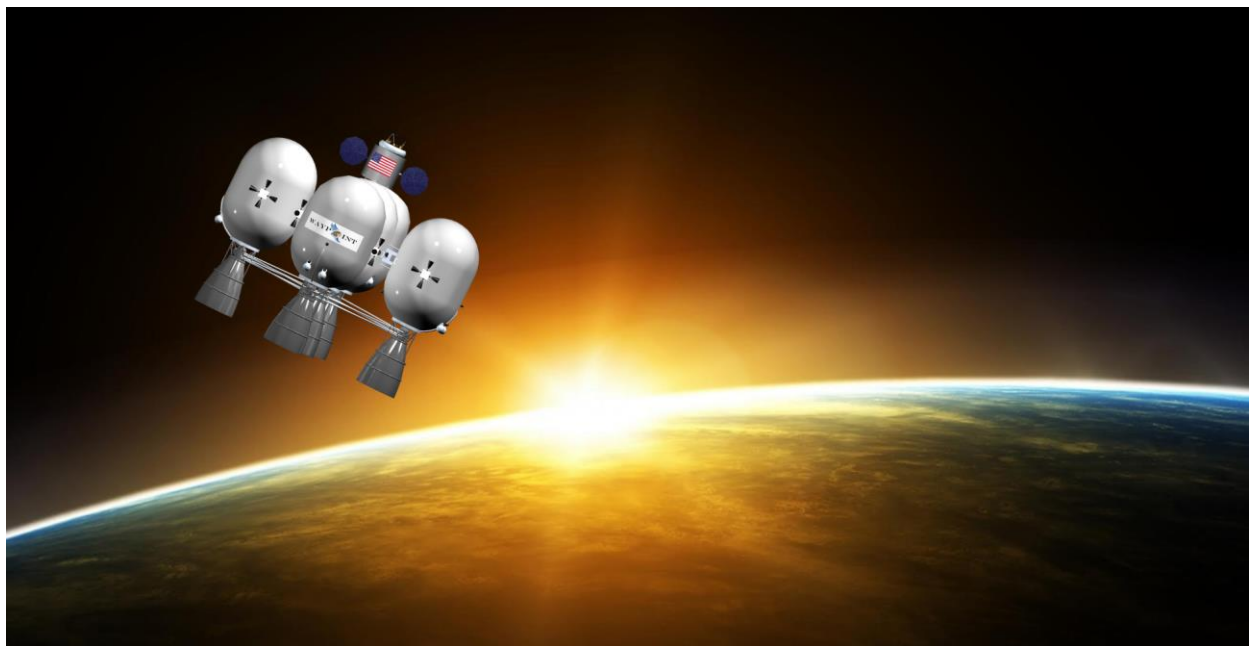


**Figure 1.1. Hermes in Orbit around Earth.**

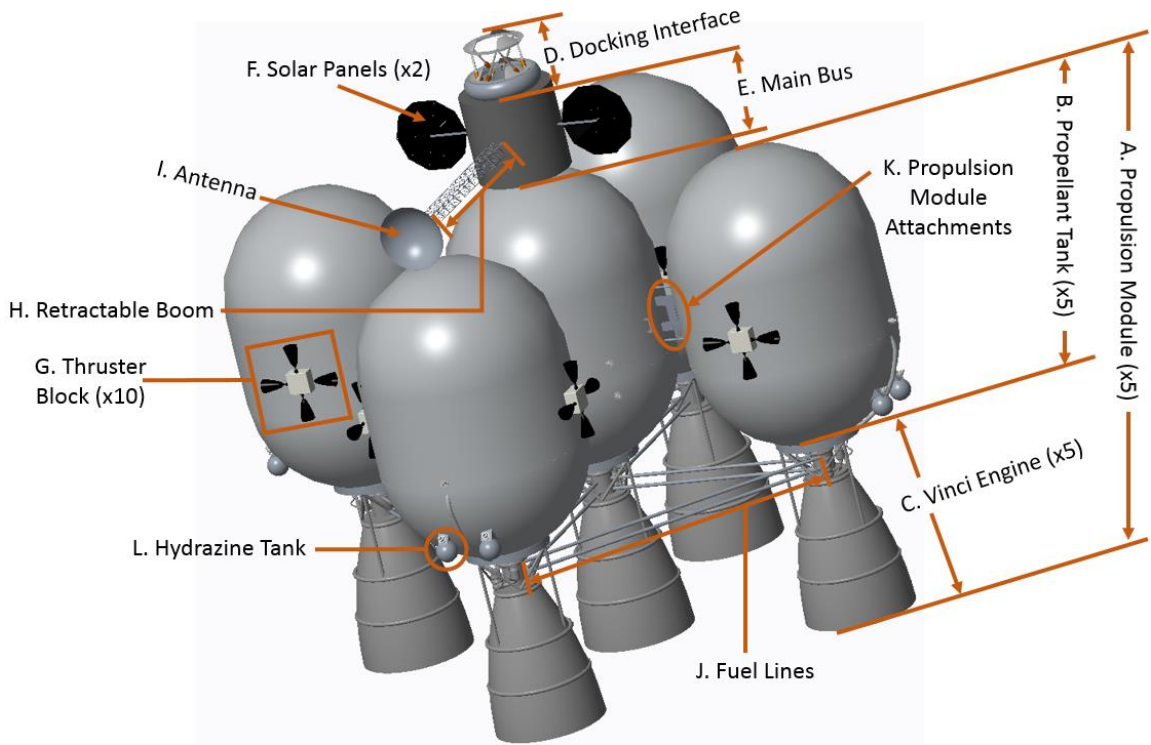


**Figure 1.2. Design Concept of Hermes.**

Delivering manned capsules and expensive scientific equipment requires a highly dependable transfer vehicle. Reliability is the key factor for a mission of this nature, as the customer payload is of utmost importance. To enhance safety for the payload, every aspect of Hermes' design is driven by reliability and safety.

Critical to mission success, the propulsion system drives the design architecture of the OTV. The layout of the vehicle features five propulsion modules (Figure 1.2, A), allowing for redundancy in the highly unlikely case of an engine failure. Each tank (Figure 1.2, B) holds LOX and LH<sub>2</sub> for the Vinci main engines (Figure 1.2, C), which have been thoroughly tested (Section 7.1.1.1). All fuel lines between the tanks are cross fed (Figure 1.2, J) so that no propellant is lost if an engine were to fail. This system also allows for single-point refueling (Section 6.2) and even fuel distribution at all times.

All non-propulsion hardware components also stress reliability, with every subsystem implementing multiple redundancies. On the outside of the main bus (Figure 1.2, E) are two solar panels (Figure 1.2, F) that provide power generation for the vehicle, and a high gain antenna (Figure 1.2, I) on a retractable boom with a gimbaled mount (Figure 1.2, H). Both these components are configured to exceed maximum mission requirements and satisfy NASA safety standards (Section 10.2 and Section 9.3). Two thruster blocks (Figure 1.2, G) are placed on each propulsion module

for ten total blocks. Only the eight blocks located on the outer modules are used during flight and easily supply the maneuvering capability required for mission lifetime (Section 7.3). Computer and power systems inside the main bus have multiple repeating units and fault tolerance in order to minimize probability of mission failure.

During transfers, the vehicle experiences high compressive loads, meaning structural integrity is of utmost importance. Structural reliability is maintained by designing the vehicle to specific requirements derived from Finite Element Analyses (FEA). After evaluating maximum force distributions on the vehicle, safety margins are enforced and material selections are made. This process is detailed in Section 5.3. The propulsion module attachments (Figure 1.2, K) require additional attention as they are critical points of failure. Reinforcement welds and high-strength interlocking connections between tanks minimize the probability of failure.

When docking with the payload, the International Docking System Standard (IDSS) androgynous docking interface (Figure 1.2, D) offers a tested industry standard. Maximum forces in conjunction with safety margins are used to confirm reliability of the IDSS mechanism. Every component of Hermes fulfills specific requirements put forth by the AIAA RFP shown in Table 1.1:

**Table 1.1. AIAA RFP Requirements and Compliance.**

#	Requirement:	Met:
1	The OTV will be stationed in 400 km AMSL circular LEO with 28° inclination.	Section 4 (pg. 14)
2	The OTV payload capability shall be 50,000 lb from LEO to EML and 15,000 lb from EML to LEO.	Section 7 (pg. 37)
3	The OTV must be capable of remaining at EML1 or EML2 for at least 30 days.	Section 4.2 (pg. 15)
4	Each transfer (from LEO to EML and from EML to LEO) should not exceed 6 days.	Section 4.2.4.1 (pg. 17)
5	The life of the OTV shall be 5 years and the OTV shall be capable of at least 10 missions to EML1 or EML2.	Section 7.1.2 (pg. 40)

Development of Hermes is driven by the value of its capabilities. As per RFP Requirement #2 (Table 1.1), the OTV boasts a 50,000 lb payload transfer ability to the Lagrange Points. The only current or proposed method that accomplishes the same task is the Space Launch Systems (SLS) Heavy Launch Vehicle (HLV). SLS Block I intends to deliver a comparable 55,000 lb to a lunar transfer [1]. However, the HLV faces numerous challenges. With launches projected at \$2 billion on average, cost is a major constraint [2]. For a full ten missions (Table 1.1, RFP Requirement #2), the SLS would cost as much as \$20 billion. In comparison, Hermes beginning to end-of-life mission cost is \$3.28 billion (Section 11), a dramatic 84% savings over the SLS cost.

Hermes also has an accelerated program timeline compared to the SLS. With high Technology Readiness Levels (TRL) of all major system components, WayPoint is available to start Hermes development as soon as funding

is available. After only seven years of development, manufacturing, and testing, Hermes will be ready to launch in 2023 (Section 2.2). Contrastingly, the SLS development is staggering as the projected debut launch date is being moved back and is set for late 2018, four years later than the original 2014 date [3].

Hermes' fast mission turnover rate is another strong asset of the design. When fully operational, the vehicle will be able to conduct four round-trip transfers to EML per year (Section 2.2). This rate of delivery is much more efficient than the SLS which reaches a max capacity of one launch per year at best [2]. Figure 1.3 directly compares the two technologies with Hermes costing \$328 million per mission and SLS costing \$2 billion per mission. As can be seen, Hermes stays well below the SLS cost, yet fulfills more than double the number of missions over 20 years.

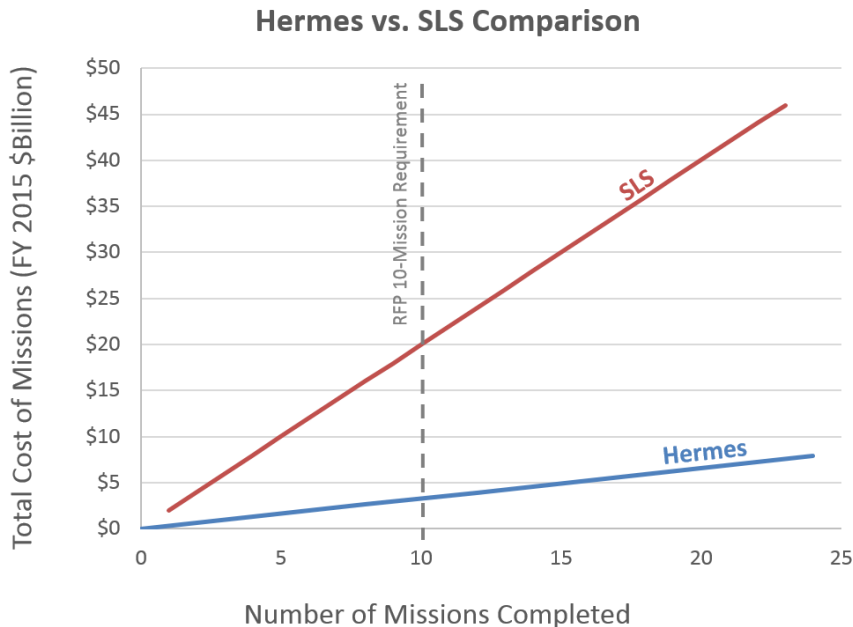


**Figure 1.3. Overall Comparison Between Hermes and SLS.**

Not only is Hermes far more cost effective long-term than the SLS, but it also offers additional capabilities that no other current technology can perform. Hermes has the ability to remain at the EML for 30 days and return a 15,000 lb payload to LEO (Table 1.1, RFP Requirements #2, #3). This shuttling service provides fast transfers between LEO and the EML, a capability not available with standard launch vehicles. Customization options are also offered to the customer, as Hermes is capable of delivering 50,000 lb to EML2 in addition to EML1 for a slightly higher price (Section 11.2.2). If more a payload more than 50,000 lb is needed to be transferred, up to 85,000 lb can be delivered to EML1 for the same price as 50,000 lb to EML2 (Section 7.1).

With a modular approach, Hermes will have longevity, reliability, and flexibility – all factors that extend Hermes' lifetime beyond the five-year requirement. Given that there is no existing method to transfer payload between LEO and EML, any supplemental missions past the original requirement extends a highly sought-after service to the customer. With a capacity of four missions per year, each additional year could bring 200,000 lb of payload to EML and 60,000 lb back to LEO, allowing for transport of large quantities of resources and tools.

## 2. Overall Mission Architecture

### 2.1. Vehicle Overview

Hermes is sectioned into nine subsystems as listed in Table 2.1.

**Table 2.1. Hermes Subsystem Breakdown.**

Subsystem Name	Section
Launch Operations	Section 3
Orbital Trajectory and Determination	Section 4
Structural Definition	Section 5
Docking Systems	Section 6
Propulsion Systems	Section 7
Attitude Determination and Control Systems	Section 8
Communications	Section 9
Power and Thermal Systems	Section 10

All subsystems work with each other for full integration throughout the design process. In each section, major design attributes and justifications are explained. Cost and risk factors drive these decisions in every stage of development.

### 2.2. Program Schedule

The Hermes program schedule is driven heavily by availability of SpaceX Falcon Heavy and Falcon 9 launch vehicles. The Falcon Heavy is expected to make its first test flight in early 2015. Considering that the Falcon 9 went from its first launch to being fully operational in five years, a similar timeline is expected for the Heavy, making it fully operational by 2020 [4].

The expected launch capacity of the Falcon family is also based off the Falcon 9. In 2015, the 9 is scheduled to launch 14 times. Of the 14 launches, NASA is scheduled for four of the slots. Taking into account the fact that SpaceX increased its production from 12 Falcon 9 vehicles in 2013 to 24 in 2014, it is reasonable to assume that NASA will be able to reserve eight Falcon 9 launches per year by the time the Falcon Heavy is fully operational in

2020 [4]. WayPoint predicts that many of the EML missions will be a joint venture with NASA, thus, a similar launch quantity of eight per year is expected for the 9 variant starting in 2020.

The Falcon Heavy follows a similar path. After being fully operational, NASA is expected to have four launches per year for four years until production is ramped up. After that, eight launches per year is assumed starting in 2024. With SpaceX's recent surge in production and launch scheduling, these figures are reasonable deductions. The entire launch and mission sequence starting with the development phase is shown in Figure 2.1. Software development time from Table 11.1 is taken to be about 2.5 years. The Vinci engines are slotted for a test flight on the Ariane 5 ME in 2018, and about two years are allotted for hardware manufacturing and vendor customization [5].

A major benefit of the Hermes design is the high Technology Readiness Level (TRL) of its components, which allows for the Research and Development (R&D) phase to be a relatively short six years. R&D for the project will commence as soon as 2017 given that funding will be in place by then. When fully operational, Hermes will be capable of performing four round-trip missions per year.

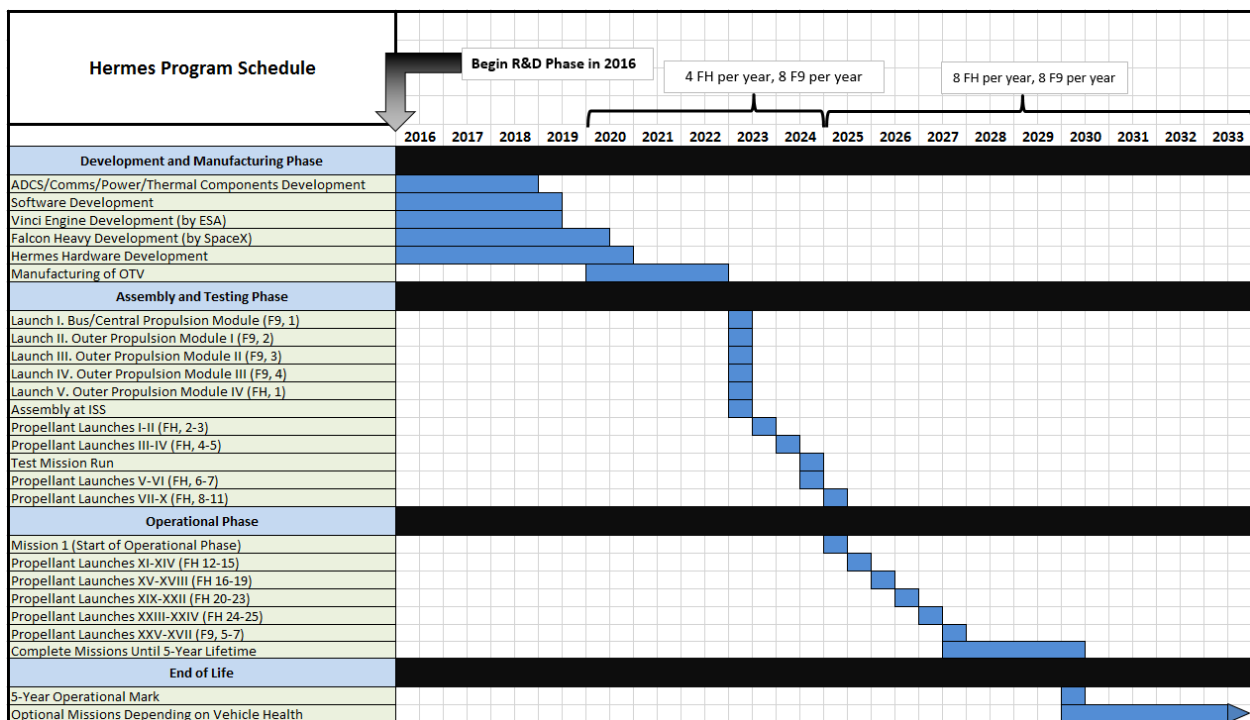


**Figure 2.1. Hermes Program Schedule.**

## 3. Launch Operations

### 3.1. Launch Vehicle

#### 3.1.1. Design Goals

Launch Vehicles (LV) are compared using the mass deliverable to a desired orbit (LEO and GTO). Choosing one to service Hermes requires the deliverable mass to meet or exceed Hermes' maximum dry mass. If this requirement cannot be met, the next logical step is to choose a LV that can send the OTV into LEO in as few launches as possible. These considerations, along with the cost of each launch, drives the choice for selecting an economically and logically feasible LV.

The first step in finding which LVs are best suited to service Hermes is calculating the total dry and wet mass of the OTV. Four classes of LVs exist: small, medium, heavy, and super-heavy (sometimes called ultra-heavy), which are split by a loosely defined range of payload masses delivered to LEO. The set of cutoffs used in our trade studies were less than 2,000 kg for small, 2,000 to 20,000 kg for medium, 20,000, to 50,000 for heavy, and greater than 50,000 kg for super-heavy. Hermes was estimated to have a wet and dry mass of 159,651 kg and 16,651 kg respectively, which shows that the small class is not an option, requiring up to 75 launches. Therefore, only medium, heavy, and super-heavy LVs are to be considered.

Another design driver is the payload fairing volume. Each LV is outfitted with specialized fairings that can vary greatly in total volume, making a design used for one LV not possible with another. In order for the design of the OTV to commence, the LV must be selected early, as it will constrain the possibilities of other subsystems.

#### 3.1.2. Mass and Cost

Table 3.1 shows a trade study comparing the specifications and prices of LVs in the medium, heavy, and super heavy classes. Values with asterisks are estimations for LVs that are currently under development. Every LV in this list, aside from the Falcon 9, is capable of lifting the entire dry mass to LEO in one launch, however none of the listed LV's can lift the entire wet mass in one launch. In order to reduce the number of possible LV choices, a simple cost analysis was performed for launching the wet mass shown in Table 3.2.

**Table 3.1. Launch Vehicle Trade Study.**

Launch Vehicle	Payload to LEO (400km) (kg)	Fairing Diameter	Cost (\$Millions)	Launch Site
<b>Falcon XX (2030)</b>	140,000	10*	350*	CC/Vand*
<b>SLS (2018)</b>	70,000 – 130,000	8.4	1000-2000*	KSC LC-39
<b>Flacon X (2020)</b>	125,000	8.4*	250*	CC/Vand*
<b>Delta IV Ultra Heavy (2025)*</b>	67,000	5.4	500*	CC/Vand
<b>Atlas V HLV (2020)*</b>	29,400	5.4	in production	CC
<b>Flacon Heavy</b>	53,000	5.2	85	CC/Vand
<b>Delta IV Heavy</b>	28,790	5	375	CC
<b>Proton M</b>	21,600	4.3	85	Baikonor
<b>Ariane 5 ECA</b>	21,000	5.4	120-220	French Guiana
<b>Atlas V 551</b>	18,850	5	226	CC/Vand
<b>Flacon 9</b>	13,500	5.2	61.2	CC/Vand

**Table 3.2. Cost Analysis of Launch Vehicles for OTV Delivery to ISS.**

Launch Vehicle	Cost per Launch (millions)	Mass to LEO (400 km) (kg)	# of launches needed	Total Cost to Launch OTV (millions)
Falcon X Heavy	85	125,000	2	500
Falcon Heavy	250	53,000	3	255
Falcon 9	61.2	13,500	12	734.4
Ariane 5 ECA	120	21,000	8	960
Delta IV Heavy	375	28,800	6	2250

The SLS was omitted from this study based on its high price compared to other launch vehicles. The Atlas V 551 was also omitted due its high price combined with low mass capabilities. Finally the Falcon XX was omitted due the estimated completion date being well outside of our selected launch date of mid to late 2023. The table clearly shows that the Delta IV family requires a very high cost compared to any of the other LVs listed. The Ariane 5 ECA also has a relatively high cost when compared to the other options presented. Leaving just the Falcon family of rockets to be considered further. The Falcon 9 has proven to be a reliable LV with a launch success rate of 94.12% [6]. The Falcon Heavy is scheduled for its first launch in 2015, giving it adequate time to reach a TRL-9 by the planned launch date. The Falcon Heavy is also derived from the Falcon 9, providing a good claim to its reliability upon completing development. The Falcon X Heavy has not officially started development adding an unnecessary risk of not having it completed by the planned launch date. Thus, the Falcon Heavy and Falcon 9 are the primary choices of launch vehicle with the choice dependent upon what is to be launched, Section 3.1.3.

### 3.1.3. Payload Fairing

Even though the Falcon Heavy can lift the entire wet mass of Hermes to LEO in three launches, this does not mean that it can fit the entire volume of the OTV inside three of its payload fairings. The static envelope of the Falcon 9 and Falcon Heavy fairing has a 4.6 m diameter, a 6.6 m cylindrical height, and a conic top section that reduces down to a 1.3 m diameter 4.8 m above the top of the cylindrical section. During lift off, the fairing housing undergoes a large amount of stress and vibrations that make the fairing flex and possibly damage the delicate instruments housed inside. The static envelope for a payload fairing is the space available to house a satellite without it being at risk of touching the sides of fairing.

Hermes' design must account for the limited space available inside the payload fairing carrying the modules into space. This issue can have profound effects on vehicle layout and the types of connections between modules. Hermes will utilize a common bulkhead design as shown in Figure 7.6 and discussed in Section 7.2 for the propellant tanks, allowing for reductions in the volume needed for those tanks. However, adding on MMOD shielding, structural supports, thruster blocks, and heat shielding will increase the diameter of each propulsion module too much to fit inside of the standard Falcon 9 payload fairing, requiring WayPoint to develop and build custom fairings to launch each module of Hermes. These custom fairings are shown in Figure 3.1.

With the addition of the shielding, tank connections, and the bus, the fairing needs a static enveloped diameter of 5.7 meters, a cylindrical height of 8.5 meters, and a total height of 12 meters. Designing and building these custom fairings will incur added costs but it has been decided that these costs are outweighed by the benefits of having larger propulsion modules.

Since Hermes will be launched in multiple sections, it is important to consider the assembly process, which is discussed in Section 3.3.1. Since assembly will be taking place at the ISS, the modules must be launched un-fueled. LV selection can then be based on dry mass. Therefore, the Falcon 9 becomes the most cost effective solution for the Central Propulsion Module (CPM) and most Outer Propulsion Modules (OPM). However, there is still need for fuel

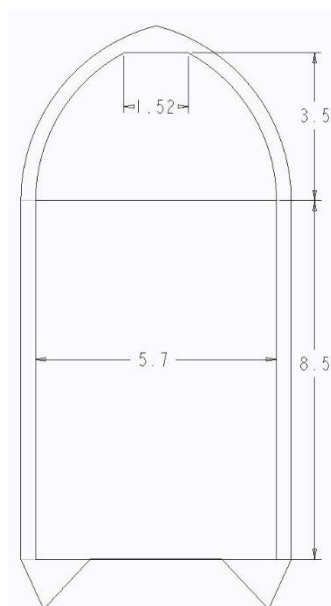


**Figure 3.1. Custom Payload Fairing Dimensions.**

on board in order to rendezvous with the fuel depot once the assembly process is complete. For this reason, the final OPM will be launched fully fueled on a Falcon Heavy.

### 3.1.4. Propellant Launch

The propellant used on Hermes makes up a majority of the mass of the OTV. For this reason a second cost analysis was performed to choose the optimal launch vehicle to deliver propellant for each mission. The propellant needed for missions to EML1 is 127,000 kg and for EML2 is 143,000 kg. This cost analysis was performed using the EML2 numbers.

Table 3.3. Cost Analysis of Launch Vehicles for Propellant Delivery to Propellant Depot.					
Launch vehicle	Cost per Launch (\$Millions)	Mass to LEO (kg)	# Launches Needed	Rounded Up	Total Cost to Launch OTV (\$Millions)
Falcon 9 Heavy	85	53000	2.70	3	255
Falcon XX	350	140000	1.02	2	700
Falcon X Heavy	250	125000	1.14	2	500
Delta IV Heavy	375	28800	4.97	5	1875
Delta IV Ultra Heavy	500	67000	2.13	3	1500
Ariane 5 ECA	120	21000	6.81	7	840

Table 3.3 shows that the Falcon XX and the Falcon X Heavy rockets, as currently specified, can launch the entire mass of the propellant into LEO in just 2 launches for EML2 and 1 launch for EML1. This fact makes the Falcon XX and Falcon X Heavy very appealing since the risk of a launch vehicle failure is minimized, however, the Falcon XX is not currently in production and, in this trade study, has not been estimated to be ready until 2030. With an initial mission date of mid to late 2024, this rules out the Falcon XX and leaves the Falcon X Heavy and Falcon Heavy to be considered. The Falcon Heavy, despite requiring an extra launch, is estimated to be \$200 million cheaper and has been chosen to deliver the propellant for each mission.

## 3.2. Launch Site

Launch sites that service the Falcon 9 Heavy include the Vandenberg Air Force Base Space Launch Complex 4 in California and the Kennedy Space Center Launch Complex 39A in Florida [7]. The Florida site offers a range of inclinations of 28-62 degrees while the California site services inclinations from 51-145 degrees. Since the ISS is at an inclination of 51.5 degrees, both launch sites can be used to launch Hermes. However, launching from the California

side would require Hermes to launch over the Continental United States in order to match the rotation of the ISS around the Earth. The Florida site allows a launch over the Atlantic Ocean. Therefore, the Florida site has been chosen.

### 3.3. Logistics and Launch Timeline

#### 3.3.1. Assembly Process

Since Hermes will be launched in multiple sections, on orbit assembly is required. Two ways that were researched were assembly with the use of a robotic arm, specifically the Canadarm, and assembly at the ISS with the use of space walks and Canadarms. Assembly at the fuel depot would require Hermes to include a Canadarm of its own, adding to the costs and power requirements of the vehicle. However, Hermes has been designed to operate without the need for a Canadarm at every other stage of operation. This makes incorporating a Candarm into the main bus of Hermes superfluous. As a result, Hermes will be launched to the ISS to undergo assembly through the use of space walks and Candarms already onboard the ISS.

The assembly process will begin with the Central Propulsion Module (CPM) and the main bus, which will dock with one of the two new ports being adapted on the ISS [8] to meet the requirements set forth in the International Docking System Standard (IDSS). These two parts will be attached on the ground prior to launch and will include the engine cross feed lines that connect the CPM to each OPM clamped to the outside of the module. These clamps resemble hose clamps commonly used in plumbing with a rubber inner part to create a tight friction contact with each line. This will secure the lines in place during launch and provide an easy way for astronauts to detach each line in order to connect modules. These clamps and the payload configurations are shown in Figure 3.2.

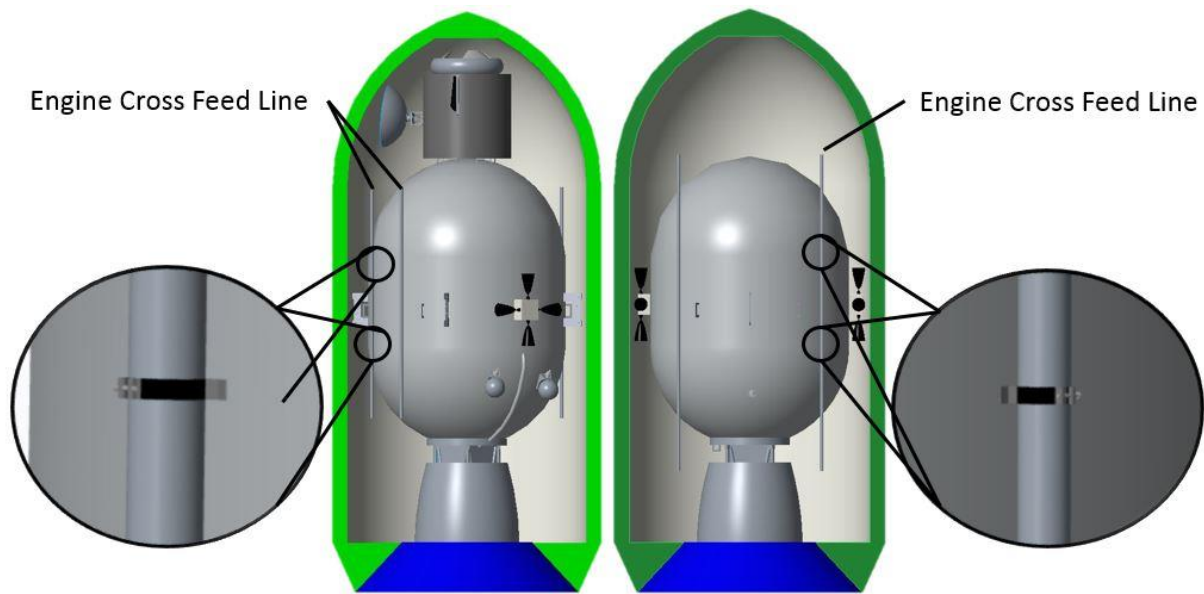


**Figure 3.2. Payload Configurations of the CPM- (left) and OPMs (right).**

The next three launches will deliver three un-fuelled OPM's, each connecting in sequence around the CPM. Each OPM will include two engine cross feed lines, which connect the OPMs to each other clamped onto the outside of the fuel tanks in the same manner as the CPM. Astronauts performing space walks will bolt structural connections and connect fuel lines with the help of Candarms to position and keep unattached modules steady. After the first three OPMs are connected, Hermes will detach from the ISS and maneuver outside of a blast zone. This is to protect the ISS from a catastrophic explosion of Hermes during the assembly phase of the last OPM. Hermes will rendezvous with the final, fully fuelled, OPM and a crew capsule sent from the ISS once outside of the blast zone. The capsule will use thrusters to keep itself within range of Hermes and depressurize itself allowing the crew to perform the final spacewalk necessary to connect the structural supports and fuel lines to the final OPM. Once the final fuel lines and supports are connected, the crew will board the capsule and return to the safety of the ISS. Hermes will then commence propellant transfer to disperse the propellant evenly throughout the five tanks. A transfer burn will then be started to rendezvous with the fuel depot to begin the refueling process and ready Hermes for its first mission to EML1. Figure 3.3 shows the assembly process in detail.

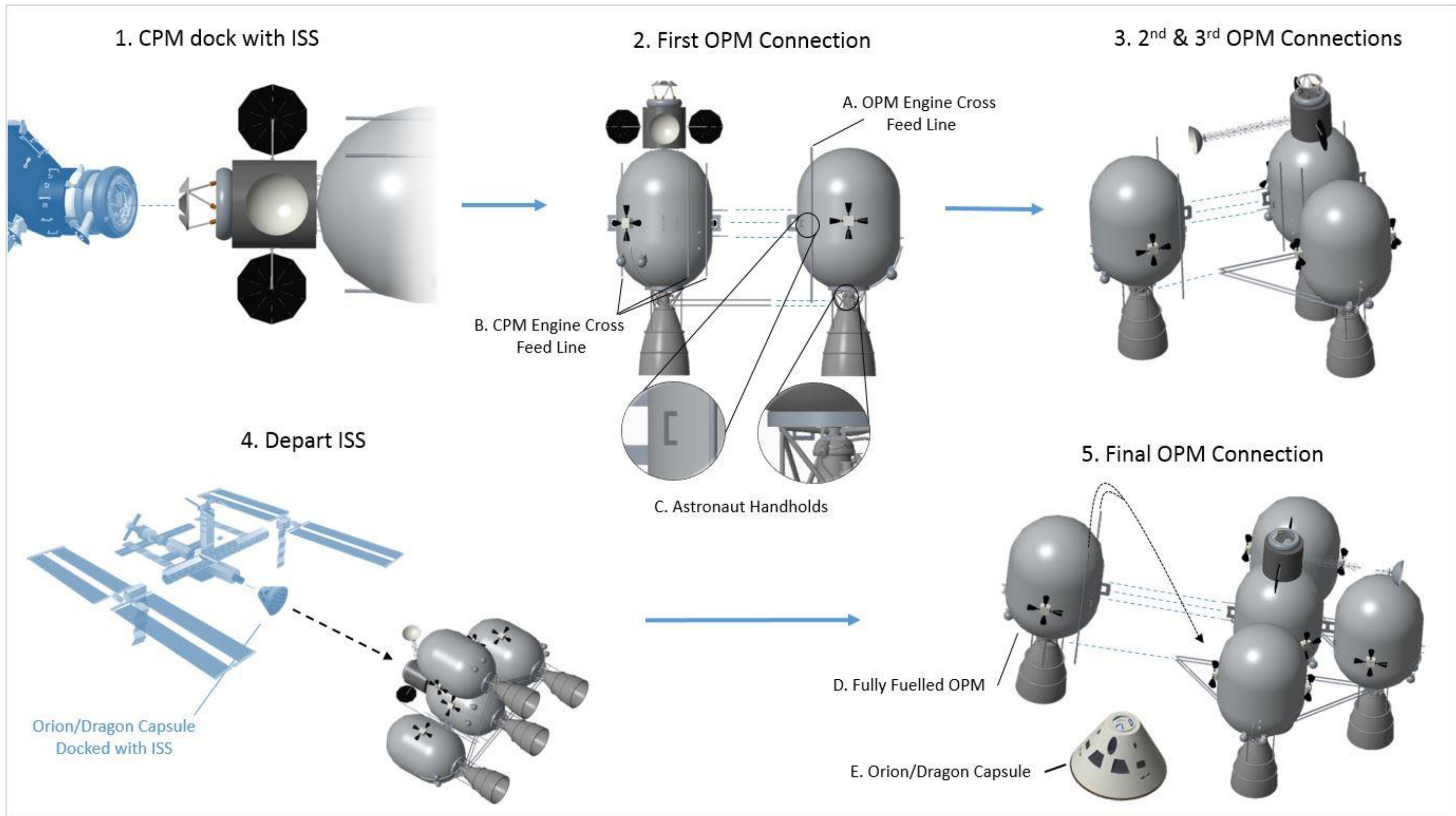


Figure 3.3. Assembly Process for Hermes.

### 3.3.2. Launch Timeline

The launch timeline for Hermes (Figure 3.4) was selected to provide optimal transfer windows to the EML points. The CPM will be launched in the first quarter of 2023 followed every 2-3 months with another section of Hermes. The first three OPM's will launch in quarters 2, 3, and 4 of 2023. The final fully fuelled OPM will launch in the first quarter of 2024. This will allow for Hermes' first mission to proceed in late 2024 to early 2025.

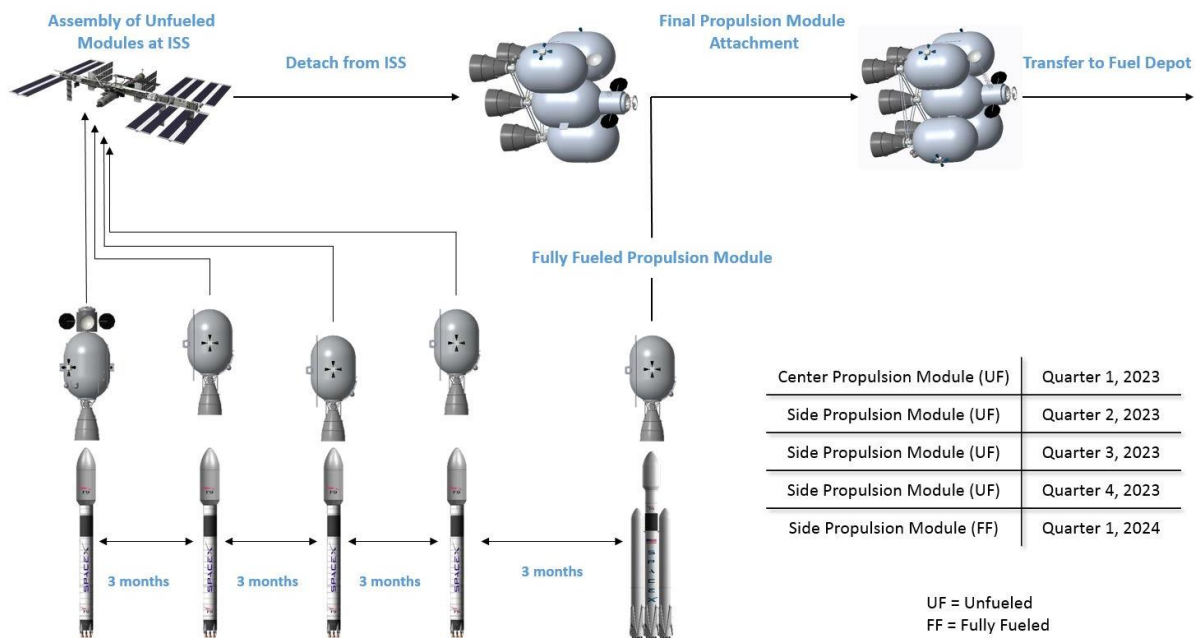


Figure 3.4. Launch Manifest.

## 4. Orbital Trajectory and Determination

### 4.1. Design Approach

One of the main design parameters of any space mission is the change in velocity ( $\Delta V$ ) budget. The amount of propellant required strongly depends on the  $\Delta V$  required over the course of the mission, and minimizing  $\Delta V$  will keep mission costs down and mission feasibility high. Other design considerations include transfer time, halo orbit selection, human safety, and eclipse conditions. These design concepts will be explored in detail in order to formulate a mission sequence that balances cost, safety, and likelihood of success.

## 4.2. Concept Development

### 4.2.1. Assembly in Orbit

As mentioned in Section 3, Hermes is assembled in orbit by astronauts at the ISS. Four of the propulsion modules will be assembled unfueled at the ISS. Once assembly is nearly complete, Hermes maneuvers away from ISS using ADCS thrusters outside of the ISS' no-go zone and into a slightly elliptical orbit. In this new orbit, Hermes circles the ISS approximately every two hours at a nearly constant distance [9]. The fifth propulsion module, which is the final piece of the assembly, is launched from Earth with enough fuel perform a plane change and altitude change to rendezvous with the Propellant Depot (PD). The  $\Delta V$  for this combined maneuver is calculated using the law of cosines,

$$\Delta V = \sqrt{(v_2 - v_1)^2 + 4v_1 v_2 \sin^2 \frac{\delta}{2}} \quad (4.1)$$

where  $v_2$  is the orbital velocity of the PD,  $v_1$  is the velocity of Hermes near the ISS, and  $\delta$  is the angle between the orbit planes of the ISS and the PD, which is 23.65 degrees. Using Equation (4.1), the required  $\Delta V$  for this maneuver has been determined to be 3,140 m/s. Because Hermes is not carrying a payload at this time in the mission, one full propellant tank will provide enough propellant to execute this maneuver.

### 4.2.2. Orbit Phasing

In order to avoid damaging the PD before or after a mission to a Lagrange point, Hermes performs an orbit staging maneuver. The staging maneuver creates separation from Hermes and the PD. As a result, Hermes avoids damaging the PD structure with high-energy gas exhausted during a Hermes main burn. An orbit staging distance of 20 km was conservatively chosen. The maneuver was also specified to take 20% of one earth orbit at a 400 km altitude, which is 18.5 minutes. In order to assess the effectiveness of the 20 km staging maneuver, the  $\Delta V$  required and main engine exhaust diffuse time were calculated. First,  $\Delta V$  was calculated using Equation (4.2),

$$\omega_{drift} = 1080 \frac{\Delta V}{V} \quad (4.2)$$

where  $\omega_{drift}$  is specified in degrees per orbit [10]. Based on the orbit fraction (0.2) and the staging distance, the drift rate can be calculated to be 0.134 degrees per orbit. Using  $V$  as  $V_{LEO}$  results in a  $\Delta V$  requirement of 0.9526 m/s.

To assess the danger posed to the PD, the time allowed for the main engine exhaust to diffuse was calculated. This was done using Equation (4.3),

$$v_e = g_0 I_{sp} \quad (4.3)$$

where  $v_e$  is the exhaust velocity relative to Hermes,  $g_0$  is the gravitational constant for Earth (9.81 m/s<sup>2</sup>), and  $I_{sp}$  is the specific impulse for Hermes' main engine, which is 465 seconds. Hermes' main engines have an exit velocity of 4,560 m/s relative to Hermes. At the start of the burn, the PD is moving at a relative velocity of 3,110 m/s to the exhaust. The relative velocity allows the main engine exhaust 6.44 seconds to diffuse before contacting the PD, which should be adequate for liquid propellant in LEO. These staging maneuvers will be performed before transfer orbit injection at the beginning of each mission and after LEO injection at the end of each mission.

An Optimized R-Bar Target Rendezvous (ORBT), with a +R-Bar pitch Maneuver, will be used to assess vehicle health during the second half of the 5-year mission via a camera on the PD. The ORBT maneuver was used by all Space Shuttle missions after the loss of *Columbia* [11]. Although more complex, the  $\Delta V$  required for the ORBT maneuver is approximated well by Equation (4.2).

#### 4.2.3. LEO Orbit Maintenance

Because Hermes will remain in a LEO parking orbit for approximately 6 months between missions, orbit maintenance will be required. Hermes will remain in an orientation that minimizes drag area while satisfying ADCS requirements for gravity-gradient stabilization. The lowest possible drag area while satisfying the ADCS requirement Hermes can achieve is 252 m<sup>2</sup>. Additionally, Hermes will be 25% fueled during this time to increase the mass, which will decrease the  $\Delta V$  required to maintain the LEO altitude. Simulating 6 months in LEO with these parameters in System Tool Kit with the Astrogator plugin (STK/Astrogator) High Precision Orbital Propagator resulted in 22.68 m/s of total  $\Delta V$  required. Figure 4.1 shows a plot of the orbit decay and boosts maneuvers over a 6 month period. Note the two pairs of burns visible in the figure. The first occurs at the start of the 6 month period, and the second occurs approximately 4.5 months into the period, when Hermes' periapse reaches 380 km.

FOR UNFUNDDED EDUCATIONAL USE ONLY

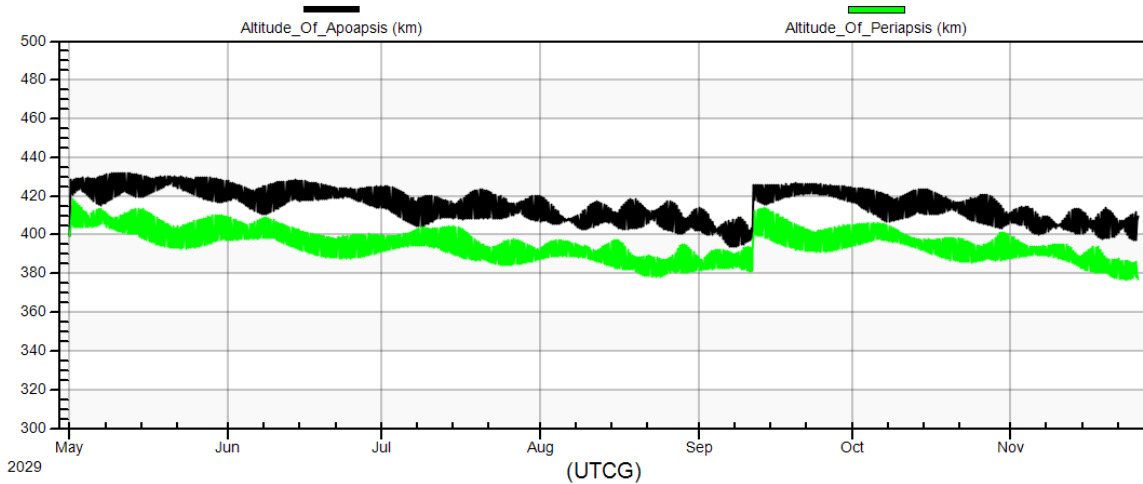


**Figure 4.1. Orbit Maintenance in LEO, as simulated in STK/Astrogator.**

#### 4.2.4. Transfer Trajectory

##### 4.2.4.1. Hohmann Transfers

A preliminary assessment of the  $\Delta V$  requirements for typical EML1 and EML2 missions was conducted through the use of a classic Hohmann transfer. The  $\Delta V$  and Time of Flight (TOF) in seconds were calculated using Equations (4.4) and (4.5),

$$\Delta V_H = \sqrt{\mu_E \left( \frac{2}{R_{LEO}} + \frac{2}{R_{LEO} + R_{EML1}} \right)} \quad (4.4)$$

$$TOF_H = \pi \sqrt{\frac{a_H^3}{\mu_E}} \quad (4.5)$$

where  $a_H$  is the semi major axis of the Hohmann transfer ellipse. The TOF for EML1 was calculated to be 3.87 days, well under the 6 day specification. The  $\Delta V$  for EML1 was found to be 3,700 m/s one way. In order to calculate EML2 requirements, another Hohmann transfer ellipse calculation was done. For EML2, the TOF is 6.19 days, and the  $\Delta V$  was found to be 4,110 m/s one way. A margin of 400 m/s, or approximately 10%, was specified for both missions. This margin allows for an emergency fast transfer to be executed on the return journey. Free return trajectories or hyperbolic rendezvous procedures would also be useful in the event of main engine failure [12-13]. In both fast transfer cases, a fast transfer ellipse with a semi-major axis of 1.3 times the Hohmann semi-major axis was chosen. Parameters

for these transfers were calculated using the method described in [12], and are summarized in Table 4.1. Using the Hohmann characteristics as a benchmark, further research was conducted into possible transfer trajectories to the Lagrange points.

**Table 4.1. Hohmann vs Fast Transfer Trajectories.**

Transfer Type	EML1 Hohmann	EML1 $\frac{a}{a_H} = 1.3$	EML2 Hohmann	EML2 $\frac{a}{a_H} = 1.3$
<b><math>\Delta V</math> Req [m/s]</b>	3,700	4,060	4,110	4,310
<b>% Hohmann <math>\Delta V</math></b>	100.00%	109.90%	100.00%	104.87%
<b>TOF [Days]</b>	3.87	2.37	6.19	3.79
<b>% Hohmann TOF</b>	100.00%	61.36%	100.00%	61.32%

#### 4.2.4.2. Direct Halo Orbit Transfers

The use of a Direct Halo Orbit Transfer, which uses a stable manifold, was considered for the Hermes mission. The first burn would insert Hermes into a Hohmann-like trajectory, and a second burn would insert Hermes into the exterior manifold of EML1, and eventually enter an EML1 halo orbit without requiring a third insertion burn. A comprehensive study of direct halo orbit transfers was compared to the Hohmann transfer data computed in STK/Astrogator [13]. These trajectories are listed in Figure 4.2.

The x-axis specifies the distance of the halo orbit's center to the center of the Earth. For reference, the Moon's average distance from the Earth places the center of the moon at  $x_0 = 384,000$  km. The transfers in Parker's study [13] were conducted assuming that a spacecraft was in a 185 km circular low earth parking orbit with an inclination between 0 and 50 degrees, as specified in Table 4.2.

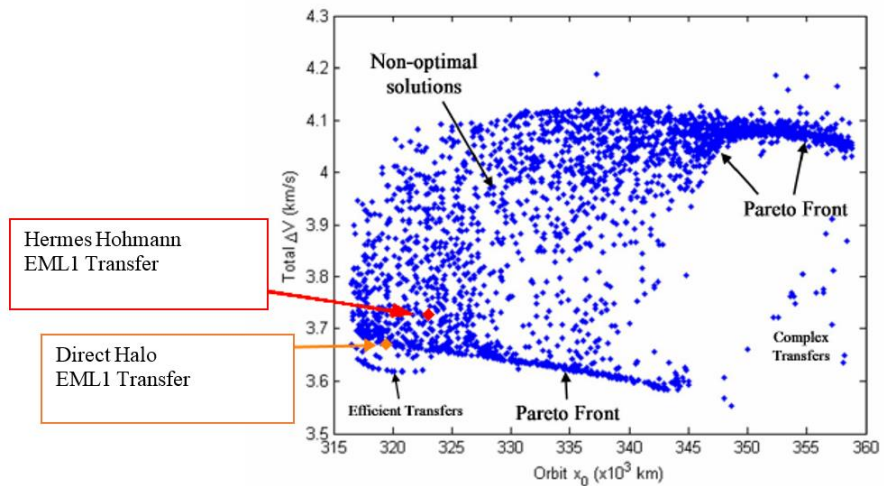


**Figure 4.2. Possible EML1 Transfers plotted against Total  $\Delta V$  required and Orbit Position (Adapted from [13]).**

**Table 4.2. EML1 Transfer Options Sorted by Total ΔV (Adapted from [13]).**

Transfer Type	$x_0$ [ $\times 10^3$ km]	Total ΔV [m/s]	Inclination in LEO [deg]	Transfer Δt [Days]
Direct Halo	320569	3670.3	30.0	5.40
Hohmann	323142	3713.4	28.0	4.24
Direct Halo	354725	4072.5	13.7	5.00
Direct Halo	350325	4073.9	8.6	5.90

Despite the slight reduction in ΔV requirement that accompanies the use of a direct halo orbit transfer, the additional time required increases risk for human missions. Additionally, the use of a Hohmann transfer eliminates the need to design a free return trajectory. Therefore, Hermes will use a Hohmann transfer trajectory, as simulated in STK/Astrogator. The ΔV requirement of the selected transfer necessitates that the five propellant tanks are only partially filled to provide the 7,340 m/s of ΔV, plus a margin of approximately 400 m/s. The transfer time, 4.24 days, also directly satisfies the RFP requirement of a 6 day transfer. Figure 4.3 illustrates the trajectory to and from EML1.

While EML2 is not the primary focus of the Hermes mission, Hermes is designed to be capable of transporting 22,679.6 kg (50,000 lbs) to EML2 and 6803.8 kg (15,000 lbs) back to a 400 km LEO, with

**Table 4.3. EML2 Direct Halo Transfers Sorted by Total ΔV (Adapted from [13]).**

Transfer Type	$x_0$ [ $\times 10^3$ km]	Total ΔV [m/s]	Inclination in LEO [deg]	Transfer Δt [Days]
Direct Halo	382074	3947.7	19	6.20
Direct Halo	383881	3949.9	18.4	5.70
Direct Halo	392708	3969.8	16.5	5.90
Hohmann	444493	4129.0	28.0	6.18

approximately a 10% ΔV margin. This mission scenario is the only case that all five propellant tanks will be fully fueled at the start of the mission, as will be discussed in Section 7. Although a common assumption is that a transfer to EML2 requires less ΔV due to the ability to use a lunar gravity assist, these transfers only require less ΔV if the target Lagrange point orbit lies in the plane of the Moon's orbit about the Earth [14]. If this orbit family is chosen, lunar eclipses will occur frequently and add design constraints to the thermal and communication systems. Additionally, these trajectories typically take over 8 days to execute, and introduce finer navigation requirements during the lunar gravity assist maneuver [15]. As a result, a Hohmann trajectory was again chosen, for the same reasons as the Hohmann trajectory was chosen for the EML1 transfer. The inability to complete a Hohmann transfer in 6 days is justified by the fact that the EML2 sequence is a supplementary objective for Hermes, rather than the main mission objective. Table 4.3 presents all orbits that were considered. A schematic of the trajectory to and from EML2 is qualitatively similar to Figure 4.4, but is not shown for brevity.

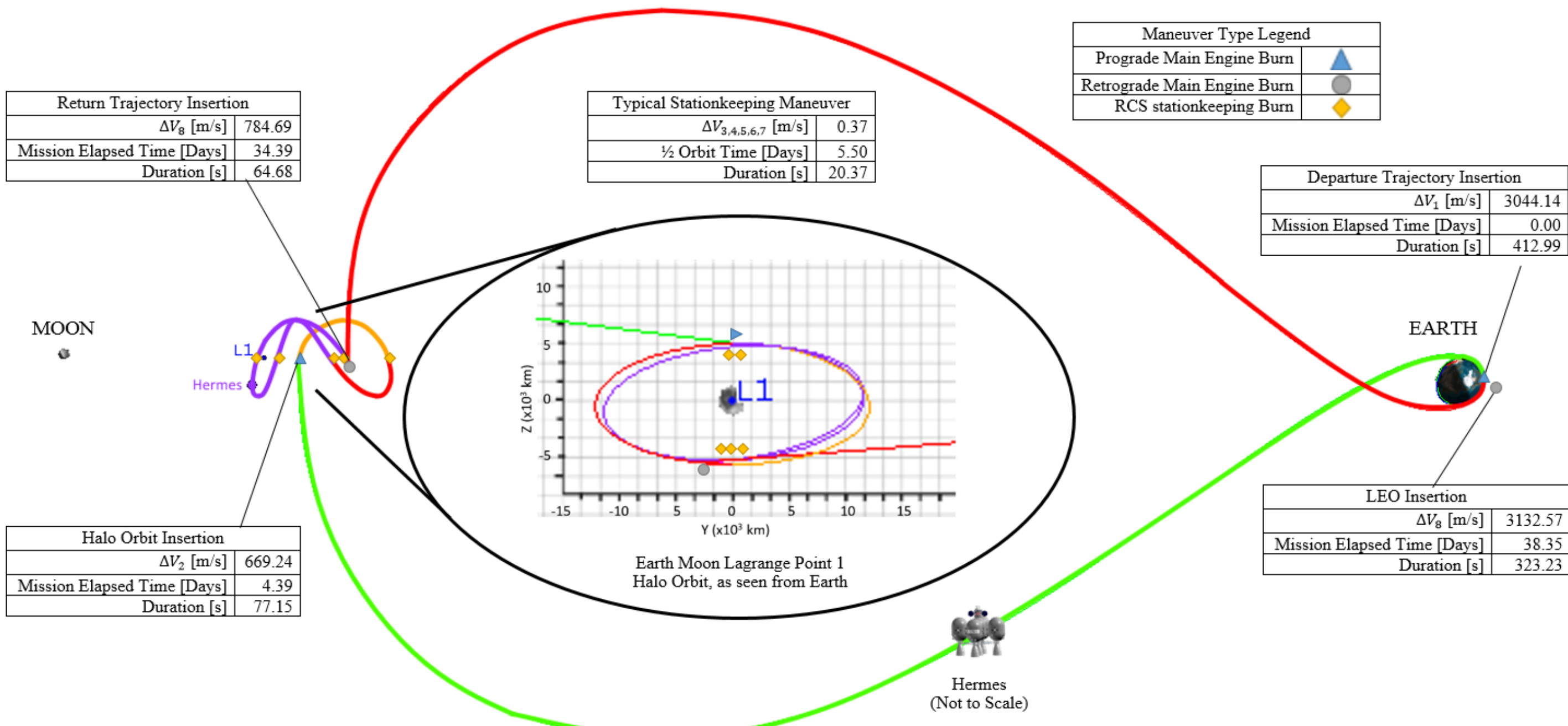


Figure 4.5. Typical Hermes Earth Moon Lagrange Point 1 Mission Sequence, as viewed in the Earth Moon Rotating Frame.

## 4.2.5. Lagrange Point Orbit

### 4.2.5.1. Station-keeping

To determine an estimate of EML1 stationkeeping requirements, the ARTEMIS spacecraft's stationkeeping budget was examined. The ARTEMIS P1 spacecraft was stationed at EML1 in a Lissajous Orbit for 11 months [16]. P1 had an average period of 13.51 days, and had a projected annual Station-keeping  $\Delta V$  of 5.28 m/s [17]. The typical station-keeping maneuver for ARTEMIS was 0.19 m/s. Afterwards, the Hermes EML1 orbit was simulated in STK/Astrogator, and the typical stationkeeping maneuver was found to be 0.365 m/s for a 5000 km radius halo orbit about EML1. Five of these maneuvers were necessary, so the 30-day total is calculated to be 1.825 m/s. In reality, the magnitude of station-keeping maneuvers vary depending on the desired customer halo orbit. For this reason, the limiting case for Hermes is the full 25 m/s of  $\Delta V$  that the RCS system is designed for to maintain the desired orbit in LEO for 6 months. This large  $\Delta V$  limit allows for a wide variety of demanding EML1 and EML2 orbit scenarios and docking maneuvers.

### 4.2.5.2. Halo Orbit Details

The halo orbit selected in Section 4.2.5.1 for calculating stationkeeping  $\Delta V$  was further investigated in order to assess performance in a full ephemeris model. Figure 4.6 shows Hermes' standard EML1 Halo Orbit, which has a maximum Y amplitude of 10,864 km and a maximum Z amplitude of 5,620 km. The figure shows a simulation of a full ephemeris model. The full ephemeris model accounted for all of the gravitational forces of the planets in the solar system. This simulation proves that Hermes' standard EML1 Lagrange point orbit is stable and quasi-periodic as long as station-keeping maneuvers are performed approximately every 7 days.

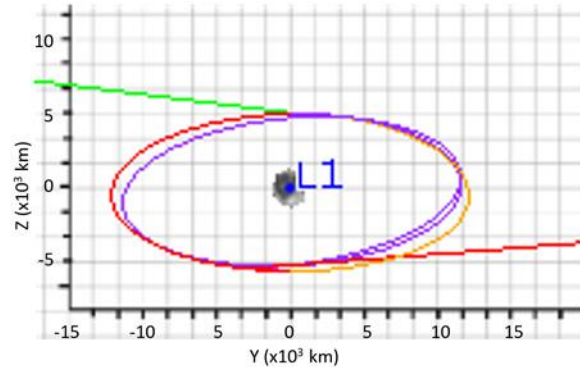


**Figure 4.6. YZ Projection of Hermes' EML1 in Halo Orbit, as Viewed from Earth.**

#### 4.2.6. Disposal Orbit Plan

In order to responsibly dispose of Hermes, an orbit raise has been developed for the end of the 5-year mission. Equation (4.6) defines the periapse radius required to place Hermes in a disposal orbit, as determined by the Inter-Agency Space Debris Coordination Committee [18].

$$R_{Graveyard} \approx R_{GEO} + 235 + \left( 1000 * C_R * \frac{A}{m} \right) \quad (4.6)$$

$C_R$  is the solar radiation pressure coefficient,  $\frac{A}{m}$  is the aspect area ( $m^2$ ) to dry mass (kg) ratio, and 235 is the protected region about GEO (200 km) with a safety margin of 35 km that accounts for gravitational perturbations by the sun and moon. Using the typical GEO radius of 35,786 km and assuming no plane change is necessary,  $R_{graveyard} = 36,066.6$  km. Using a standard Hohmann transfer, as discussed in Section 4.2.4.1, results in a required  $\Delta V$  of 2690 m/s. Although the  $\Delta V$  requirement to place Hermes in a disposal orbit is much higher than the  $\Delta V$  requirement to deorbit Hermes, the ability to reactivate Hermes could save Waypoint money in the future.

#### 4.3. Orbital Sequence Summary

A major design driver for the orbital trajectory determination and propulsion system is providing a thrust to weight ratio (T/W ratio) of at least 0.5 in order to stay in the design space of high-thrust space systems. In these systems, gravity losses can be safely neglected, simplifying the design process [19]. Table 4.4 shows the lowest T/W ratio is within 3% of 0.5, which eliminates the need for extensive modeling of finite burn losses. Table 4.4 also lists the duration of all orbit maneuvers. These T/W ratios were achieved by altering the number of active engines during each burn, and will be discussed further in Section 7. A diagram of the mission sequence can be found Figure 4.5.

**Table 4.4. Orbital Mission Sequence (Nominal EML1 Mission).**

Burn	$\Delta V$ [m/s]	Engine	T/W Ratio	Duration [sec]
<b>Phase from Depot</b>	0.96	8 RCS Thrusters	-	1113.80
<b>Transfer Orbit Insertion</b>	3044.14	5 Main Engines	.503 (Start) - .787 (End)	412.99
<b>Coast to EML1</b>	-	-	-	375075.84
<b>Halo Orbit Insertion</b>	669.24	4 Main Engines	.486 (End)	77.15
<b>Station-Keeping Maneuver (x5)</b>	0.37	8 RCS Thrusters	-	20.37
<b>½ Halo Orbit (x5)</b>	-	-	-	514404.24
<b>Transfer Orbit Insertion</b>	784.69	3 Main Engines	.759 (End)	64.68
<b>Coast to Earth</b>	-	-	-	342010.32
<b>LEO Insertion</b>	3132.57	2 Main Engines	1.486 (End)	323.23
<b>Phase to Depot</b>	0.96	8 RCS Thrusters	-	1113.80
<b>Totals</b>	<b>7632.47</b>			<b>3316805.94</b>

## 4.4. Aerobraking Trajectory Consideration

STK/Astrogator was used to simulate possible aerobrake maneuvers. A one pass approach was used, due to the time constraint of 6 days. Even at a very low aerobraking altitude of 50 km, the  $\Delta V$  savings of 4.35% per mission are not enough to justify the increase in risk and development cost of Hermes. Significant negative effects for other subsystems are cited as a driving factor in this decision. Structures would need to include a large heat shield and a layer of insulation, which would add mass. Additionally, structures would need to account for the extreme thermal gradients that would be experienced during the aerobrake maneuver. Thermal systems would need to carefully monitor and respond to the heating encountered by Hermes. Communications and ADCS would need to anticipate blackout conditions during the aerobraking maneuver due to ionized gas effects. Propulsion is the only subsystem that benefits from the  $\Delta V$  savings.

## 5. Structural Definition

### 5.1. Design Approach

#### 5.1.1. Design Goals

The most important aspect of the structural design is ensuring that the OTV maintains structural integrity throughout the mission. Because the six day transfer time requires higher stress maneuvers, the loads on the structures will be more severe. The connections between propulsion units will experience high shear stresses during these maneuvers, and the walls of the main bus and propulsion units will experience compression while the engines are operating. Due to the ten-mission requirement presented by the RFP, the structures must be either easily replaceable or able to withstand the stresses placed on them throughout the mission.

Limiting the mass of the OTV is critical because it reduces cost. Lower dry mass reduces propellant needs, and therefore results in smaller propellant tanks. In this way mass reduction decreases propellant costs as well as material costs. A smaller mass and volume can also result in smaller launch vehicles, reducing launch costs. Finally the smaller propellant tank requires less assembly, therefore lowering manufacturing costs.

## 5.2. Design Consideration

### 5.2.1. Vehicle Size

The overall size of Hermes impacts on design choices because the material will have to cover a large surface area. Each propellant tank will have a surface area of approximately  $115 \text{ m}^2$  and therefore cannot be constructed in one piece. Therefore, any material chosen must be welded, bonded, or bolted together.

### 5.2.2. Space Environment

The 10-year mission will expose the OTV to several dangers in the space environment, including micrometeoroids and orbital debris (MMOD), radiation, and atomic oxygen. These threats must be considered and mitigated. Micrometeoroids and orbital debris (MMOD) can endanger the spacecraft, especially while in LEO where the vehicle is stationed for several months at a time. Meteoroids in LEO cannot be tracked if they are less than 10 cm and can have impact speeds up to 20 km/s [10]. If MMOD were to strike electronic equipment in the main bus, it could result in a mission failure. Therefore, the exposed surface area of the main bus has additional MMOD shielding.

Electronic equipment in the main bus will be radiation hardened. In order to reach EML1 the orbit will go through the Van Allen radiation belts, an area of high energy electrons. The reason for this orbital path is discussed in Section 4.2.4.

In LEO atomic oxygen is prevalent and can degrade spacecraft materials [10]. Atomic oxygen must be a consideration in choosing materials. Metals are not as reactive to atomic oxygen as polymers, and despite their higher mass, are a safer choice [20]. Any polymers that will be exposed to the space environment will need to be coated in a protective material.

### 5.2.3. Assembly

Considering the size and modularity of Hermes, it will need to be launched in multiple pieces, and will be assembled in orbit. While a Canadarm could make all the connections, because these intricate maneuvers will be near the propellant tanks, using a robotic arm would add unnecessary risk. Astronauts can fasten the connections, with minimal risk of harming the vehicle and therefore will complete the assembly process. The final connections are

simple enough to be completed in orbit and the design will ensure the astronauts can physically reach the necessary locations.

On the ground assembly must also be considered. As previously mentioned, the vehicle materials shall be easily weldable to more efficiently construct the structural shell. Certain materials are hazardous to humans and should not be used for the safety of machinists working with them. Other structures may simply be difficult to construct, or require extensive R&D in order to complete. These facts will have an impact on the final decision.

#### **5.2.4. Current Availability**

Technologies that are currently available for use are favorable. Research and development for technologies that are not ready for use creates an added expense, but more importantly would delay the production of Hermes. Using undeveloped technologies also adds risk to the mission. Technologies already in production can be used more confidently since they have been proven successful in past missions.

### **5.3. Concept Development**

#### **5.3.1. Materials Choices**

A trade study has been completed to determine the choice of materials for the structural shell, which is mainly constructed of a single material. The main possibility of failure stems from buckling because the structural shell will be under compression for the duration of any orbital maneuvers. During some of these maneuvers, the shell experiences the full thrust of the engines. The primary material shall be the one that most efficiently handles that thrust.

The tank shell is made of panels; efficiency of panel buckling is determined by Equation (5.1) below, where C is a constant [21].

$$\frac{P}{\text{mass}} = C * \left( \frac{P_{\max}}{L^4} \right)^{\frac{2}{3}} * \frac{E^{\frac{1}{3}}}{\rho} \quad (5.1)$$

Material efficiency is determined by  $E^{1/3}/\rho$ . Table 5.1 below lists characteristics of several metals and alloys. Aluminum is the most efficient choice of the three; because of that, most metals listed are aluminum alloys. Shear strength is not always readily available information, and in those cases is estimated.

Composite materials were considered, but decided against due to reasons listed in Section 5.3.1. Perhaps most importantly, a composite tank has yet to be produced and flown. Waiting for this tank to become fully developed would push back production of Hermes, whereas an aluminum tank could begin production immediately. In addition, if the space environment damages a composite section, not only would its strength be greatly reduced, but it would also be difficult to repair. Finally the use of composites makes adding necessary connecting structures more challenging than with metals.

**Table 5.1. Material Properties.**

Material	Density (g/cc)	Young's Modulus (GPa)	Yield Strength (Mpa)	E/ρ	E <sup>1/2</sup> /ρ	E <sup>1/3</sup> /ρ	Yield Strength/ρ	UTS(Mpa)	Shear Strength (Mpa)*
Aluminum Alloys									
6061-T6	2.80	68.00	276.00	24.29	2.95	1.46	98.57	310.00	201.50
7075-T6	2.70	71.00	503.00	26.30	3.12	1.53	186.30	572.00	371.80
2090-T83	2.59	79.69	455.00	30.77	3.45	1.66	175.68	503.00	326.95
2099-T83	2.63	78.00	520.00	29.66	3.36	1.62	197.72	560.00	364.00
2195	2.71	74.40	565.00	27.45	3.18	1.55	208.49	589.00	382.85
Titanium									
Ti6Al4V	4.43	113.80	970.00	25.69	2.41	1.09	218.96	950.00	550.00
Steel									
AM 350	7.70	200.00	480.00	25.97	1.84	0.76	62.34	1035.00	621.00
Inconel 625	8.44	207.50	414.00	24.59	1.71	0.70	49.05	827.00	496.20

Aluminum 2090-T83 is an Al-Li alloy and is the primary material for the main bus. The main bus experiences the most force of any component of the vehicle, so it is especially critical for the bus to use the most efficient material. Al 2090-T83 is commercially available, and has the advantage of being a very weldable aluminum alloy [22].

Because the main bus houses all electronic equipment, it is also important to consider a materials effect on such systems. Some metals, including some aluminum alloys, can produce noise in communication systems. However, aluminum 2090 has been used in the fuselage skin of both commercial and military aircrafts [23]. Since communication is equally important in those vehicles, it is safe to use this alloy in this situation as well.

Aluminum 2195 is also an Al-Li alloy. It will be used for the fuel tanks. Even though its efficiency is average for aluminum alloys, it specifically designed for the space shuttle external tank. It has been proven to not only survive

the necessary thrust, but also to be effective in cryogenic cooling. The second point is critical, due to the nature of our fuel and the length of the missions (Section 10.6).

### 5.3.2. MMOD Shielding

As discussed in Section 5.3.2, MMOD presents a serious threat to spacecraft. The whipple shield was designed to protect the spacecraft from such threats. This shield consists of a thin sheet of metal, followed by a “standoff zone”, and ending with a thicker sheet of metal [24]. The outer layer acts a bumper. If the outside wall is pierced, it shatters the MMOD. As the debris moves through the standoff zone, it spreads; so when it impacts the back wall, the pressure is reduced.

A variant on the Whipple design is the “stuffed Whipple”. The difference in this design is the addition of a ceramic cloth between the two metal sheets [24]. A third option for additional shielding is the multi shock system which consists of several layer or ceramic bumpers before a rear wall [24].

Figure 5.1 shows a comparison of the major types of MMOD shielding. Considering that the overall volume of the propulsion units will be a factor for launch, the stuffed whipple design was chosen for the tanks. It is volume efficient while still offering mass savings. For the main bus, where volume is not an issue, the multi-shock Nextel shield was chosen because it is the most mass efficient of the shields.

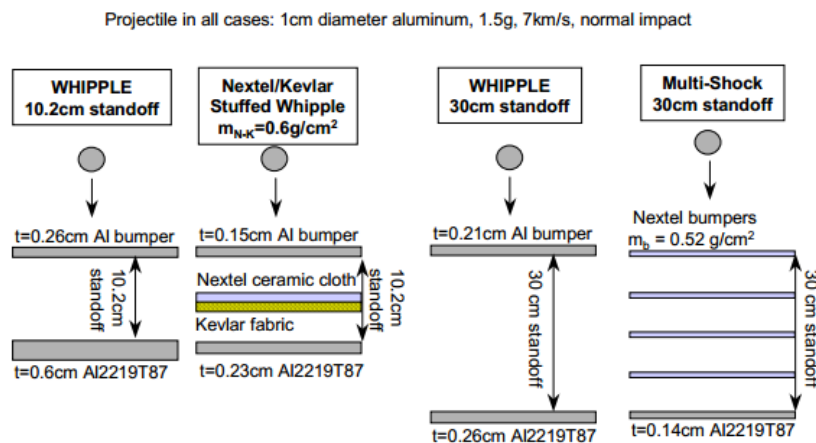


**Figure 5.1. MMOD Protection [24].**

### 5.3.3. Deployable Structures

Deployable structures include any structure that is not at its fully extended state at the time it is launched into LEO. This could include, but is not limited to, trusses, booms, solar panels, and antennas. Deployable technologies will be utilized in communications; antennas will be attached to a coilable boom and then deployed once in orbit. Solar panels also benefit. A large mast of solar panels could be unfurled from the main body of the spacecraft. This process results in a much larger area covered than possible if they needed to be at full length at launch. The coilable boom to be used is seen in Figure 5.2.

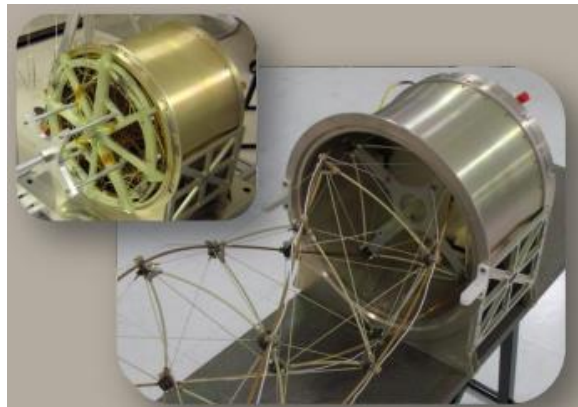


**Figure 5.2 ATK Coilable Boom [25].**

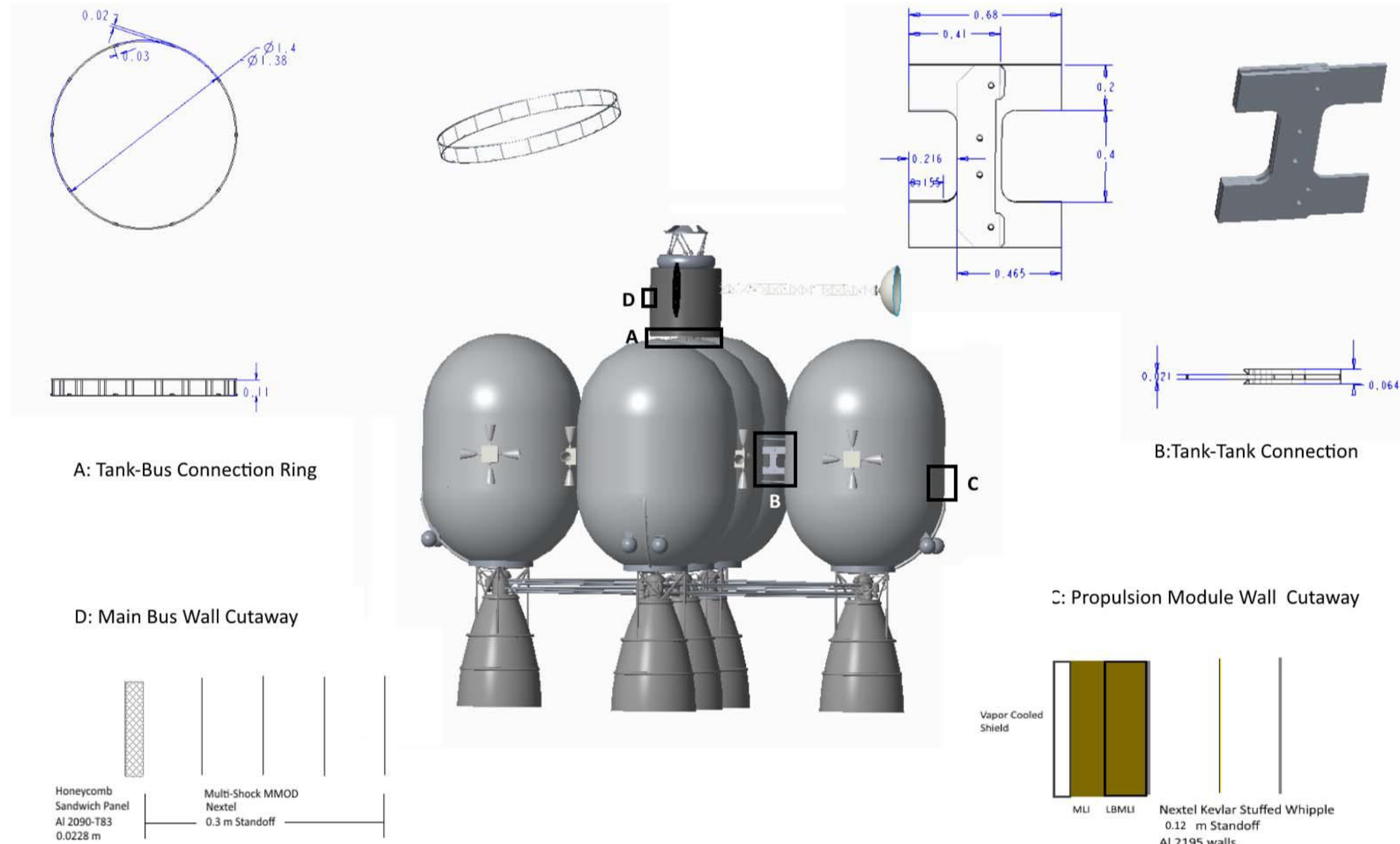


Figure 5.3. Structural Overview.

### 5.3.4. Design Architecture

Figure 5.3 shows an overview of Hermes' structure with several key components highlighted. Due to the five-tank system shown, the tanks will need to be connected using the structure in Figure 5.4. Because Hermes is being assembled in orbit, the propulsion units can be placed together with little complication using a Canadarm. The male connection will be on the outside tanks while the female connections are on the central tank. The connections will slide into place such that the holes align, which will allow astronauts to connect the parts with bolts. The shear bolts being used are made of Inconel forging, and are the same that were used on the space shuttle [26]. Since the connections on the shuttle had to endure much larger shear forces than Hermes, these bolts can be used with great confidence

The connector plates will be welded to the outside of their respective propulsion units and consist of Al 2195. The welds will be 4 m long and 4 mm deep. This will satisfy the necessary shear force requirements with a safety factor of two. The total width of connection system will be 0.06 m in order to accommodate the bolts. The bolts themselves will have a 2.5 cm diameter. The connection system will span 0.68 m between propulsion units. This width will be enough for astronauts connecting the two modules to reach the system [27]. This connection system facilitates disconnecting and replacing propulsion modules in case of failure.

A FEA analysis was performed to optimize the shape of the connection system. While the dimensions above still needed to be satisfied, excess material was removed to reduce weight. Figure 5.5 shows the final FEA for the current connections. The top of the scale represents the yield stress of the material. As the figure shows, all stresses are safely below that critical stress.

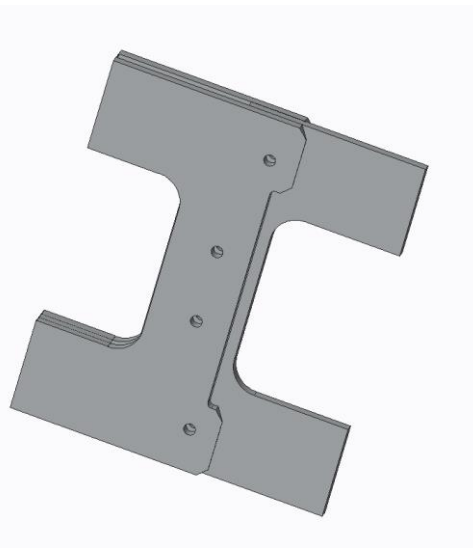


**Figure 5.4. Interlocked Tank-Tank Connection (dimensions shown in Figure 5.3).**

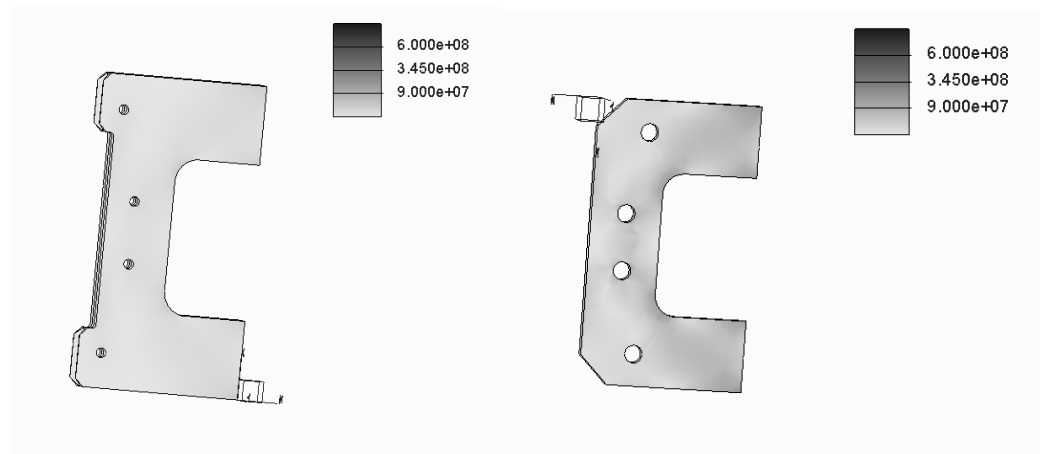


**Figure 5.5. Final FEA Analysis.**

Similarly the connection between the main bus and central propulsion unit, shown in Figure 5.6, allows for easy disconnection and replacement if necessary. The truss ring will be launched attached to the main bus and connected by weld. It will attach to the central propulsion unit via the interlocking connection ring as shown in the figure. The two pieces will also be bolted together using Inconel forged bolts. The aluminum rods of the truss structure are designed to withstand the compressive forces during burns and the applied torques during ADCS maneuvers.

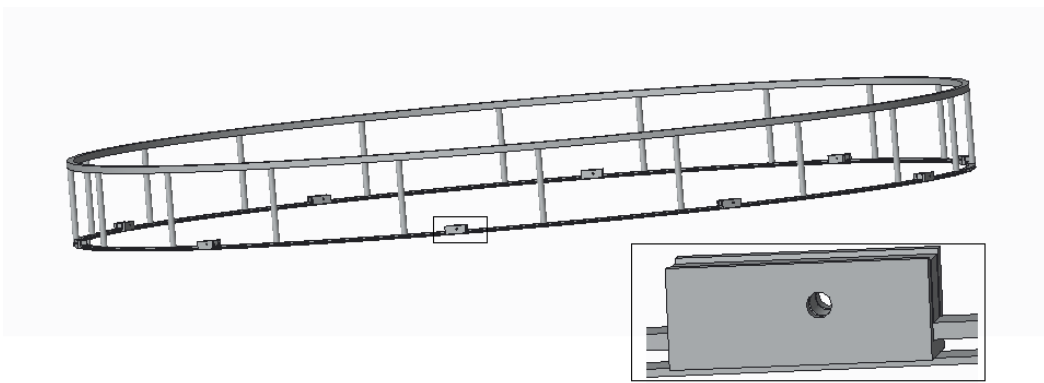


**Figure 5.6. Bus-Tank Connection (dimensions shown in Figure 5.3).**

The wall of the propulsion module will consist of the stuffed whipple shield (Section 5.3.2) and is constructed with Al 2195 (Section 5.3.1). A representation can be seen in Figure 5.7.



**Figure 5.7. Propulsion Unit Wall (side and front view).**

The interior aluminum wall of the propellant tanks will be reinforced with a skin stringer system. The stringer system involves lining the walls with thin vertical strips of aluminum and several horizontal reinforcement rings. . Stringers are an efficient way to increase buckling strength without significantly increasing mass or volume. A cutaway can be seen in Figure 7.6.

The main bus is attached to the top of the central propulsion unit and is cylindrical with a base diameter of 2 m so it can accommodate the Orion docking system. All electronic systems will be housed in the main bus. Solar panels and antennas will be attached to the outside. The bus is connected to the top of the central propulsion unit using the support structure in Figure 5.6. The outside of the bus is supported by a small aluminum support structure. The structure transfers thrust from the propulsion system to the bus. The top and bottom plates of the bus are connected via a central aluminum truss for additional support.

The walls of the main bus are a sandwich structure consisting of two aluminum plates with a honeycomb core. The honeycomb core is a lightweight option to increase the depth of the wall, therefore increasing buckling strength. The main bus shell consists of Al 2090-T83 (Section 5.3.1) and the Multi-shock MMOD shield (Section 5.3.2). Figure 5.8 is a representation of this configuration.

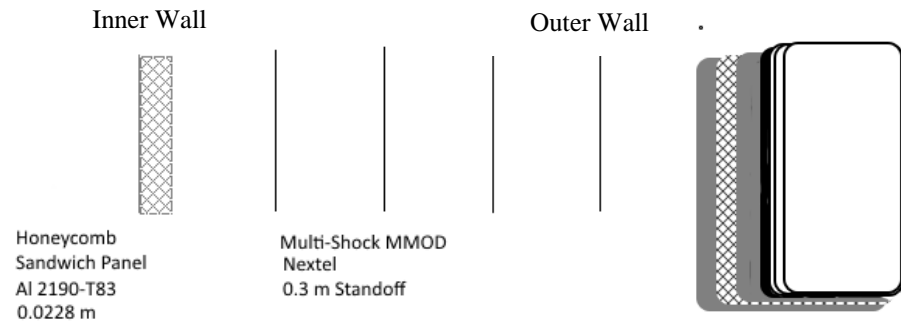


**Figure 5.8. Main Bus Wall Side and Front View.**

## 6. Docking Systems

### 6.1. Docking Interfaces

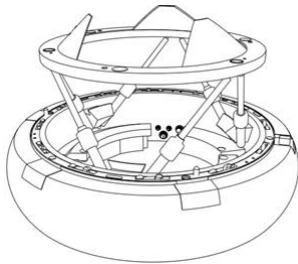
#### 6.1.1. Payload Interface

The first step in determining the docking interface for Hermes, is to calculate the forces experienced during the lifetime of the vehicle. The maximum force that will be experienced occurs during full throttle engine burns to a Lagrange Point. A breakdown of the dry mass components is needed to accurately calculate the forces exerted on specific connections. The payload connection, while accelerating at the same rate as the entire OTV, will feel a compressive force due to the payload mass only.

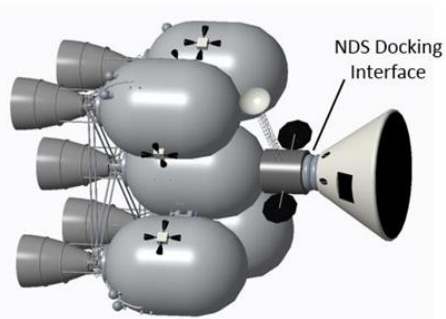
Other considerations include the need for a universal and androgynous interface to accommodate the largest variety of payloads originating from different countries. Existing technologies already address this issue, namely the NASA Docking Standard (NDS) which adheres to the specifications set forth in the International Docking System Standard (IDSS) [28].

Table 6.1 shows calculations of the acceleration of the OTV and the resulting force exerted on the payload docking interface. The compressive forces calculated show the force experienced at the beginning and end of each burn. For our proposed design, all maneuvers at full throttle of any combination of the five Vinci engines will never exceed the IDSS design limit of 300 kN [29]. The NDS interface will be the new US standard for docking mechanisms and will be able to dock with any other interface that adheres to the IDSS. For this reason, the NDS docking interface

was chosen to secure the payload to the main bus. The specific configuration of the NDS interface being used is the 302 as it has a much longer lifespan compared to the 301 model. This model currently does not support active docking cycles. In order to work around this limitation, all payloads planning on using Hermes will be required to support active docking. This is the same stipulation that the ISS has for all of its docking interfaces. This presents a challenge, however, as the docking mechanism will need to dock with the ISS a minimum of one time during the assembly process. In the event of the 302 not being able to perform any active docking cycles the Canadarms aboard the ISS will be used to secure Hermes during the assembly process.



**Figure 6.1. Active Configuration of the NASA Docking Standard Interface [28].**



**Figure 6.2. Orion Docked with Hermes.**

**Table 6.1. Compressive Forces on Payload Docking Interface.**

	To EML1		To Earth	
	Initial	End of Transfer	Initial	End of Transfer
<b>Dry Mass (kg)</b>	15,651	15,651	15,651	15,651
<b>Fuel (kg)</b>	122,000	43,725	33,030	25,797
<b>Total (kg)</b>	158,651	71,651	71,651	25,651
<b>Payload Mass (kg)</b>	22,727.27	22,727.27	6,818.18	6,818.18
<b>Force per Engine (kN)</b>	180	180	180	180
<b>Total Force (kN)</b>	900	720	540	360
<b>OTV acceleration (m/s<sup>2</sup>)</b>	5.61	8.77	9.73	7.46
<b>Max Compressive force (N)</b>	249.1	229.2	76.3	109.2

## 6.2. Refueling

In order to perform more than one mission it is essential to design for the ability to refuel the OTV while in LEO. Without this ability, the size and mass of the OTV would quickly exceed anything that could be launched into orbit. Technologies are currently being developed and tested by NASA to put a refueling station into LEO [30]. Those technologies do not specify an exact design for nozzle geometry or what type of connection is to be made with a vehicle undergoing the refueling process. However, NASA has demonstrated the ability of Dextre, the two-armed robotic handyman aboard the ISS, to use NASA developed tools and procedures to connect to and refuel satellites in orbit [31]. The satellite nozzle that is connected to is easily incorporated into the design of Hermes with a nozzle for the LH<sub>2</sub>, LOX, MMH, and N<sub>2</sub>O<sub>4</sub> tanks on each module. Figure 6.3 shows the nozzle geometry on the CPM. The nozzles on each OPM will be located on the outside of each module for easy access while at the fuel depot. Figure 6.4 shows one of the nozzles being tested with Dextre and will resemble the actual nozzles attached onto Hermes. While this means there are a total of 20 nozzles located on Hermes, not all of these will be used for refueling between missions. Hydrazine and N<sub>2</sub>O<sub>4</sub> tanks on the center propulsion module are only used to rendezvous with the ISS before and during the assembly procedure and will not need to be refilled during the operational lifetime of Hermes.

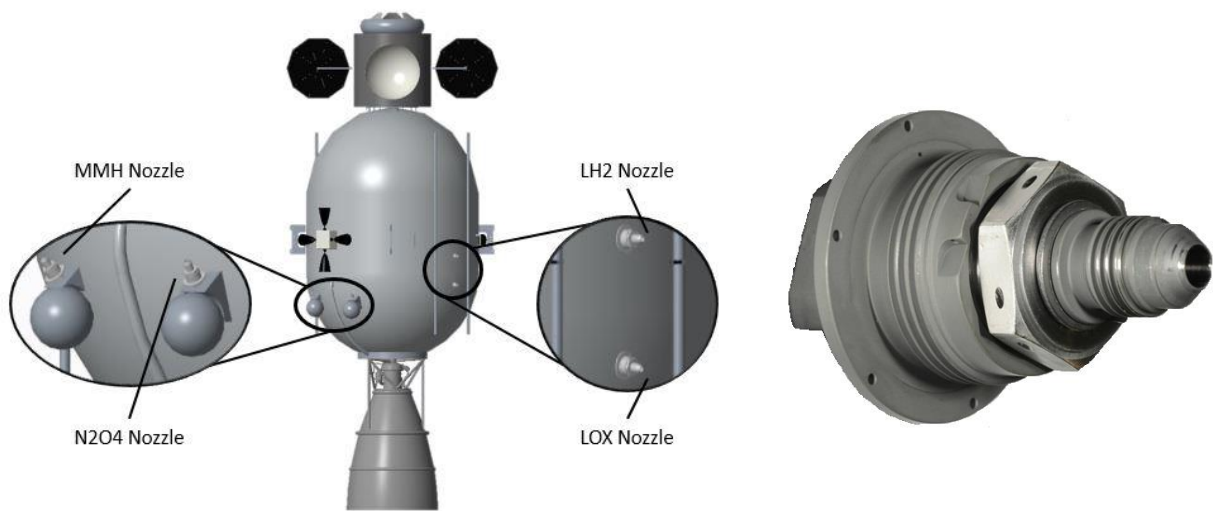


**Figure 6.3. CPM Nozzle Locations.**

**Figure 6.4. LH<sub>2</sub>, LOX, MMH, N<sub>2</sub>O<sub>4</sub> Nozzle [32].**

The refueling process will follow a “zero-vent fill” process for the LH<sub>2</sub> and LOX tanks. This process, used to fill the propellant depot as well [30], starts by chilling the transfer lines and receiving tank. This is done by pumping

gaseous fuel (either LH<sub>2</sub> or LOX depending on which tank is being filled) into the empty tank. Once the tank has reached an acceptable temperature, sub-cooled liquid fuel is pressure fed into the tank quenching the gaseous fuel and sucking in additional liquid fuel. This process has been demonstrated to retain almost 100% of the fuel after successful transfers [33].

Autonomous refueling of hydrazine has been demonstrated on the Orbital Express mission performed in March 2007 [34]. This process followed 7 key steps: coupling mating, leak check of the coupling using helium gas, venting of the helium gas used to do the leak check in the coupling, priming of the coupling with liquid, fluid transfer, gauging of receiving tank to validate amount of propellant transferred, purging and de-mating of the coupling. This method will be used to refuel the MMH and N<sub>2</sub>O<sub>4</sub> tanks onboard Hermes. This process has been routinely used to refuel the ISS with hydrazine, albeit not autonomously. Figure 6.5 shows a schematic of internal refueling components.

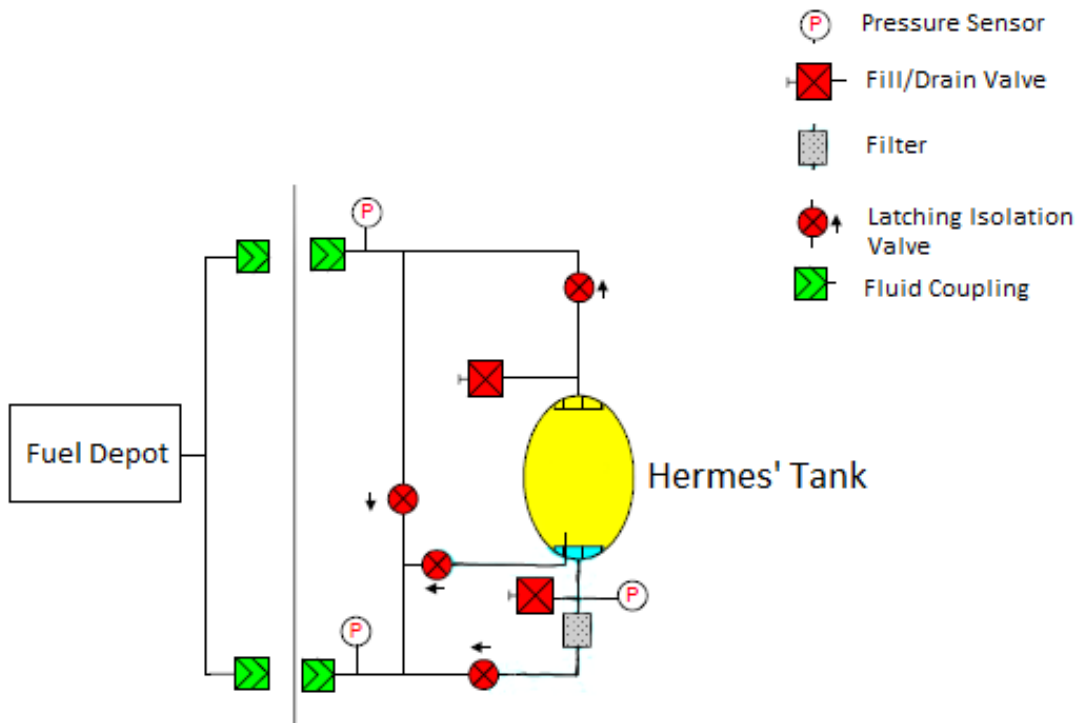


**Figure 6.5. Hydrazine Refueling Scheme [34].**

## 7. Propulsion Systems

### 7.1. Main Engines

Hermes' main propulsion system provides the  $\Delta V$  to initiate and terminate orbital transfers. Major requirements for this system are given in Table 7.1.

The propulsion system is designed to

Table 7.1. Main Engine System Requirements.	
Characteristic	Required Value
EML1 Mission $\Delta V$	3.774 km/s Each Way
EML2 Mission $\Delta V$	4.1 km/s Each Way
Payload to EML	50,000 lb
Payload to LEO	15,000 lb
Minimum Thrust-to-Weight Ratio	0.5
Maximum Thrust-to-Weight Ratio	1.5

provide the vehicle with 4.1 km/s of  $\Delta V$  on each half of the mission. A total  $\Delta V$  of 8.2 km/s is sufficient for Hermes to transfer the RFP payloads to and from EML2, as described in Section 4.2.4.1. The available  $\Delta V$  also allows the OTV to exceed the requirements of the EML1 mission. As an example, Hermes is capable of transferring 85,000 lb to EML1 and 15,000 lb back to LEO when fully fueled.

Constraints are also placed on the thrust of Hermes' engine system. The engines must be sized to accelerate the vehicle at an appropriate rate of 0.5 to 1.5 g. A maneuver with a thrust-to-weight ratio of at least 0.5 is deemed high thrust, and can be considered approximately impulsive [19]. These impulsive burns decrease transfer times and increase fuel efficiency, as discussed in Section 4.2.4. The upper acceleration limit of 1.5 g prevents adverse health effects on human passengers. An engine system with a fixed thrust is unlikely to meet these acceleration criteria throughout the entire mission. Because the weight of the OTV changes dramatically throughout the mission, the total thrust must also be capable of varying to keep thrust-to-weight ratios in the desired range.

In addition to conforming to sizing constraints, the vehicle must be practical to assemble and launch. The system shall utilize a modular design to simplify construction and replacement of failed major components. These modules must be sized appropriately to launch on an economically feasible launch vehicle with high launch frequency.

#### 7.1.1. Main Engine Selection

To begin the propulsion system design process, the overall propulsive method of the vehicle was first selected. Chemical, nuclear and electric propulsion options were considered, and findings of the trade study are given in Table 7.2. Each system was evaluated using a different dry mass because of differing propellant requirements and tank sizes of the systems.

**Table 7.2. Propulsive Method Trade Study [37-39].**

	<b>Chemical</b>	<b>Nuclear Thermal</b>	<b>Electric</b>
<b>Dry Mass (kg)</b>	15,000	10,000	5,000
<b>Minimum Thrust to Weight Ratio</b>	0.57	0.98	6E <sup>-6</sup>
<b>External Power Required (W)</b>	1,000	0	50,000
<b>TRL</b>	9	6	9
<b>Lifetime Propellant Launch Cost (Million USD)</b>	3,500	1,718	61
<b>Approximate Engine Cost (Million USD)</b>	125	5,000	10
<b>Total Engine and Propellant Launch Cost (Million USD)</b>	3,625	6,718	71

Nuclear propulsion was eliminated because of its low Technology Readiness Level (TRL), high development cost, safety concerns, and political issues. Electric propulsion systems are not capable of providing the high thrust required to perform a 6 day transfer; an electric system requiring an excessive 50 kW of electrical power would take over 18 days to transfer the payload between the desired orbits. Therefore, traditional chemical rockets are used on the Hermes OTV.

Based on the decision to use chemical rockets, compatible engines and propellant types were considered. A cost optimization was conducted for each system to obtain the cheapest possible launch cost on the Falcon vehicles (Section 11.2.1). The estimated OTV dry mass used for calculations was 14,300 kg plus the weight of the engine system.

The relevant findings of this trade study are given in Table 7.3. The lifetime cost corresponds to completing 10 missions to EML1, as well as an additional test mission. Acceleration values account for altering the number of active engines during each burn. The desirable qualities in this trade study are minimum propellant launch costs and accelerations in the range of 0.5 to 1.5 g.

**Table 7.3. Main Engine Trade Study [40-44].**

<b>Engine/ Fuel</b>	<b>Quantity</b>	<b>Propellant Per Mission (kg)</b>	<b>Minimum Acceleration (g)</b>	<b>Maximum Acceleration (g)</b>	<b>Total Max Thrust (kN)</b>	<b>Lifetime Propellant Launch Cost (Billion USD)</b>	<b>Total Engine Cost (Million USD)</b>
Vinci/ LH <sub>2</sub>	5	127,000	0.57	1.49	900	2.31	120
RL-10-B2/ LH <sub>2</sub>	5	130,500	0.34	1.192	550	2.31	190
XR5M15 / CH <sub>4</sub>	5	185,000	0.08	0.48	167	2.78	45
Merlin 1C / RP1	3	234,520	0.46	2.70	1,233	3.07	60
Kesl / RP1	5	286,700	0.05	0.30	124	3.68	20

The RL-10, XR5M15 and Kestrel engines do not provide sufficient thrust to meet the desired acceleration range. Although the addition of three RL-10 engines would achieve the required accelerations, the added engines would increase the costs and structural mass of the OTV. Three Merlin engines provide appropriate thrust at the beginning of the mission, yet even a single Merlin engine is too powerful to safely propel the rocket when the OTV is nearly empty of fuel. Development of a new Rocket Propellant 1 (RP-1) or Methane ( $\text{CH}_4$ ) engine with appropriate thrust would still not decrease fuel launch costs; propellant Specific Impulse (Isp) affects launch costs more than engine thrust. Therefore, WayPoint also eliminated the option of developing a new engine. Based on this trade study, the Vinci engine was selected for use on Hermes.

### **7.1.1.1. Vinci Engine**

The Vinci burns Liquid Hydrogen ( $\text{LH}_2$ ) and Liquid Oxygen (LOX) with a Isp of 465 s, and is produced by Snecma for use on the Ariane 5. In general,  $\text{LH}_2$  encounters boil off issues on long term missions; however, the procedures and systems described in Section 10.6.3 limit boil off to 250 kg of  $\text{LH}_2$  per mission. To offset boil off, Hermes carries an additional 250 kg fuel margin split evenly between the five propulsion units.

The selected engine is well-suited for use in the very near future. The Vinci engine has undergone significant ground testing, and is projected to begin flight in 2017. A single Vinci engine has been tested for 6,000 seconds, 1,000 seconds fewer than the OTVs engines would be fired throughout Hermes' lifetime [35]. Should Snecma not complete additional testing, WayPoint would perform its own engine lifetime tests. Regardless, the proven endurance of the engines provides evidence that the Vinci is well suited for applications of high reusability.

The mission profile requires the engines to restart multiple times during a mission. The Vinci engine is designed for five restarts without reloading the ignition system, which utilizes a gaseous hydrogen/oxygen torch with an electric spark igniter [36]. The engine operates on an expander cycle, as shown in Figure 7.1. In an expander cycle, liquid hydrogen flows through channels in the engine nozzle, boils while cooling the nozzle, and is injected into the thrust chamber. Chamber valves are used to allow propellant into the thrust chamber, and purge valves vent propellant to the exterior of the vehicle. Figure 7.2 shows the physical components represented in the propellant flow system.

In case the Vinci engine is not ready for use on Hermes, a backup engine system has been chosen. Although slightly below the desired thrust range, the RL-10 may serve as a replacement engine if the Vinci engine development is delayed. However, the RL-10's low thrust-to-weight ratio requires a less than optimal orbital trajectory. A loss of

efficiency may eliminate the possibility of the vehicle transferring payloads to EML2, or reduce the amount of mass transferred to EML1.

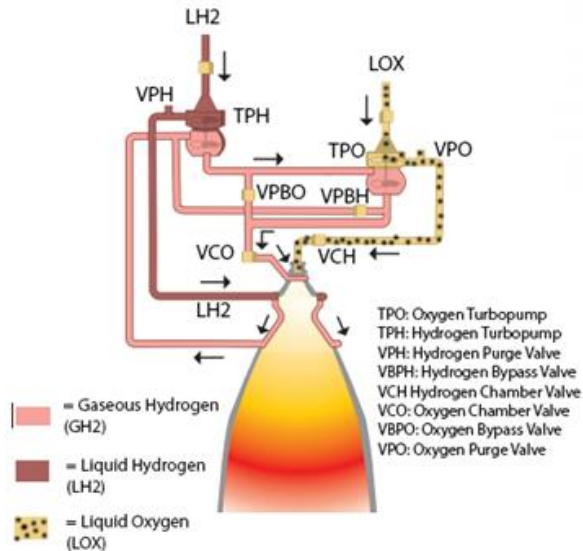


**Figure 7.1. Vinci Flow Schematic [36].**

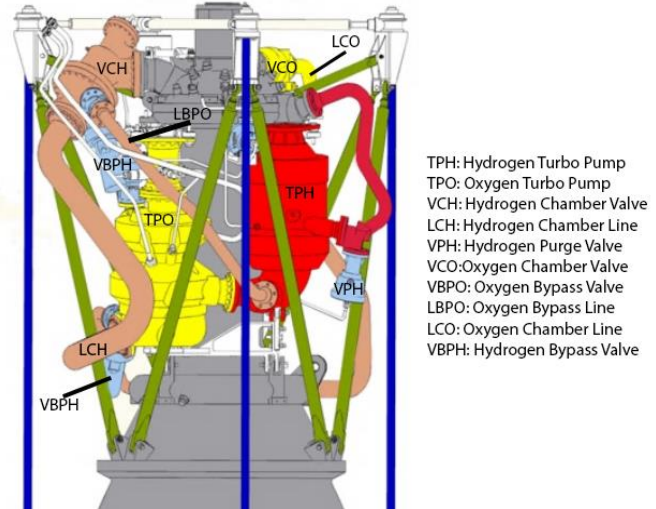


**Figure 7.2. Vinci Engine Component Layout [37].**

### 7.1.2. Propulsion Profile

A profile of engine operation throughout a round trip mission to EML1 is given in Table 7.4. Engines are numbered as shown in Figure 7.3. The number of engines operating during any maneuver varies throughout the mission to maintain a thrust-to-weight ratio in the desired range of 0.5 to 1.5. This engine firing sequencing also prolongs the operational lifetime of the Vinci rockets, since no engine is active throughout the full duration of the mission.

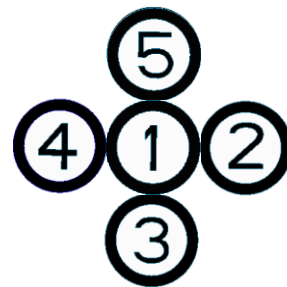


**Figure 7.3. Module Numbering.**

**Table 7.4. Propulsion Mission Profile.**

Event	Engines Operating	Burn Time (s)	Propellant Used (kg)
LEO Departure	1-5	413	81,589
EML1 Arrival	2-5	77	12,196
EML1 Departure	1,2,4	65	7,731
LEO Arrival	3,5	323	25,484

## 7.2. Propellant Tanks

### 7.2.1. Tank Sizing

Hermes' propellant tanks are sized to contain enough propellant for 8.2 km/s of  $\Delta V$ , corresponding to the amount required for the EML2 missions. An additional 10% propellant margin is also applied to the tank volume requirements. The propulsion units are designed to launch on SpaceX Falcon 9 rockets with custom payload fairings. A five tank propulsion system is used because of launch fairing size constraints. When coupled with the five-engine system, five propellant tanks allow for a very high degree of modularity and redundancy. With a five-unit arrangement each tank holds up to  $21.54 \text{ m}^3$  of LOX and  $59.82 \text{ m}^3$  of LH<sub>2</sub>, corresponding to 24,555 kg of LOX and 4,222 kg of LH<sub>2</sub> per propulsion unit. On an EML1 mission with the payloads stated in the RFP, each tank is only filled with  $18.29 \text{ m}^3$  of LOX and  $50.78 \text{ m}^3$  of LH<sub>2</sub>, which includes a 10% fuel margin.

The overall shape of the propellant tank is a pill, which has well-known structural properties and manufacturing requirements [10]. The LOX tank comprises the bottom portion of the propellant tank; geometrically the LOX tank is roughly hemispherical with a slight concavity in the upper surface. The remainder of the pill volume is filled with LH<sub>2</sub>. By placing the heavier LOX tank at the bottom of the pill and moving the vehicle center of mass towards the thrust of the engines, stability is increased. The lower mass concentration also decreases the effective buckling length of the tank, mitigating the risk of structural failures.

To decrease the propulsion system mass, the propellant tanks are designed to include a common bulkhead. In the common bulkhead configuration, the LOX and LH<sub>2</sub> tanks share a structural wall. The bulkhead eliminates the need for a heavy intertank assembly to rigidly support the separate propellant vessels. Eliminating these attachments reduces the mass of the structure by almost 20% [38]. The common bulkhead is constructed of insulation sandwiched between two layers of aluminum. The core insulation material is Airex R82.80 foam, which is capable of limiting heat leak to acceptable levels for a common bulkhead application [38]. In areas of high stress concentration, such as the joints between the bulkhead and tank walls, the foam core is reinforced with a high strength honeycomb material.

A cutaway image of the propellant tank layout is given in Figure 7.6 with dimensions given in meters in Figure 7.5. False color has been applied to the cutaway image to visually distinguish components. The LOX feed line connects directly from the LH<sub>2</sub> sponge to the engine, and is not shown in these diagrams. The LH<sub>2</sub> feed line passes through the common bulkhead and then continues down the side of the tank, as on the Space Shuttle external tank

[39]. All feed lines match the geometry and construction of the Vinci engine fluid lines, corresponding to a 5 cm inner diameter for the LOX feed line, and a 7 cm inner diameter for the LH<sub>2</sub> piping. Structural considerations of the propellant tanks and connections to adjacent units are discussed in Section 5.3.4. A separate cutaway image in Figure 7.8 shows the skin and stringer system used to reinforce the propellant tanks against buckling.

### 7.2.2. Thrust Ring

A structural attachment is required to connect these propellant tanks to the engine system. To accomplish this, a thrust ring is used to attach each Vinci engine to its respective propellant tank. The ring structure is shown in Figure 7.7 and is welded to both the engine and the propellant tank. False color has been applied to the ring in the image to enhance visibility. Applying a safety factor of three to the engine thrust, the thrust ring is designed with a buckling strength of 540 kN. The structure is composed of Aluminum 2090-T83, and consists of twelve bars spanning a 0.127 m gap between two solid rings. The bars have square cross sections with side lengths of 1.5 cm.

### 7.2.3. Propellant Management

The propellant tanks also require a method of holding fluid near the feed lines in low gravity. For propellant management, Hermes uses a propellant sponge at the bottom of each propellant tank. Surface tension effects cause propellant to naturally cling to the vanes of the device in a low gravity situation. Feed lines connecting the propellant tanks to the engines attach to the tanks at the location of the sponge devices. Once a small amount of propellant from the sponges is burned by the engines, inertial forces cause the liquid to be pushed towards the propellant lines. Accelerations as small as 0.001 g are sufficient to push the remainder of the propellant to the bottom of the tanks. During the settling process, the sponge also refills, and retains enough propellant to smoothly restart the engines during the next burn [40]. When fuel is being fed between tanks, as will be discussed in Section 7.2.4, Hermes' reaction control thrusters are used to provide the required acceleration to fill the sponges.

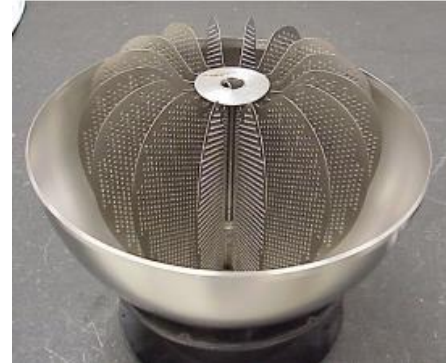


**Figure 7.4. Small Scale Propellant Sponge [40].**

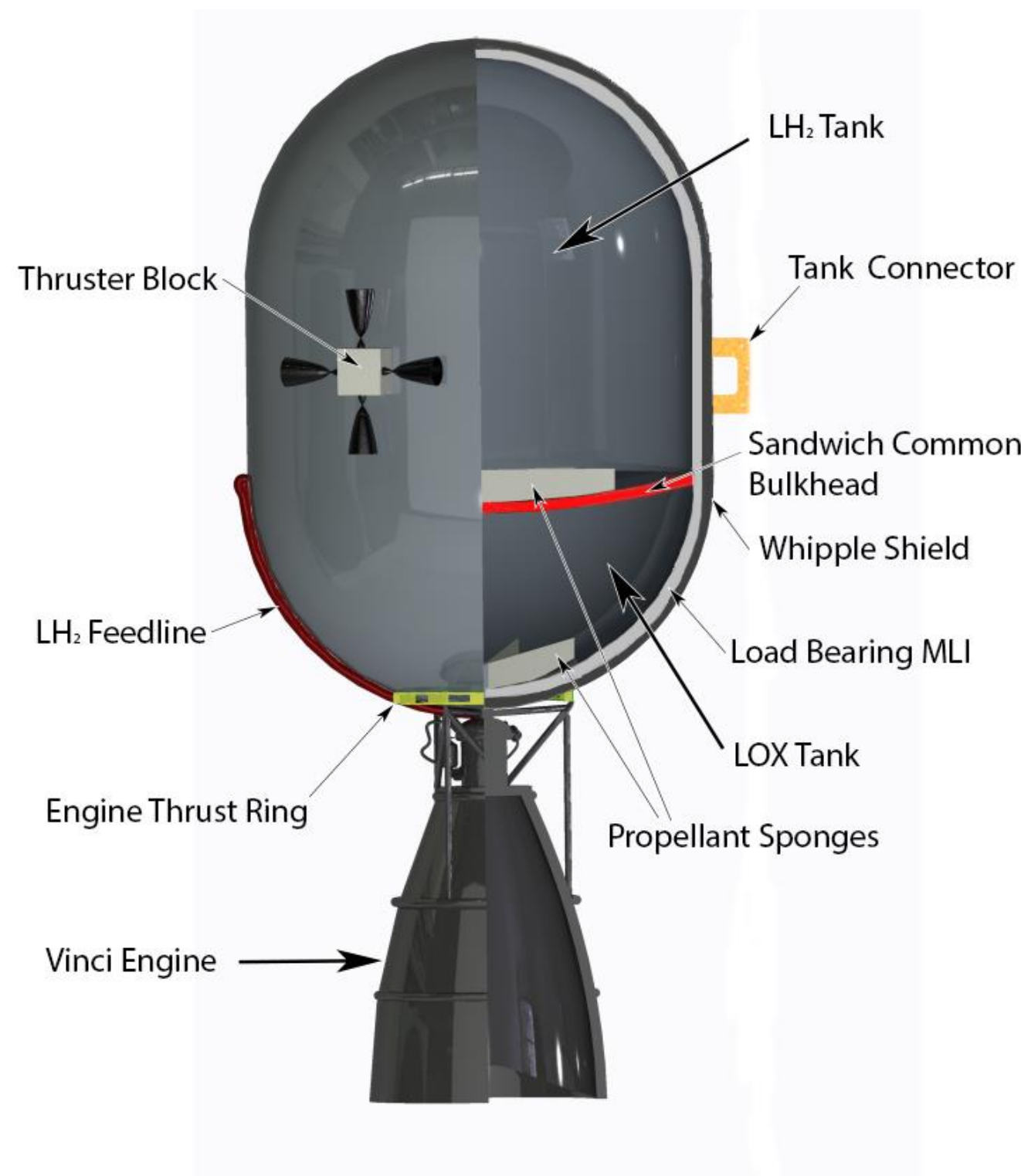


Figure 7.6. Quarter Section Cutaway View of Propulsion Unit.

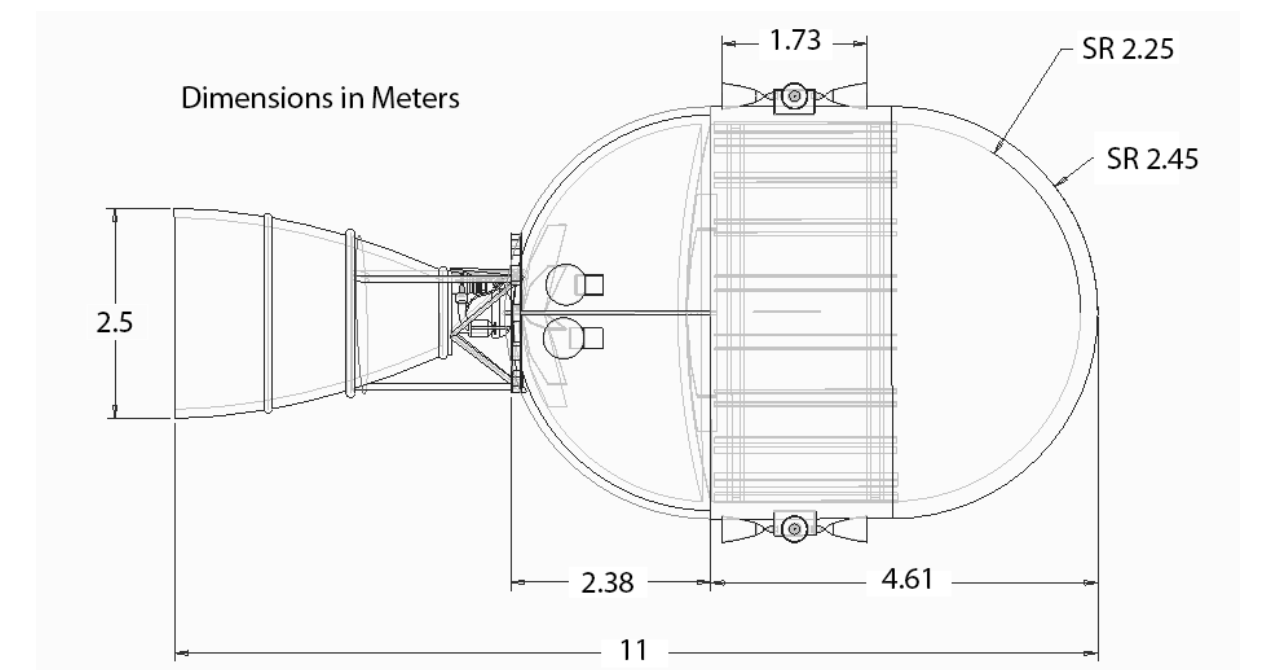


Figure 7.5 Propulsion Unit Dimensions.



Figure 7.7. Engine Thrust Ring.

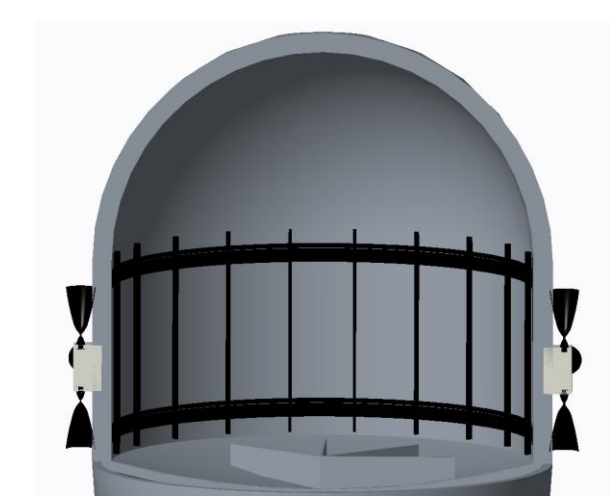
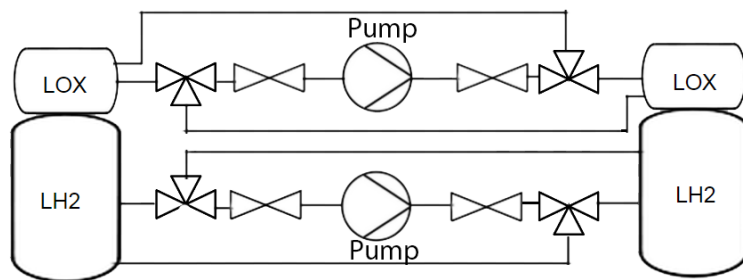


Figure 7.8. Skin and Stringer System.

#### 7.2.4. Tank Cross Feed

Hermes' propulsion systems feature tank and engine cross feeding capabilities with three main utilities. The cross feed system allows for passive connections between propellant tanks. The connection allows the vehicle to be refueled using only one LOX and one LH<sub>2</sub> port, instead of one per propulsion module. However, each propulsion unit contains the required refueling ports for redundancy purposes. The system also allows propellant to be slowly pumped between tanks in between burns. The pumping utility maintains the nominal center of mass later in the mission when all propulsion units do not operate for equal durations. The pumping system is combined with the above passive cross link system as shown in Figure 7.9. Each exterior LOX and LH<sub>2</sub> tank is connected to the center LOX and LH<sub>2</sub> tanks as shown in the diagram.



**Figure 7.9. Tank Cross Feed System.**

The tank cross feed system uses two three-way valves to switch the direction of the flow. Either tank can be set as the inlet or outlet of the pump using these valves. Additionally, the pump may be bypassed completely, fulfilling the passive cross feed requirement. The pump system uses 1 kW cryogenic pumps operating at 250,000 Pa; the pumps create a volumetric flow rate of 0.004 m<sup>3</sup>/s. At this rate, emptying a full propulsion unit takes 5.65 hours. The transfer process does not occur during burns, only between orbital maneuvers. During these times, the vehicle's down time is anywhere from six days to one month. Therefore, the designed propellant transfer rate is more than sufficient to relocate propellant between maneuvers.

The propellant lines are composed of extruded stainless steel, as recommended by NASA for use with cryogenic propellants. Extruding the pipes avoids welding, since welds introduce a failure point along the propellant line [41]. The propellant piping has an inner diameter of 2.5 cm, relating to a maximum flow velocity of 40 m/s. A

Fanno flow analysis confirmed that the fluid will not choke in the pipe due to frictional effects, since the flowing propellant only reaches a maximum Mach number of 0.1.

### 7.2.5. Engine Cross Feed

Hermes also includes an engine cross feed system to allow an engine to burn propellant from a different tank. Direct cross feed is desirable if an engine were to fail during a thrusting maneuver. If an engine failed, the vehicle could be placed on an undesirable trajectory, and not have time to transfer propellant using the pumping system described above. An engine feed linkage allows propellant to flow from the feed lines of one engine directly to the feed lines of another. The engine cross feed system includes additional propellant lines and valves, but no additional pumps. Propellant from any given tank enters the cross feed system and flows into the turbo pump of a functional engine. A simplified diagram cross fed engine flow system is given in Figure 7.10.

These linkages exist for both the LOX and LH<sub>2</sub> feed lines of each engine. The propellant lines themselves mimic the materials and diameter of the standard Vinci feed lines. As previously mentioned, the Vinci feed lines have a 5 cm inner diameter for the LOX feed line, and a 7 cm inner diameter for the LH<sub>2</sub> piping. This linkage introduces additional complex valves and connections to the engine system, and therefore shall only be used as an emergency contingency.

When not in operation, all fluid feed lines are closed from all tanks using isolation valves. Incident heat on the propellant lines causes the residual propellant in the pipes to boil off. Before opening the isolation valves and reinitiating a connection to the tanks, purge valves actuate in the cross feed system. These valves release any boiled off propellant from the feed lines, reducing the risk of gas bubbles flowing through the engines.

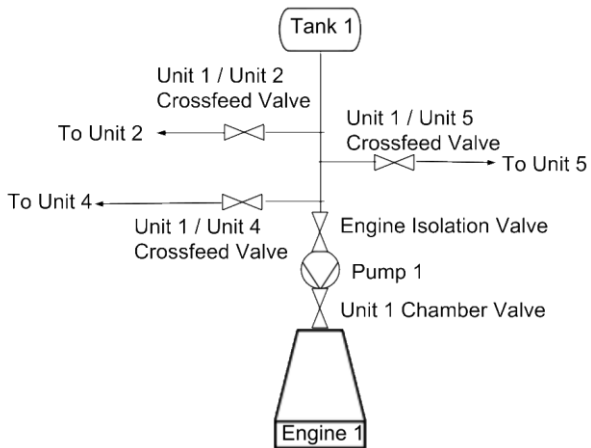


**Figure 7.10. Engine Cross Feed System.**

## 7.3. RCS and Maneuvering System

### 7.3.1. Maneuvering Thrusters

To apply  $\Delta V$ s on the order of 10 m/s, maneuvering thrusters must be used instead of the main engines. A trade study of thrusters is given in Table 7.5 using inputs characteristic of each system. The required propellant was calculated with a total  $\Delta V$  of 25 m/s for rendezvous and station keeping maneuvers, using a vehicle dry mass of 15,600 kg. Calculations accounted for the instantaneous mass of the OTV during each maneuver.

The burn times column represents the time to provide 10 m/s of  $\Delta V$  when the vehicle is arriving at EML1, since this will be the longest single burn. Exact burn times are not critical, but it is important that they remain on the order of several minutes. The projected rendezvous maneuver time is approximately 1,200 seconds. Therefore, the burn times should be significantly below this value.

**Table 7.5. Maneuvering Thruster Analysis [39, 51-52].**

	Propellant Required (kg)	Burn Times (s)	Power Required (W)	Thrust (N)
<b>Bipropellant Hydrazine</b>	310	390	35	445
<b>Monopropellant Hydrazine</b>	450	400	35	400
<b>Ion Thruster</b>	10	550,000	50,000	10
<b>Cold Gas Thruster</b>	1,100	115,000	10	300

Ion thrusters require restrictive amounts of power and burn times outside of the required range. Cold gas systems require over four times the propellant mass of hydrazine systems, and also exhibit excessive required burn times. Although the toxicity of hydrazine adds a risk to the mission, alternative systems are not feasible for use on a vehicle of Hermes' size. Hydrazine has been safely used on other large vehicles such as Apollo and Space Shuttle missions, and is planned to be used on the Orion spacecraft. Based on the thruster trade study, Hermes uses a bipropellant hydrazine thruster system which burns a mixture of Monomethylhydrazine (MMH) fuel and Nitrogen Tetroxide ( $N_2O_4$ ) oxidizer.

A trade study was also conducted to select the specific thruster model. The relevant values are given in Table 7.6. The propellant required represents the amount needed for a  $\Delta V$  of 25 m/s throughout a mission, and the burn times represent a 10 m/s  $\Delta V$  when arriving at EML1.

**Table 7.6. Maneuvering Thruster Analysis [39, 51-52].**

Thruster	Propellant Required (kg)	Burn Times (s)	Number of Cycles
Airbus S400-15	320	395	135
Moog DST-12	340	7700	50,000+
<b>Aerojet HiPAT 445N</b>	<b>305</b>	<b>380</b>	<b>672</b>

Based on the thruster analysis, the Aerojet HiPAT 445N was selected for Hermes. The smaller Moog DST-12 thrusters require more propellant and longer burn times than the S400 and HiPAT thrusters. The Aerojet and Airbus thruster are similar, but the HiPAT was chosen due to its slightly lower propellant requirement and higher number of allowable cycles.

The selected HiPAT thrusters are limited to a cycle life of 672 burns [42]. The thrusters are projected to require 40 cycles per mission for ADCS purposes and six cycles per mission for propulsion purposes. However, the thrusters do not cycle equally. The maximum usage of any one thruster per mission is approximately 20 cycles. During assembly, which is a one-time process, each thruster is used a maximum of 6 times. Therefore, the 672 cycles are sufficient for the entire lifetime of Hermes, including the test flight and assembly.

During standard missions, Hermes uses eight blocks of four thrusters each, with two blocks on each exterior propulsion module. For assembly purposes, the central propulsion unit will also include two blocks of thrusters. These central actuators are not be used once the OTV is assembled, since exhaust from the thrusters impinge on the adjacent propulsion units. Figure 7.11 shows the configuration of a thruster block. The block's multiple available thrust vectors allow the thrusters to be used for ADCS purposes as well as small propulsion burns and vehicle assembly.

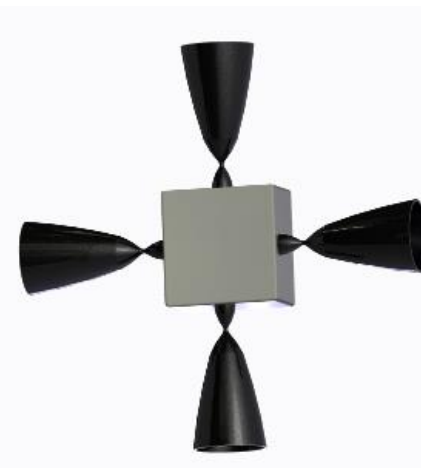


**Figure 7.11. Thruster Block.**

### 7.3.2. Hydrazine Tanks

Hermes' maneuvering propellant requirements determine the size of the vehicle's hydrazine tanks. ADCS propellant requirements are projected at 10 kg per mission as discussed in Section 8.1.2. Summing the ADCS requirements with the propellant value in Table 7.6, Hermes needs at least 315 kg of hydrazine during each mission.

The final thruster propellant requirement derives from station keeping in LEO between missions. During these six months, the OTV is 25 percent fueled and uses 340 kg of hydrazine. However, since hydrazine is refueled upon returning to LEO, these 340 kg are not carried by Hermes during the EML transfers. Therefore, the most hydrazine Hermes expends without refueling is 340 kg. Applying a safety factor of 1.5, the OTV tanks contain 500 kg of hydrazine total. Each propulsion module contains a fuel and oxidizer tank; both are spherical with a radius of 0.22m. The hydrazine tanks are shown on the right side of Figure 7.12.

Since Hermes' tanks only hold enough propellant for one mission, the hydrazine is refueled after arriving and before departing LEO. Based on current NASA procedures for refueling hydrazine at the ISS, Hermes' hydrazine tanks are refueled through direct fluid transfer with the Fuel Depot. Direct refueling is much simpler than swapping empty hydrazine tanks for new, full tanks; switching tanks would require much more complex robotic and mechanical systems. Because hydrazine is an easily storable propellant, boil off in these tanks is not a concern. Hydrazine refueling is discussed further in Section 6.2.

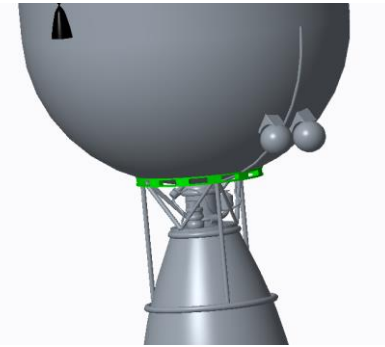


**Figure 7.12. Hydrazine Tanks and Attachment.**

## 8. Attitude Determination and Control Systems

### 8.1. Control Actuators

#### 8.1.1. Requirements

The requirements of the Attitude Determination and Control System (ADCS) consist of pointing accuracy requirements and the ability to perform large slew maneuvers. Pointing includes requirements from the propulsion,

docking, thermal, and communications subsystems. Given the designed mission profile, the pointing requirements during the vast majority of the phases of the mission are flexible. The main requirement is to ensure that the solar panels face the sun. However, docking and refueling procedures will require a high degree of pointing accuracy. Table 8.1 gives a summary of the pointing requirements throughout the mission.

**Table 8.1. Pointing Requirements During all Mission Phases.**

	LEO Inactive Period	Orbit Transfers	EML Inactive Period	Burns/Docking
Accuracy Required [deg]	Uncontrolled/Undefined	5	5	0.1

To achieve these pointing requirements, Hermes must have control actuators. Actuators are components that change the angular momentum and pointing direction of the spacecraft. The main concerns when selecting these components are meeting specified pointing and slew requirements and sizing the actuators to meet the physical constraints of the vehicle. Hermes is a large vehicle with large moments of inertia as shown in Table 8.2, which means that it is difficult to turn. These moments of inertia will act as requirements for sizing the control actuators.

**Table 8.2. Spacecraft Moments of Inertia.**

	LEO with No Fuel and No Payload	LEO with Full Fuel Large Payload	Transfer to EML	EML With No Payload	EML With Small Payload	Transfer to LEO
<b>Mass [kg]</b>	1.55e4	1.81e5	9.22e4	5.18e4	5.86e4	4.73e4
<b>I<sub>z</sub> [kg·m<sup>2</sup>]</b>	3.23e5	3.27e6	1.46e6	1.03e6	1.04e6	8.10e5
<b>I<sub>x</sub>/I<sub>y</sub> [kg·m<sup>2</sup>]</b>	2.64e5	4.21e6	2.65e6	8.10e5	1.31e6	1.13e6

The other main challenge in designing the control actuators is providing the ability to reject all disturbance torques experienced in the space environment. The main sources of disturbance torques include solar radiation pressure, aerodynamic drag, magnetic fields, and gravity gradient effects [10]. These disturbances cause the pointing direction of the spacecraft to slowly diverge from the desired direction.

### 8.1.2. Control Actuator Selection

Hermes uses bipropellant hydrazine thrusters in the form of a reaction control system as the main method of attitude control as described in Section 7.3. Other actuators considered include control moment gyroscopes, magnetic torquers, and momentum wheels. Table 8.3 gives a summary of the typical performance and characteristics of these different actuators. Thrusters have been selected primarily because they serve the dual purposes of performing the station-keeping and rendezvous maneuvers required while also being powerful enough to perform all necessary slew

maneuvers. Thrusters are also capable of maintaining fine enough pointing for precise maneuvers such as docking [10]. This dual usage minimizes the mass on-board Hermes. Specific selection of thrusters was performed in Section 7.3.

**Table 8.3. Typical Attitude Actuators [10].**

Actuator	Performance Range	Mass [kg]	Power [W]
<b>Hydrazine thrusters</b>	0.5-9000 N	0.4-1.6	18-58
<b>Momentum Wheels</b>	Max Torques: 0.01-1 N-m Momentum Storage Capacity: 0.4 to 3000 Nms	2-20	10-100
<b>CMG</b>	25-500 N-m	>10	90-150
<b>Magnetic Torquers</b>	1-4000 A-m <sup>2</sup>	0.4-50	0.6-16

Magnetic torquers are not applicable to Hermes since a large portion of the mission will take place far from the Earth where the magnetic field is not strong enough to provide sufficient torques. Control moment gyroscopes would require the inclusion of unnecessary mass and power requirements as Table 8.4 shows that the additional propellant mass of ADCS is significantly less than the mass caused by including CMGs. Momentum wheels were also considered for their ability to maintain fine pointing. However, they were determined to be unnecessary as the pointing requirements for the majority of the mission are not fine enough to justify their inclusion.

To create a reaction control system utilizing thrusters, Hermes will include 32 thrusters in eight blocks of four, one of which is

**Table 8.4. Summary of ADCS Control Actuators.**

<b>Number of Thrusters</b>	32
<b>Propellant Mass Per Mission (kg)</b>	10
<b>Number of Burns Per Mission</b>	43

shown in Figure 8.1. These thrusters can apply force about any of the three axes which will generate pure moments. In this manner the angular momentum vector can be changed without altering the translational motion of the spacecraft. The assembly control system will also use these thrusters as described in Section 8.4, so they have been placed for the maximum re-use of components as shown in Figure 8.2. Although this placement does not maximize the moment arm of each thruster which would minimize the fuel cost, it allows for multiple uses of each thruster which helps create a reliable and redundant reaction control system while having only a small effect on the amount of hydrazine required for each mission.



**Figure 8.1. Thruster Block.**

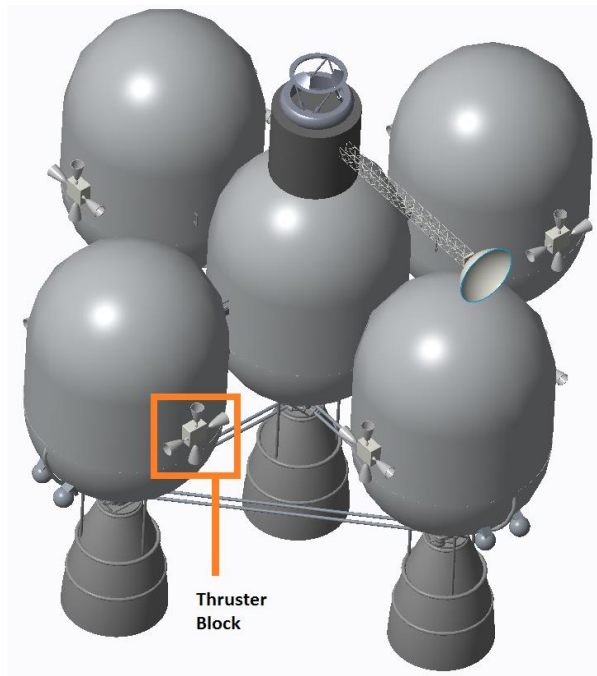


**Figure 8.2. Thruster Block Placement.**

## 8.2. Attitude Sensors

### 8.2.1. Sensor Selection

Sensors are required onboard the OTV to determine the spacecraft's attitude, or pointing direction. Several types of ADCS sensors have been examined and based on their operational methods, their applicability to both the LEO and EML1 environments has been determined. Table 8.5 details the performance characteristics and utilities of these sensors. Earth sensors would not function properly at EML1. As a result of the extreme distance from the Earth, the Earth's disk would subtend a small angle of the visual field, drastically decreasing the sensor's accuracy. The magnetometer would also not work at EML1 as there is no appreciable magnetic field from the Earth that far out. Finally, the GPS receiver would also not function as GPS satellites orbit at a lower altitude than EML1.

**Table 8.5. ADCS Sensor Characteristics and Applicability [10].**

	Accuracy	Mass [kg]	Power [W]	Use in LEO	Use at EML1
<b>Inertial Measurement Unit</b>	0.003 to 1 deg/hr	0.1 to 15	1 to 200	Yes	Yes
<b>Sun Sensor</b>	0.005 to 3 deg	0.1 to 2	0 to 3	Yes, when not in eclipse	Yes
<b>Star Sensor</b>	0.0003 to 0.01 deg	2 to 5	1 to 4	Yes	Yes
<b>Magnetometer</b>	0.5 to 3 deg	0.3 to 1.2	<1	Yes	No
<b>Earth Sensor</b>	0.05 to 1 deg	1 to 4	5 to 10	Yes	No
<b>GPS Receiver</b>	0.25 to 0.5 deg	6 to 10	1 to 100	Yes	No

By combining the specified pointing requirements with Table 8.5, appropriate sensors were selected. Inertial Measurement Units (IMUs) serve to provide rate information for the spacecraft, which is critical for docking procedures and thrusting maneuvers. As these maneuvers occur frequently throughout the life of the spacecraft, accurate and robust IMUs must be included.

Accurate external references are needed in addition to IMUs, which necessitates a star sensor, as it is the only sensor that accurately provides an external pointing reference in both LEO and at EML1. However, accurate star sensors generate large amounts of data. To decrease the amount of data being generated while in idle mode in LEO, it is beneficial to include an additional external reference sensor. Earth sensors, magnetometers, and GPS receivers are all capable of performing this task. However, GPS receivers are heavy and consume excess power in comparison to other sensors so they will not be used. A magnetometer has been chosen over an Earth sensor due to its lower mass and power requirements and the low pointing accuracy required while in idle mode in LEO. This sensor will however, not be used while at the Lagrange points.

Coarse sun sensors, which are simply small solar cells, are less accurate versions of sun sensors. These sensors provide rough pointing estimates based on the angle of incidence of sunlight on their surface. Since they do not require any power and are relatively inexpensive, including several coarse sun sensors enables an effective and cheap fault recovery mode if other sensors were to temporarily fail.

### 8.2.2. Component Selection

To accurately describe the entire ADCS system, specific commercial off the shelf hardware has been selected for use on Hermes. A star sensor, sun sensor, magnetometer, and an inertial measurement unit (IMU) have all been

selected based on favorable component traits. Flight heritage and reliability was also considered in the selection process to continue Waypoint's goal of creating a reliable and proven system.

Table 8.6 details several commercially available star trackers. The  $\mu$ STAR-200H has been selected based on its very high accuracy, low mass, and fast update rate. The high accuracy provided by this star tracker will assist in accurate docking and refueling procedures as well as in navigational assistance.

Table 8.6. Commercially Available Star Trackers [54-58].					
Name	Mass (kg)	Operational Temperature (C)	Update Rate (Hz)	Accuracy (arc-sec)	Power (W)
CT-602	<5.5	50 to -30	10	3	8
CT-633	2.5	45 to -25	5	5	8
ST-16	0.164	50 to -30	2	7	1
HE-5AS	2.2	70 to -40	4	5	7
<b><math>\mu</math>STAR-200H</b>	2.7	61 to -24	10	<1	9

Table 8.7 gives a list of several commercially available sun sensors. The BASS sensor from Airbus has been selected based on its large field of view as well as the fact that it is a passive component. Since the primary purpose of these sensors is to assist in a recovery mode, the wide field of view will assist in maximizing the number of sensors that can view the sun.

Table 8.7. Commercially Available Sun Sensors [59-63].					
Name	Mass (kg)	Operating Temperature (C)	Power (W)	Field of View (deg)	Accuracy (deg)
CubeSat	<0.005	50 to -25	<0.01	114	<0.5
Coarse Sun Sensor	0.365	90 to -80	<0.2	128	<1
LIASS	0.23	100 to -100	0	90	0.18
<b>BASS</b>	0.065	95 to -40	0	180	0.18
MSS-01	0.086	93 to -40	0	60	1

Table 8.8 lists several commercially available magnetometers. The SSBV Magnetometer has been selected based on the desire to decrease the amount of data generated in LEO and this magnetometer's slow update rate. As the magnetometer's primary function will be to act as a backup and redundant attitude check while in LEO, generating large amounts of data is not necessary.

**Table 8.8. Commercially Available Magnetometers [64-67].**

Name	Mass [kg]	Operating Temperature [C]	Resolution [nT]	Update Rate [Hz]	Power [W]
<b>SSBV Magnetometer</b>	0.2	75 to -35	13	10	0.4
<b>HMR2300</b>	0.098	85 to -40	6.7	25	0.5
<b>HMC1043L</b>	0.01	150 to -55	12	25	0.03
<b>Tri-Axial External Magnetometer</b>	0.14	70 to -55	1	250	<1

Table 8.9 gives information about several models of inertial measurement units (IMUs). IMUs measure the accelerations on all three orthogonal axes of the spacecraft and contain gyroscopes to ensure that the accelerometers are always pointing in the correct direction. The units will be used extensively in navigational roles to provide data to the on-board orbit propagator as well as to precisely measure how long the vehicle undergoes acceleration during a thrusting maneuver. Due to the complex orbital trajectories Hermes follows, obtaining the correct trajectory is critical to the mission success so extremely precise and reliable information must be gathered in this area. To accomplish this, the Miniature Inertial Measurement Unit (MIMU) manufactured by Honeywell has been selected to provide acceleration data to Hermes. The MIMU has a very low gyroscope drift rate and has been proven on many missions including deep space missions such as New Horizons [43]. Therefore, it is capable for use on Hermes as well.

**Table 8.9. Commercially Available IMUs [69-71].**

Name	Mass [kg]	Operational Temp [C]	Drift Rate [deg/hr]	Max Acceleration [g's]	Power [W]
<b>MIMU</b>	4.44	65 to -30	<0.005	25	22
<b>LN-200S</b>	0.748	71 to -54	<0.1	40	12
<b>HG1700</b>	0.91	85 to -54	1	12	8

Table 8.10 provides a complete description of all attitude determination sensors that will be on board Hermes.

### 8.3. On-Board Processing

Computers are necessary on-board Hermes to perform all on-board processing tasks including processing data from sensors, making control decisions, controlling on-board systems, and preparing data to be communicated. Because Hermes will not be carrying a science payload, the processing requirements result mostly from ADCS and Command requirements and not from Data Handling.

**Table 8.10. Sensors on Board.**

Sensor Type	Name	Number of Units
<b>Star Sensor</b>	$\mu$ STAR-200H	2
<b>Sun Sensor</b>	BASS	6
<b>Magnetometer</b>	SSBV Magnetometer	1
<b>IMU</b>	MIMU	2

The space environment is very harsh for electronics. Processors are constantly bombarded with ionizing radiation that builds up over time and will eventually render the computer useless. Processors are also prone to Single Event Upsets (SEUs) that are caused by high energy particles colliding with the board and temporarily disrupting computation. Because these electronics are prone to these failures in space and many decisions made by the flight computers will translate into actual control commands, it is important that redundancy is implemented in the computer system. For this reason, Hermes will feature three identical flight computers that will form a voting system where all computers perform the same task and then compare the results. If all three computers agree, then that choice is made. If two agree and one differs, the voting system determines that an error occurred with the third computer and its result is disregarded.

Table 8.11 shows a selection of commonly used radiation hardened flight computers. The Proton 400k computer has been selected for use on-board Hermes on the grounds of its comparable maximum radiation dose, a fast processor with 7200 Million Instructions per Second (MIPS), and large amount of RAM. The Proton 400k also has a proven flight heritage which is critical as Hermes will be ferrying human passengers.

**Table 8.11. Commercially Available Radiation Hardened Computers [72-74].**

Name	Mass [kg]	Power [W]	Temperature Range [C]	Instructions [MIPS]	Max Radiation Dose [kradSI]	RAM [MB]
<b>Maxwell Single Board</b>	1.5	19	65 to -30	1800	>100	8
<b>RAD750 6U Compact PCI</b>	<2	<25	50 to -20	260	>100	52
<b>Proton 200k Lite</b>	0.2	1.5	61 to -24	1200	>100	512
<b>Proton 400k</b>	<1	8	61 to -24	7200	>100	512

In addition to these hardware components, software is required to run and process data from all the various sensors as well as to execute control commands. Advanced algorithms will be used in the code including Kalman filtering, orbit propagation for complex environments, complex ephemerides, and fault detection. Table 8.12 gives an estimation of the number of source lines of code that will be necessary to implement all of these algorithms.

## 8.4. Assembly Maneuvering System

Before Hermes is fully assembled, the individual propulsion modules and main bus must be maneuvered into position for assembly as is discussed in Section 3. To accomplish this, each module must have its own control and maneuvering systems. These systems will enable them to rendezvous with the ISS as well as control their pointing direction. A diagram of

**Table 8.12. Source lines of code estimation [10].**

Software Component	Source Lines of Code
Executive	1,000
Communication	5,500
Sensor Processing	4,500
Attitude Determination and Control	20,500
Attitude Actuator Processing	2,100
Fault Detection	6,500
Utilities	7,300
Other Functions	5,000
<b>Total:</b>	<b>52,400</b>

the system Hermes will use is shown in Figure 8.3. This system has been sized so that its main components are applicable to all launches.

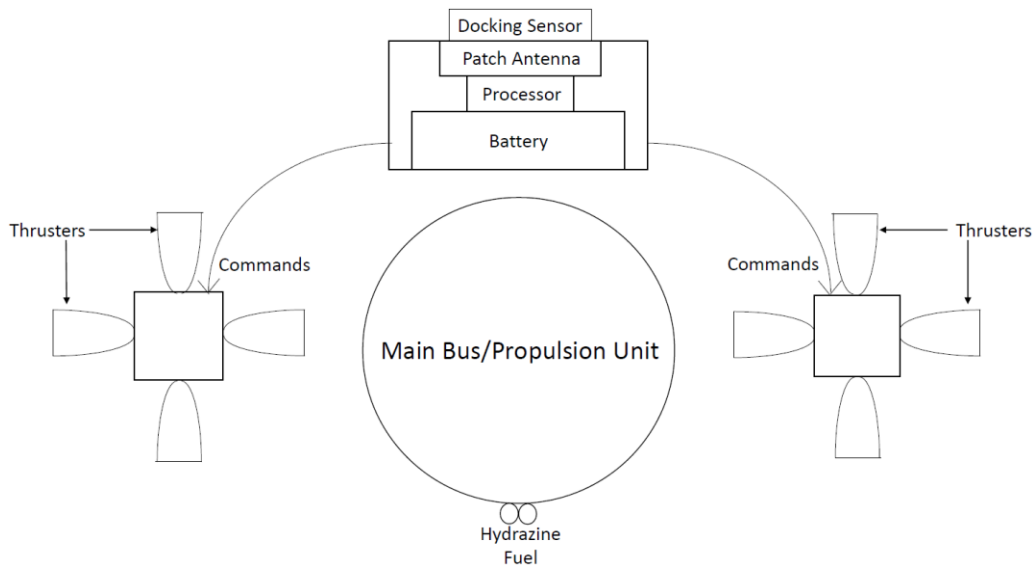


**Figure 8.3. Assembly Maneuvering System.**

The main feature of this system is the dual quad-blocks of thrusters. These allow for full three-axis control of each unit as well as provide the ability to the necessary  $\Delta V$  for rendezvous procedures. Both of these quad blocks will be reused for the fully assembled RCS system on Hermes to allow for maximum reuse of system components. Because these thrusters will be re-used in the main RCS system, the main RCS system hydrazine fuel tanks will be used as well. The ~12 kg of hydrazine fuel that is necessary for assembly procedures for each module will be launched in these tanks as well.

The other component of the maneuvering system is the control block. This block will be placed at the top of each module and will have the ability to send and receive control commands. A Microstrip patch antenna as selected in Section 9.3.2 will be used for ground and ISS communication and a DragonEye flash LIDAR camera will be used to provide range information for the individuals controlling the approach of these modules. Table 8.13 details the selection of this sensor. The main criterion was the small resolution with the mass differentiating it from the GoldenEye sensor.

**Table 8.13. Commercially Available Docking Sensors [75-78].**

Name	Mass [kg]	Maximum Range [km]	Resolution [m]
ELRF-3	1.23	30	2
LRF	0.91	20	2
GoldenEye	4	3	0.1
DragonEye	<3	1.5	0.1

## 8.5. Navigation

Since the primary purpose of Hermes is to act as an orbital transfer vehicle, knowledge of its position in space at all times is a necessity. Small errors in position estimation may result in mistimed thruster firings, incorrect orbit insertions, or even total mission failure. For these reasons, advanced techniques to determine the vehicle's precise position will be implemented.

One primary form of position determination that Hermes employs is high accuracy star trackers. Star trackers are capable of position determination by recording multiple successive images of the same group of stars. "Two different sightings are enough to establish the spacecraft's position in space or to align the IMU stable member, but a third or more additional fixes are used for confirmation and greater accuracy" [44]. Since the highest accuracy star sensor available has been selected, the system will provide accurate spacecraft position determination.

In addition to star trackers, the IMUs on-board will be crucial for navigational purposes. The accelerations that the units measure will serve several purposes. The data will be used to precisely time and measure thruster firings and their measurements will also be fed back into the flight computer's orbit propagator to accurately model the satellite's position and velocity. The orbit propagator utilizes well-known orbital mechanics to calculate the predicted position and velocity of Hermes.

One final form of navigation is used: the Deep Space Network described in Section 9.2.2 will provide ranging information to Hermes' communication system. This is a common use of ground station communication that Hermes

uses to verify and update all estimates of its position. All of these redundant forms of space navigation provide an accurate and reliable navigation system for Hermes.

## 9. Communications

### 9.1. Design Approach

The primary functions of the communications system for Hermes are to perform Telemetry, Tracking and Command (TT&C) and downlinking health data for the purpose of system calibration. Throughout the mission, communicating at the Lagrange points is the most challenging task due to the large free space losses experienced by the signal. For this reason, the communications system is designed around this requirement.

To meet these system requirements, it is necessary to select a ground station to communicate with, and to determine appropriate antenna and other communication technology to be placed on-board the spacecraft. Another component of the communications system is the selection of a frequency band over which communication signals are sent. These various choices are based around a link budget analysis.

### 9.2. Ground Station

#### 9.2.1. Trade Study Significance

To communicate between Earth and Hermes, a ground station on Earth is needed. Due to the large distances being traversed, the antennas at these stations will need to be large and powerful. As such, using existing ground stations, rather than constructing one, is more economically feasible. Several link analyses have been performed involving both the Deep Space Network (DSN) and the Near Earth Network (NEN).

#### 9.2.2. Trade Study Findings

A link budget consists of trading several different inputs including data rate, satellite antenna size/gain, and satellite transmit power in order to create a usable link on both uplink and downlink. An initial assessment of required data rates is performed in Table 9.1. This table shows that the absolute minimum data rate that should be available for

downlink should be 200 kilobits per second (kbps). All attempts to maximize the possible data rate will be made in order to decrease the required frequency of downlinks.

Specifications on the available ground station data links are given in the *Space Mission Engineering: The New SMAD* [10]. Table 9.2 shows the link budget for the main high-gain antenna that is required to communicate from EML1. Tradable items

(i.e. adjustable parameters) were marked with shaded cells and unnecessary items were blacked out. All available links from both the DSN and NEN have been analyzed with links in both the S-band and X-band. Data rates have been maximized and satellite transmit power was minimized while taking into consideration ground station limitations such as maximum data rates supported and maximum receive power allowed. Link margins were kept low, but positive, to avoid over-engineering the system while still maintaining a good link.

In addition to a high-gain antenna, several low-gain antennas must be included to communicate when the high-gain antenna cannot be pointed at Earth with at the EML. This emergency mode form of communication can allow the vehicle recover from unforeseen attitude control loss situations. These low-gain antennas may also be used to communicate in LEO. Table 9.3 shows several link budgets for use of low-gain antennas. All tradable items are in shaded cells.

**Table 9.1. Estimated Data Rates Required [45].**

Source	Data Rate (bps)
Telemetry	100,000
Communications	50,000
Health Data	50,000
<b>Total:</b>	200,000

**Table 9.2. High-gain Antenna Link Budget [10].**

		DSN ELM1 (S-band)		DSN EML1 (X-band)		NEN EML1 (S-band)		NEN EML1 (X-band)
Link Cases	Units	Uplink	Downlink	Uplink	Downlink	Uplink	Downlink	Downlink (Uplink not supported)
<b>Transmit Frequency</b>	GHz	2.025	2.2	7.145	8.4	2.1	2.25	8.025
<b>Data Rate</b>	Mbps	5	5	5	125	5	15	150
<b>Transmit Diameter</b>	m	34	1.2	34	1.2	11.3	2.2	2.2
<b>Transmit Beamwidth</b>	deg	0.3050108	7.9545454	0.0864446	2.0833333	0.8849557	4.2424242	1.1894647
<b>Transmit Efficiency</b>	%		0.7		0.7		0.7	0.7
<b>Transmit Gain</b>	dB		27.28305		38.920191		32.74308	43.788334
<b>Transmit Power</b>	W		3		3		125	125
<b>Backoff + Line Loss</b>	dB		-5		-5		-5	-5
<b>Transmit EIRP</b>	dBW	78.7	27.05427	89.5	38.691403	66	48.71218	59.757434
<b>Propagation Range</b>	km	320009	320009	320009	320009	320009	320009	320009
<b>Space Loss</b>	dB	-208.68174	-209.4016	-219.63328	-221.03882	-208.99762	-209.5968	-220.64214
<b>Atmospheric losses</b>	dB	-5	-5	-5	-5	-5	-5	-5
<b>Receive Diameter</b>	m	1.2	34	1.2	34	2.2	11.3	11.3
<b>Receive Beamwidth</b>	deg	7.9545454	0.280748	2.0833333	0.0735294	4.5454545	0.8259587	0.2315772
<b>Receive Efficiency</b>	%	0.7		0.7		0.7		
<b>Receive Gain</b>	dB	26.563105		37.514649		32.143819		
<b>Backoff and Line Loss</b>	dB	-2	-2	-2	-2	-2	-2	-2
<b>System Noise Temp</b>	dB-K	27		27		27		
<b>Receiver G/T</b>	dB/K	-0.4368941	40.5	10.514649	53.9	5.1438199	23	35
<b>Receiver C/No</b>	dB-Hz	91.181361	79.752574	101.98136	93.152574	83.746190	83.715290	95.715290
<b>Eb/No</b>	dB	2.42E+01	1.28E+01	3.50E+01	1.22E+01	16.75649012	1.20E+01	1.40E+01
<b>BER</b>	-	0.00001	0.0001	0.00001	0.0001	0.00001	0.0001	0.0001
<b>Required Eb/No</b>	dB	9.6	7	9.6	7	9.6	7	7
<b>Implementation Loss</b>	dB	-2	-2	-2	-2	-2	-2	-2
<b>Link Margin</b>	dB	12.59	3.76	23.39	3.18	5.16	2.95	4.95

**Table 9.3. Low-gain Antenna Link Budget at EML1 and LEO [10].**

Link Cases	Units	DSN EML1 (X-Band)		NEN EML1 (S-band)		NEN LEO (S-band)	
		Uplink	Downlink	Uplink	Downlink	Uplink	Downlink
Transmit Frequency	GHz	7.145	8.4	2.1	2.25	2.1	2.25
Data Rate	Mbps	0.2	0.2	0.2	0.2	5	5
Transmit Diameter	m	34		11.3		11.3	
Transmit Beamwidth	deg	0.086444655		0.884955752		0.884955752	
Transmit Efficiency	%						
Transmit Gain	dB		6		16		6
Transmit Power	W		10		80		2
Backoff + Line Loss	dB		-5		-5		-5
Transmit EIRP	dBW	89.5	11	66	30.03089987	66	4.010299957
Propagation Range	km	320009	320009	320009	320009	2500	2500
Space Loss	dB	-219.6332885	-221.0388296	-208.9976297	-209.5968942	-166.8531861	-167.4524505
Atmospheric losses	dB	-5	-5	-5	-5	-5	-5
Receive Diameter	m		34		11.3		11.3
Receive Beamwidth	deg		0.073529412		0.825958702		0.825958702
Receive Efficiency	%						
Receive Gain	dB	6		16		6	
Backoff and Line Loss	dB	-2	-2	-2	-2	-2	-2
System Noise Temp	dB-K	27		27		27	
Receiver G/T	dB/K	-21	53.9	-11	23	-21	23
Receiver C/No	dB-Hz	70.46671148	65.46117043	67.60237025	65.03400565	99.74681393	81.15784942
Eb/No	dB	1.75E+01	1.25E+01	1.46E+01	1.20E+01	3.28E+01	1.42E+01
BER	-	0.00001	0.0001	0.00001	0.0001	0.00001	0.0001
Required Eb/No	dB	9.6	7	9.6	7	9.6	7
Implementation Loss	dB	-2	-2	-2	-2	-2	-2
Link Margin	dB	5.86	3.45	2.99	3.02	21.16	5.17

In addition to technical feasibility, the cost of utilizing these ground stations must also be considered.

Table 9.4 lists these costs, as well as the total time required to downlink a week's worth of telemetry, communications, and health data. The Deep Space Network X-band connection was chosen for communication from the Lagrange points because it has a much shorter link time than the DSN S-band connection and requires significantly less transmit power than either of the NEN links. Because generation of power onboard our craft will be via a solar array (Section 10.2.2), decreasing the required power will assist other systems. This connection accomplishes all of this while maintaining a comparable weekly cost to using the NEN.

**Table 9.4. Cost of Using Ground Station Connections [46].**

Ground Station Link	Downlink Data Rate (Mbps)	Link Time Per Week (hours)	Cost Per Week (\$FY2015)
<b>DSN (S-band)</b>	5.0	6.72	\$6528
<b>DSN (X-band)</b>	125.0	0.268	\$1073
<b>NEN (S-band)</b>	15.0	2.24	\$1882
<b>NEN(X-band)</b>	150.0	0.224	\$252

One concern that exists with using the DSN is that obtaining time on the antennas can be very difficult due to the large number of satellites that must communicate with the small number of antennas available. However, because of the very low downlink time required (~15 minutes per week), this will not pose a problem to Hermes [47], and viable backup options exist if arrangements cannot be made for DSN X-band.

For communication in the LEO period of the orbit, the NEN S-band connection will be utilized because the DSN is not designed to communicate with LEO satellites. The NEN's X-band connection will not be used because uplink is not supported. Additionally, while in LEO the high-gain antenna will not be utilized because it is unnecessarily powerful and difficult to point. For these reasons, the low-gain, broad-beam antennas will be used in this phase of the mission.

## 9.3. Antenna Selection

### 9.3.1. Trade Study Significance

To communicate with Earth, Hermes must have a selection of antennas on board. Selection of these antennas must meet the performance requirements specified in Table 9.2 and Table 9.3 along with minimizing system mass and power requirements.

### 9.3.2. Trade Study Findings

Table 9.2 shows that the gain of the high-gain antenna needs to be near 38.9 dBic and the gain of the low-gain antenna needs to be 6 dBi. Table 9.5 provides descriptions of several types of antennas that will be compared with these required gains and performance features.

**Table 9.5. Various Antenna Types [10].**

Antenna Type	High-gain Parabolic Reflector	Phased Array	Medium Gain (Horn)	Low-gain (Broad-beam)
Typical Max Gain [dBic]	15 - 65	5 - 20	5 - 20	0 - 6
Half-Power Beamwidth [deg]	0.5 - 5	N/A	10 - 90	90 - 180
Mass [kg]	10 - 30	20 - 40	1 - 2	0.1 - 1
Features	Mechanical Steering Lightweight High EIRP	Flat packing Multiple Beams High EIRP	Low-gain applications with broad coverage areas	Normal LEO communication Emergency Mode coverage

For the high-gain antenna, Hermes utilizes a high-gain parabolic reflector because this is the only antenna type capable of achieving high enough gains and producing the necessary Equivalent Isotropic Radiated Power (EIRP), a measure of the useful transmitted power. However, the 6 dB low-gain antenna requirement falls into several antenna categories. Hermes also uses four low-gain, broad-beam antennas for this low-gain purpose because their mass is significantly less than their counterparts and the half-power beamwidth is also significantly larger. Two antennas will be for X-band emergency communication at EML1 while the other two are for S-band communication in LEO.

Table 9.6 provides a summary of several commercially available low-gain antennas that Hermes could use. Of these, the Microstrip Patch antenna was selected because of its ability to come in both S and X band varieties as well as its comparable transmit power, half power beamwidth and maximum gain.

Table 9.6. Commercially Available Low-gain Antennas [83-85].					
Name	Mass [kg]	Frequency Band	Max Transmit Power [W]	Half Power Beamwidth [deg]	Max Gain [dB]
S-Band Patch Antenna	0.08	S	10	35	6
Cubesat S-Band Patch Antenna	0.08	S	2	30	8
Microstrip Patch Antenna	0.12	S or X	10	35	6

These patch antennas, along with the main 1.5 meter high-gain parabolic reflector, are placed at the end of a coilable boom that is attached to the main bus of the spacecraft as shown in Figure 9.1. These antennas are placed here because this minimizes the risk that it will be shadowed by the payloads with unknown geometries that Hermes will be ferrying. This antenna is gimbaled so the pointing requirements for Hermes can be reduced and a more accurate connection can be maintained. Finally, this boom will be structurally supported at the end by mounting the antenna end to the top of one of the external fuel tanks. This allows the boom to support its own weight during thrusting maneuvers and the resulting accelerations. Otherwise the coilable boom would have to extend and contract multiple time per mission which introduces unnecessary risk.

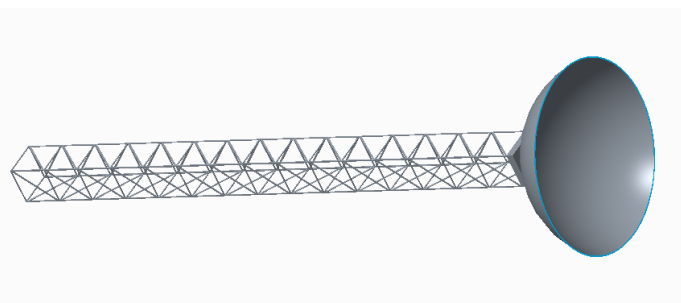


**Figure 9.1. Antenna Placement On a Coilable Boom with Gimbal Mount.**

A final component that must be selected for the communications subsystem is the transponder that will generate the communications signals. The SDST transponder has been selected for X band

communication because of its high transmit power with relatively low power consumed. The CXS-610 transponder has been selected for S-band communication because of its slightly lower consumed power.

**Table 9.7. Commercially Available Transponders [86-88].**

Name	Mass [kg]	Frequency Band	Transmit Power [W]	Power Consumed [W]
SDST	3.2	X	<20	15.8
X <sup>2</sup> PND	3.1	X	<6	38
X-Band	4.0	X	<6	30
S/S DST	3.0	S	<11	120
<b>CXS-610</b>	<b>2.6</b>	<b>S</b>	<b>&gt;5</b>	<b>30</b>
MSX-765	2.6	S	>5	35

## 9.4. Other Design Considerations

All previous analysis has been for communication from EML1, however, missions to EML2 may also be performed. Waypoint has generated several feasible solutions to this problem. One such solution would be the insertion of Hermes into a halo orbit that is at least 960 km radius which ensures that Hermes would be able to glimpse a limb of the Earth's surface at the far reaches of its orbit. Another possibility would be to place an additional satellite in orbit around the moon that could act as a relay between Hermes and Earth. These communication methods broaden the type and number of missions that Hermes can perform and make for a more flexible spacecraft.

# 10. Power and Thermal Systems

## 10.1. Subsystem Requirements

Hermes has a mission profile with three specific modes of operation: low earth orbit (LEO), engine burn, and Lagrange points. Additionally, emergency procedures in case of engine failure must be considered. These four different cases can be seen in the following power budget:

Table 10.1 shows the variation in requirements across the operational modes. The power generation and storage system must be robust enough to account for the differences across the different modes, while still minimizing weight and size. In particular, 650 Watts are required constantly while in Low Earth Orbit

(LEO), and 1720 Watts must be provided over a period of five hours. These two requirements apply to the most power intensive operational modes for long and short periods of time, respectively.

**Table 10.1. Operational Power Budget [48].**

<b>Duration</b>	# of Units	Low Earth Orbit		During Burn		Transfer/EML1 /2		Emergency Fuel Pump	
		~5 months		8 minutes		42 days		5 hours	
<b>Component</b>	Peak Power (W)	Avg Power (W)	Peak Power (W)	Avg Power (W)	Peak Power (W)	Avg Power (W)	Peak Power (W)	Avg Power (W)	
S-Band Transponder	2	2	0	2	0	0	0	2	0
X-band Transponder	1	0	0	3	1	3	1	3	1
<b>Communication Total:</b>		<b>4</b>	<b>0</b>	<b>7</b>	<b>1</b>	<b>3</b>	<b>1</b>	<b>7</b>	<b>1</b>
Control Computers	3	20	20	20	20	20	20	20	20
RC Thrusters	4	35	1	35	1	35	1	35	1
Star Sensor	2	9	8	9	8	9	8	9	8
IMU	2	22	22	22	22	22	22	22	22
Magnetometer	1	1	1	1	1	1	1	1	1
<b>ADCS Total:</b>		<b>270</b>	<b>130</b>	<b>270</b>	<b>130</b>	<b>270</b>	<b>130</b>	<b>270</b>	<b>130</b>
Thruster Gimballing	3	0	0	300	300	0	0	0	0
Ignition	5	0	0	180	0	0	0	0	0
Fuel Pumps	1	0	0	0	0	0	0	1000	1000
<b>Propulsion Total:</b>		<b>0</b>	<b>0</b>	<b>1800</b>	<b>900</b>	<b>0</b>	<b>0</b>	<b>1000</b>	<b>1000</b>
Orion Docking Heating	1	400	280	400	280	400	230	400	230
Patch Heaters	1	210	142.5	210	142.5	150	100	150	100
<b>Thermal Regulation Total:</b>		<b>610</b>	<b>422.5</b>	<b>610</b>	<b>422.5</b>	<b>550</b>	<b>330</b>	<b>450</b>	<b>330</b>
PPT with Boost Converter	1	0.94	0.94	1	1	0.94	0.94	0.94	0.94
Buck Converter	1	0.94	0.94	0.94	0.94	0.94	0.94	0.94	0.94
Batteries	1	0.96	0.96	0.96	0.96	0.96	0.96	0.96	0.96
<b>Regulation Efficiency :</b>		<b>0.85</b>	<b>0.85</b>	<b>0.90</b>	<b>0.90</b>	<b>0.85</b>	<b>0.85</b>	<b>0.85</b>	<b>0.85</b>
<b>Total:</b>		<b>1040</b>	<b>650</b>	<b>2980</b>	<b>1610</b>	<b>970</b>	<b>540</b>	<b>2150</b>	<b>1720</b>

## 10.2. Power Generation Selection and Sizing

When choosing a power generation system, a critical factor is longevity. It is imperative that power is generated consistently throughout the entire mission lifetime. Reliability is a necessity, because the safe return of astronauts during manned missions is of paramount importance.

### 10.2.1. Power Source Trade Study

A trade study comparing different methods of power generation was conducted, with the results shown in Table 10.2.

Table 10.2. Power Generation Trade Study [49].				
Alternatives	Specific Power [W/kg]	Specific Cost [\$USD/W]	Long Term Sustainability	Safety and Reliability
<b>Solar PV</b>	25 - 200	800 - 3000	Unlimited energy source	Industry standard
<b>Solar Thermal Dynamic</b>	9 - 15	1000 - 2000	Unlimited energy source	Low risk, not widely used
<b>Radioisotope Thermoelectric</b>	5 - 20	16k - 200k	Low availability, difficult to refuel	Medium risk, used for deep space satellites
<b>Nuclear Reactor</b>	2 - 40	400k - 700k	Low availability, difficult to refuel	Bad reputation, history of failure
<b>Fuel Cells</b>	275	50k - 100k	Refueling required	Low risk, not widely used

Long term sustainability and specific power are the most important factors when selecting power generation. Sustainability ensures that the OTV is self-sufficient, while specific power limits mass which in turn reduces cost. Both solar photovoltaic (PV) and solar thermal dynamic offer an unlimited energy source in the form of sunlight, but ultimately solar PV was chosen for its high specific power and proven reliability [49].

NeXt Triple Junction Solar Cells were then chosen; they characteristically achieve 29.5% efficiency at the beginning of life and 25% efficiency at the end of life. With more than 820 kW of cells in orbit, the NeXt cells also offer considerable reliability to the mission [50].

### 10.2.2. Photovoltaic Array Sizing

With PV solar selected as the power generation source, the solar array must be properly sized to accommodate all of the spacecraft's power needs. Power generation is sized for the largest consistent load: 650 W required while orbiting in LEO. Throughout the orbital trajectory, the Earth will shade the spacecraft for approximately 36 minutes out of the 92 minute orbit. To account for this, Equation (10.1) is used to calculate the additional power generation needed to sustain the OTV during eclipse.

$$Power_{Total} = \frac{t_{orbit} Power_{Req}}{t_{daylight} \cos(20^\circ)} \quad (10.1)$$

In Equation (10.1),  $t_{orbit}$  is the total time in orbit,  $t_{daylight}$  is the time spent in the sun,  $Power_{Req}$  is the power for the OTV, and  $\cos(20^\circ)$  gives a 20 degree margin of angular error for the solar panels. This results in a required power output of 1150 W. With a safety margin of 1.5, the solar panels must be rated to provide 1700 W of power at the end of life. Equation (10.2) is used to calculate solar panel area required to generate this much power.

$$A = \frac{Power_{Total}}{S_c \eta_{EOL}} \quad (10.2)$$

In Equation (10.2),  $S_c$  is the solar constant,  $\eta_{EOL}$  is the end of life efficiency, and  $Power_{Total}$  is the power that the solar panels must generate. The result is solar cells must cover about 5 m<sup>2</sup> to supply 1.7 kW EOL power. The solar array chosen for Hermes was the ATK Ultraflex solar array; with the Ultraflex 5 m<sup>2</sup> of solar cell coverage corresponds to two circular arrays of diameter 1.9 meters [51]. The Ultraflex system offers many built in mechanical advantages, such as the fully gimbaled system and an unfolding deployment mechanism [51].

## 10.3. Battery Selection and Sizing

### 10.3.1. Battery Selection

Because solar PV cannot provide full power in eclipse, burn, or emergencies, batteries must be included to provide constant power to Hermes. There are three different types of batteries typically used for spacecraft: Nickel-Cadmium, Nickel-Hydrogen, and Lithium-Ion. Lithium-Ion offers the highest efficiencies

and energy densities per kg, the average values of which are seen in Table 10.3 [49]. For these reasons Lithium-Ion batteries were chosen as the backup power source.

**Table 10.3. Battery Selection Trade Study [49].**

Alternatives	Energy Density [W-h/kg]	Energy Efficiency	Temperature Range
Ni-Cd	30	72%	0 to 40 °C
Ni-H <sub>2</sub>	60	70%	-20 to 30 °C
<b>Li-Ion</b>	<b>105</b>	<b>98%</b>	<b>10 to 35 °C</b>

### 10.3.2. Battery Sizing

The limiting factor for battery sizing is the excess power required in case of emergency: 1720 W over a period of five hours. With power generation conservatively rated at 1150 W, 570 W must be provided during the five hour time period while fuel is pumped between tanks. This corresponds to 2850 W-h distributed over three batteries with a 90% depth of discharge (DOD), or 950 W-h per battery. Using Saft VES 16 batteries with five parallel rows of 15 cells in series provides battery packs with 22.5 A-h, 54 V, and 1200 W-h [52].

The architecture for the main bus includes three primary batteries as well as two equivalent redundant batteries. Therefore, during normal operation all five batteries will have a lower

DOD than a three battery system.

Should two fail the spacecraft can still operate as normal, albeit inefficiently. The characteristics of these batteries are displayed in Table 10.4.

Additionally, battery

**Table 10.4. Battery Characteristics [52].**

Characteristic	Value
<b>Battery Type</b>	Saft VES 16 Li-Ion battery
<b>Individual Capacity (W-h)</b>	1200
<b>Individual Weight (kg)</b>	11.6
<b>Individual Size (mm x mm x mm)</b>	495x165x60
<b>Number of non-redundant batteries</b>	3
<b>Number of redundant batteries</b>	2
<b>Non redundant Capacity (W-h)</b>	3600
<b>Total Weight (kg)</b>	58

specifications for all requisite modes of operation are listed in Table 10.5. The required energy for each mode is given, and using the battery configuration listed above, the DOD for three and five batteries is shown. The low DOD for normal operations aids longevity of the battery; for emergency situations the focus is ensuring human safety, and a high DOD is acceptable. Notice that all operations are satisfied using three batteries, but with five batteries a lower DOD and increased redundancy against failure offer a superior system.

**Table 10.5. Operational Mode Depth of Discharge.**

	<b>Low Earth Orbit</b>	<b>Burn</b>	<b>Transfer/EML</b>	<b>Emergency</b>
<b>Required Energy [W-h]</b>	390	268	0	2850
<b>3 Battery DOD</b>	10.8%	7.4%	0%	79.2%
<b>5 Battery DOD</b>	6.5%	4.47%	0%	47.5%

## 10.4. Power Distribution and Regulation

Hermes' main bus is configured using a standard Peak Power Tracking (PPT) architecture. The PPT consists of an integrated boost converter with a modulated duty ratio; changing this switching ratio adjusts the voltage of the solar panels to generate maximum power. The solar panel voltage of 30 – 50 V will be boosted to 54 V, the operational voltage of the batteries. However, should a boost converter fail, current will still be passed through at a lower efficiency.

The two solar panels charge five batteries, each with an associated buck converter. The buck converter drops voltage from 54 V to the bus voltage of 28 V while also shunting excess power to charge the batteries. Before reaching the loads, power is routed through the Power Distribution Unit (PDU), which contains the switches and fuses to protect the power system from equipment faults [48]. This architecture can be seen in Figure 10.1.

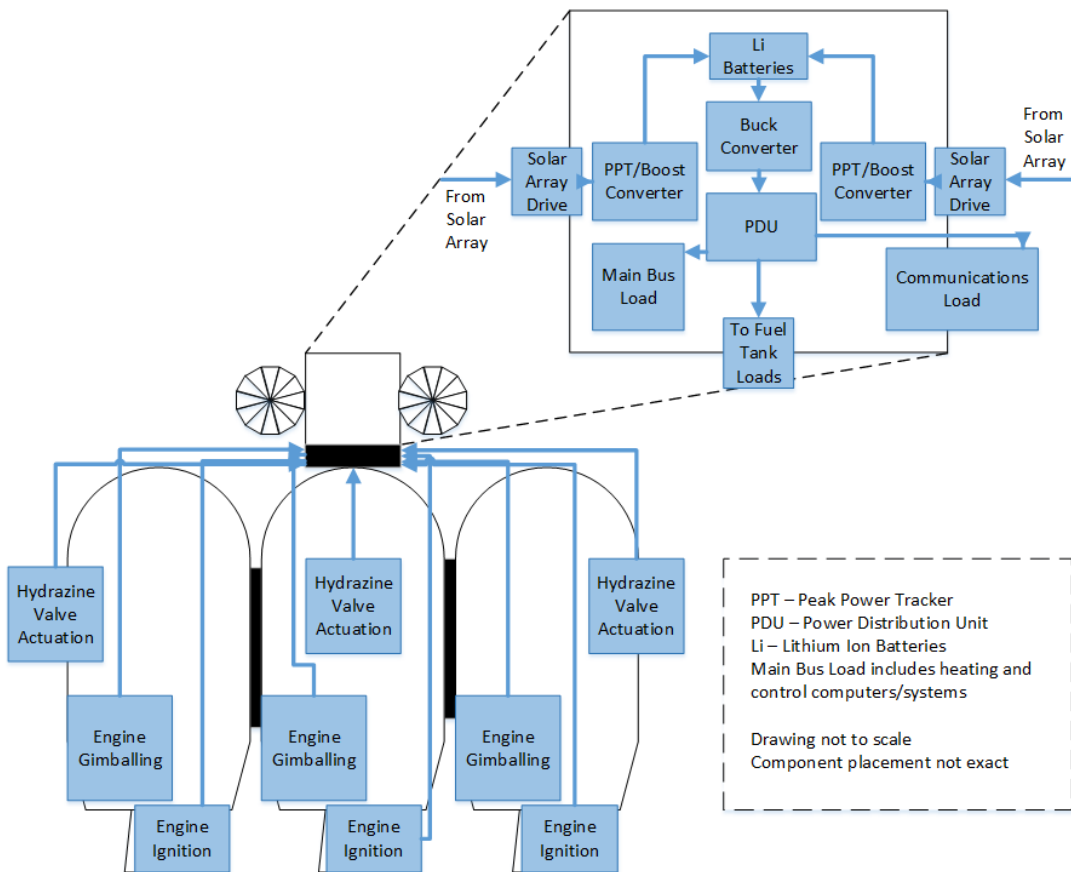


**Figure 10.1. Electrical Power System Architecture.**

## 10.5. Main Bus Design and Thermal Analysis

### 10.5.1. Main Bus Design

To prevent heat from the main bus radiating to the fuel tanks, regulation and load components are placed close to the top of the bus. This placement can be seen in Figure 10.2, looking from the bottom of the bus up to the top.

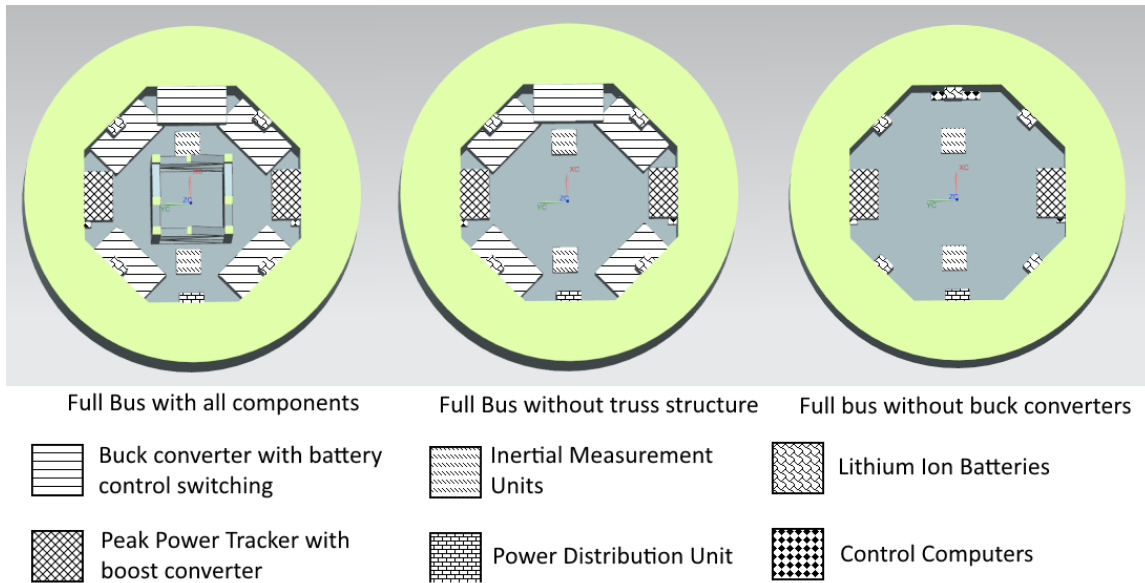


**Figure 10.2. Component Placement Within the Main Bus.**

Components are spaced radially around the center of the bus to ensure even heating, and a central truss is included to add structural integrity. The side with the PDU contains fewer heat generating components to offset one-sided heating during transfer.

### 10.5.2. Main Bus Thermal Analysis

Hermes' mission profile includes two distinct long term modes of operation: an average of five months in LEO and a 42 day round trip mission to EML1/2. While in LEO, orbital heating occurs much like any other satellite. An NX simulation was used to model the solar flux and albedo from the Earth incident on the spacecraft, with internal components generating heat based on the expected loads or inefficiencies. A list of these generated heats can be seen in Table 10.6.

Using the values in Table 10.6, each component in the main bus is defined by its contact points with the walls of the bus and generates heat distributed around the body. Thermal conductivity across the whipple

**Table 10.6. Heat Generated by Electrical Components.**

Component	Heat (W)
Peak Power Tracker/Boost converter	22
Control Computers	20
Buck Converter/Battery Control	5
Lithium Ion Batteries	5
Inertial Measurement Units	22

shield is modeled with a value estimated from experiments conducted by 3M, the supplier of Nextel material

[53]. Heat conductivity through the top and bottom of the bus is limited by the honeycomb structure, modeled with the same thermal properties as low-pressure air.

To control internal temperature, patch heaters are applied to individual components. Exterior coatings are chosen to attain desirable temperatures for the warmest case, and active heating is added to compensate for the coldest case. For Hermes, time spent at transfer and the EML are the warmest case. During this period, the spacecraft is continuously oriented with one side facing the sun to maximize solar array effectiveness. Because of this constant heat flux, the interior of the bus is heated significantly on one side while the other is cooled. Active heating applied to one side can mitigate this difference and provide even heating around the bus.

To simulate transfer in NX, 1350 W/m<sup>2</sup> of heat flux was applied to one side of the bus. Using an iterative approach changing absorptivity, emissivity, and active heating on the cold side of the bus, a desirable steady state solution was produced. The results of the simulation can be seen in Figure 10.3.

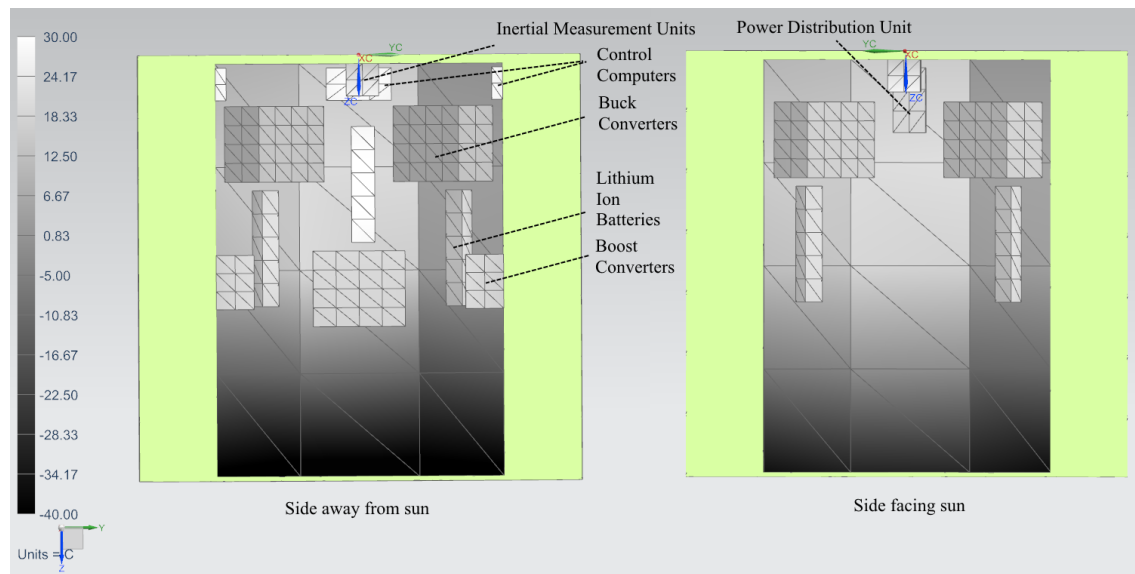


**Figure 10.3. Thermal Simulation Map During Transfer.**

The IMUs and two computers reached peak temperatures of 27° C and the five batteries sit at about 17-22° C, all of which are within the appropriate operating temperatures. The allowable temperature range for the docking interface in LEO is -39 to 50 °C [54], and although it is not shown the docking block sits at around 0 °C. Finally, the buck/boost controllers don't require warm operational temperatures, and 8-15 °C is appropriate.

The other mode in the mission profile is the waiting period in LEO. In order to simulate this environment, the same absorptivity and emissivity of 0.35 and 0.85 are used as above, representing the same coating applied throughout all stages of the mission. To accurately simulate the environment, a propellant tank is placed below the bus to block the Earth's albedo at all times. ADCS requirements are such that Hermes is gravity gradient stabilized. An iterative process is used once again to find a desirable steady state solution, which results in the thermal map of the bus components seen in Figure 10.4.

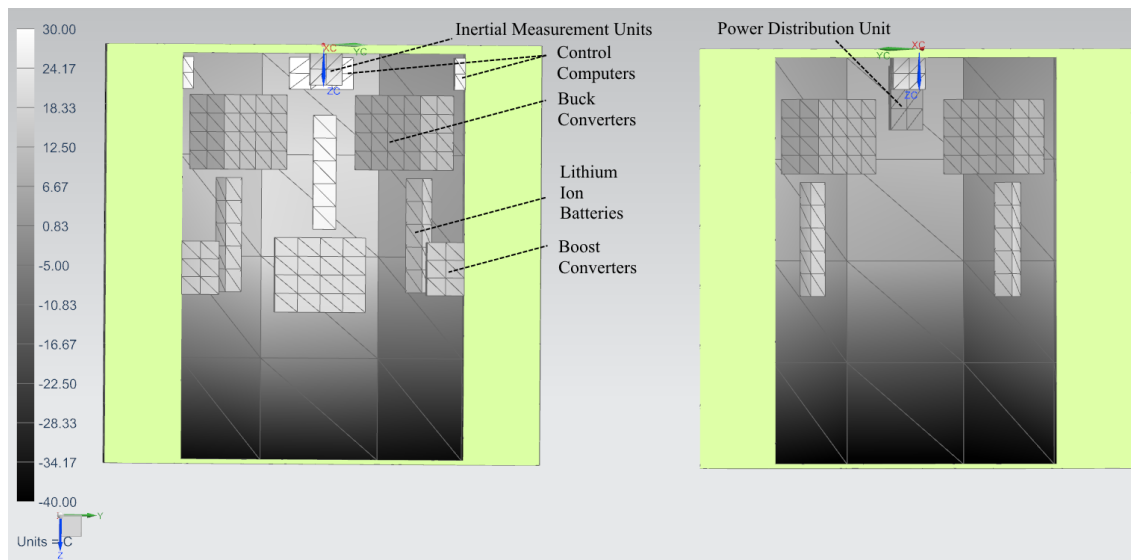


**Figure 10.4. Thermal Simulation Map in Low Earth Orbit.**

The batteries, IMUs, and computers all remained within the 15-30 °C range. Although the fuse box reached subzero temperatures, this is an acceptable operational temperature for simple components such as switches and fuses. All other components sit at 5-15 °C, and the docking system is heated to just above 0 °C; these temperatures are acceptable for these more robust components.

Table 10.7 displays a complete summary of all thermal characteristics for the main bus. White paint is applied to the outside of the bus to meet the design specifications for emissivity and absorptivity [49]. Patch heaters are applied to all necessary components with temperature gauges. The patch heater can be activated when a low temperature threshold is reached. The steady state of the system is expected to follow closely to the simulations, with 100 W of heating required during transfer and 142.5 W needed in LEO.

**Table 10.7. Summary of Main Bus Thermal Characteristics.**

Characteristic	Value
Outer Coating	White Paint
Transfer Active Heating	100 W
Transfer Docking Heating	130 W
Transfer Critical Component Temperature Range	17-27 C
LEO Active Heating	142.5 W
LEO Docking Heating	280 W
LEO Critical Component Temperature Range	15-28 C
LEO Critical Component Temperature Range	15-30 C

## 10.6. Fuel Tank Thermal Protection

### 10.6.1. Fuel Tank Requirements

Hermes' five Vinci engines use Liquid Hydrogen ( $\text{LH}_2$ ) and Liquid Oxygen (LOX) for propellant. The boiling point for  $\text{LH}_2$  at atmospheric pressure is 20.28 K while the boiling point for LOX is 90.19 °C [55]. Consequently, the internal temperatures of the propellant tanks must be below these values to enable Zero Boil Off (ZBO). However by building a 10% contingency into the propellant tank volume, Reduced Boil Off (RBO) could be an acceptable alternative.

### 10.6.2. Active vs. Passive Cooling

An active cooling system would require a cryo-cooler running a refrigeration cycle through the five propellant tanks. While this could effectively eliminate boil off, it adds significant power and weight to the system, on the order of kW and thousands of kilograms [56]. An alternative is using passive cooling techniques: advanced MLI blankets, Vapor Cooled Shields (VCS) filled with boiled off hydrogen gas, and ortho-para conversion of the hydrogen molecules [56]. Seen in Table 10.8 is a trade study comparing the merits of these two methods.

Table 10.8. Passive Insulation with Ortho-para Conversion vs. Active Cryo-cooling [49].					
Alternatives	Boiloff Reduction	Power Required	Mechanical Complexity	Size	Weight
Active Cryocooler	Complete	10 kW	Working fluid, valves, pumps	1 m <sup>3</sup> plus broad area shield	1700 kg
Advanced Passive Insulation	9 kg/day	0 kW	Route vented air through VCS	Broad area shield; routing apparatus	1200 kg

As seen in the trade study above, the reduced weight and power requirements make passive insulation a much more attractive choice. Although an active cryocooler would achieve minimal gains in boiloff reduction over passive insulation, Hermes' active mission lifetime is only 42 days, and boiloff during that time period is sufficiently small, as shown in the next section.

### 10.6.3. Passive Cooling Design

Passive cooling is a combination of techniques to minimize the amount of heat incident on the propellant tanks. The first technique is applying 8 mil Quartz Mirrors to the outside of the tanks. With an absorptivity of 0.05 and emissivity of 0.80, solar flux is minimized while radiation to the environment is maximized [49]. Layered beneath this coating is load bearing multilayered insulation (LBMLI) that supports a broad area vapor cooled shield (VCS), followed by additional layers of traditional multilayered insulation (MLI)

[57]. The VCS routes boiled off hydrogen through the shield as an additional thermal protection layer; the gaseous hydrogen absorbs heat before it is able to reach the LH<sub>2</sub>. Shown in Figure 10.5 is a layered diagram of a Hermes propellant tank, displaying the outside coating and three layers of insulation used to protect the fuel from insipient heat.

Additionally, the use of para-ortho conversion before launch will minimize the effect of heat which seeps through the insulation. Para-ortho conversion is the practice of changing the spin state of hydrogen to increase the enthalpy of vaporization from 450 kJ/kg to 700 kJ/kg [56]. The spin conversion is accomplished by subcooling the hydrogen and flipping the spin while manufacturing the fuel [58]. Using the process results in 50% more heat required to boil off a kilogram of propellant.

Using experimental values from tests conducted on the MLI/LBMLI combination, heat flux is estimated to be 0.50 W/m<sup>2</sup> [57]. This includes a safety factor of 2. Half the surface area of three tanks is

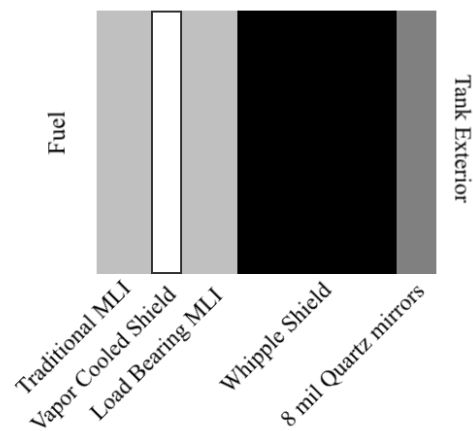


**Figure 10.5. Layer Diagram of the Hermes Fuel Tank.**

exposed to the sun while in transfer and at the Lagrange Points, caused by Hermes' side towards the sun orientation.

$$Boiloff = \frac{Q \left[ \frac{W}{m^2} \right] * PSA[m^2] * 86400 \left[ \frac{s}{day} \right]}{h_{vap} \left[ \frac{J}{kg} \right]} \quad (10.3)$$

In Equation (10.3),  $Q$  is incoming solar flux,  $PSA$  is the projected surface area, and  $h_{vap}$  is the enthalpy of vaporization. Using Equation (10.3), the boiloff because of incident heat was calculated to be 5.5 kg total per day, which is a total mission boil off of 0.2%. However it is also possible that boiloff will occur while fuel is being transferred through minimally insulated fuel lines. This line boiloff is given by:

$$Line\ Boiloff = \frac{Q \left[ \frac{W}{m} \right] * length[m] * 3600 \left[ \frac{s}{hour} \right]}{h_{vap} \left[ \frac{J}{kg} \right]} \quad (10.4)$$

where  $Q$  is incoming solar flux,  $length$  is the line length, and  $h_{vap}$  is the enthalpy of vaporization. To analyze this, an estimated length of 5 m for the propellant line is used. Heat is incident on insulated propellant lines at about five Btu/hr (1.47 Watts) per ten inches [56]. Using Equation (10.4), about 0.15 kg/hr of boiloff is expected during fuel transfer. Considering transfer times of less than an hour, this is a negligible amount. Overall, the amount of fuel that is expected to boil off during the mission is acceptably small.

## 11. Cost Analysis

The RFP does not state a specific budget for this project, however WayPoint aims to keep mission costs drastically lower than the Space Launch System (SLS). As mentioned in Section 1, to complete 10 missions as per the RFP, the total SLS cost would be approximately \$20 billion. The total mission cost for Hermes, including recurring and non-recurring factors, is \$3.28 billion. The process for calculating this value is detailed in the following sections. All costs are inflated to reflect fiscal year 2015 U.S. Dollars.

## 11.1. Non-Recurring Costs

Non-recurring costs account for aspects of the project that do not incur additional expenses as the mission goes on, or one-time costs. Included in this sector are expenses associated with: initial design and drafting at system level, software development, assembly at ISS, vehicle hardware, and test flight.

### 11.1.1. Development Costs

Development for both software elements and systems design must be taken into account. Software development costs are determined from Source Lines of Code (SLOC). SLOC requirements are driven by ADCS and Communications subsystems. Table 11.1 outlines how the software development cost is calculated. A total of \$9.58 Million and approximately 30 months are required for developing code for the mission.

In addition to software, the initial system design incurs development cost.

Drafting of engineering drawings and refining early conceptual design are important aspects of this phase. As mentioned in Section 2.2, five years are allotted for systems engineering development in the Research and Development (R&D) phase. 100 Full Time

Table 11.1. Software Development Cost [59].	
Total Number SLOC:	52,400
Cost per Man-Month:	\$25,000
Man-Months Required:	383
Total Development Time:	29.4 Months
<b>Total Cost to Develop Code:</b>	<b>\$9.58 Million</b>

Table 11.2. Engineering Development Cost [10].	
Number of Years Required for R&D:	5
Number of FTE Engineers Required per Year:	100
Cost of FTE per Year:	\$200,000
<b>Total Engineering Development Cost:</b>	<b>\$100 Million</b>

Equivalent (FTE) engineers are estimated to be required for the project during that duration. Table 11.2 summarizes the total engineering development cost. After combining both elements of development costs, the total R&D cost for the Hermes program is \$110 million.

### 11.1.2. Assembly Cost

Determining the cost of assembly at ISS requires extrapolation of available data. Figures for WayPoint's assembly cost are based off of STS125: the final Hubble Telescope repair mission in 2009. Below is a budget breakdown of that mission in Table 11.3:

**Table 11.3. STS125 Hubble Repair Mission Cost [101-102].**

Total Number of Spacewalk Hours:	35
Hours Spent Training on Earth per Spacewalk Hour:	7
Total Number of Mission Specific Training Hours:	231
Total Number of Mission Specific Training Work Days:	29
Mission Specific Training Cost (\$FY2015):	\$10 Million
Cost/Month of Mission Team (\$FY2015):	\$10 Million
2-Year Base Training for Astronauts in Months (\$FY2015):	24
Base Training Cost (\$FY2015):	\$240 Million
<b>Total Servicing Cost for Mission (\$FY2015):</b>	<b>\$250 Million</b>

The total servicing cost for that mission is estimated to be \$250 million in Fiscal Year 2015 U.S. Dollars, and with a comparable complexity to the Hermes project, WayPoint estimates the same figure for cost of OTV assembly at the ISS.

### 11.1.3. Theoretical First Unit Cost

The Theoretical First Unit (TFU) cost for Hermes is \$1.1 billion. To determine the TFU, a full bottom-up analysis was conducted to account for all subsystem components. Costs were determined through various techniques including requesting quotes from companies, researching similar technologies, and visiting company websites. The TFU cost is the basis for calculating the actual production costs, which are discussed in Sections 11.1.4 and 11.1.5 [10]. In this section, the TFU is broken down into vehicle launch costs and the hardware costs for the OTV.

#### 11.1.3.1. Launching the OTV Modules

For the OTV structure, a total of five launches are required. There are four launches for the outer propulsion modules and one launch for the central propulsion module and main bus assembly. Due to assembly process outlined in Section 3.3.1, the first four dry propulsion modules can launch on Falcon 9s, while the last fueled module must launch on a Falcon Heavy. Table 11.4 summarizes the cost to launch the vehicle.

**Table 11.4. OTV Launch Cost Breakdown.**

Dry Mass of Propulsion Module:	2,500 kg
Wet Mass of Propulsion Module:	17,888 kg
Mass of Main Bus and Components:	1,340 kg
Falcon 9 Payload to LEO:	13,500 kg
Falcon Heavy Payload to LEO:	53,000 kg
Number of Falcon 9/Heavy Launches:	4/1
Custom Fairing Cost:	\$500,000
Cost of Falcon 9/Heavy:	\$61.2/85 Million
<b>Total Launch Cost for Vehicle:</b>	<b>\$332 Million</b>

### 11.1.3.2. OTV Structure Cost

The cost of the OTV structure includes all hardware components that make up the vehicle. Table 11.6 breaks down the spacecraft cost into applicable subsystems.

**Table 11.5. OTV Hardware Cost Breakdown (TFU)  
(Detailed Costs in Table 11.14).**

Subsystem/Process	Cost	% of Total Vehicle Cost
ADCS/Communications Components:	\$6,884,460	4.1 %
Propulsion Components:	\$130,020,000	77.31 %
Power/Thermal Components:	\$2,533,498	1.51 %
Structural Components:	\$25,784,125	17.1 %
<b>Total Cost for Vehicle:</b>	<b>\$168,186,083</b>	

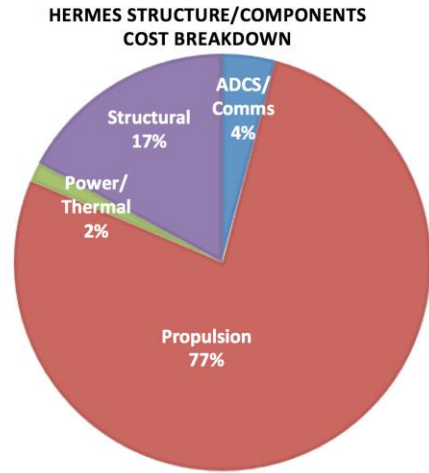

**Figure 11.1. Hermes Structure/Component Cost Breakdown.**

Figure 11.1 shows that the propulsion subsystem accounts for the majority of the hardware costs at 77%. This result is to be expected, as propulsion components are most critical for meeting all RFP requirements.

### 11.1.4. Learning Curve Discount

Once the TFU is calculated, a learning curve is applied to determine the actual production costs. The learning curve discount mathematically models the rise in production efficiency for parts that are

produced in large quantities. Equation (11.1) is the model that is used to determine true production costs after the discount.

$$\text{Production Cost} = \text{TFU} * N^{1 - \frac{\ln(\frac{1}{S})}{\ln(2)}} \quad (11.1)$$

$N$  is the number of units produced, and  $S$  the learning curve slope. Table 11.6 describes the relationship between  $N$  and  $S$  for the aerospace industry.

Due to Hermes being a singular vehicle,  $N$  is generally low for most parts. However, it is worth noting that if the market for OTVs were to expand, the learning curve discount would greatly help bring down production costs. The learning curve discount is applied in Table 11.14.

**Table 11.6. Learning Curve Relationship [10].**

<b><math>S</math></b>	<b><math>N</math></b>
95 %	< 10
90 %	10 - 50
85 %	> 50

### 11.1.5. Reserves

In determining production budgeting, higher-level cost factors need to be taken into account when trying to predict accurate estimates. Technology Readiness Level (TRL) and management reserves are accounted for. TRLs help determine the risk level of components and their ability to pass testing and substantiation [10]. Table 11.7 defines TRL reserves.

**Table 11.7. TRL Reserves [10].**

<b>TRL</b>	<b>Definition</b>	<b>Reserves</b>
9	Actual system “flight proven” through successful mission operations	5 %
8	Actual system completed and “flight qualified” through test and demonstration	10 %
7	System prototype demonstration in space environment	10 %
6	System/subsystem model or prototype demonstration in relevant environment	15 %
5	Component and/or breadboard validation in relevant environment	20 %
4	Component and/or breadboard validation in laboratory environment	20 %
3	Analytical & experimental critical function and/or characteristic proof-of-concept	25 %
2	Technology concept and/or application formulated	30 %
1	Basic principles observed and reported	40 %

Since many technologies onboard Hermes are chosen with a high TRL in mind, the total TRL reserves are kept low. The most significant TRL factor is the vapor cooled shield for each tank – its lower TRL level requires an added 20% TRL reserve cost.

In addition to reserves concerning technology, management reserves are enforced for higher-level uncertainty factors such as scheduling, vendor cost variability, and project complexity [10]. Table 11.8 quantifies management reserves:

<b>Table 11.8. Management Reserves [10].</b>	
<b>Development Status</b>	<b>Reserves</b>
Off the shelf; hardware exists; no mods required	10 %
Modifications required to existing hardware	15 %
New hardware but design passed CDR; vendor quotes	20 %
New hardware but design passed PDR	25 %
New design but within state of the art; cost estimate from Cost Estimating Relationships (CER); vendor Request of Materials (ROM)	35 %
New design; remote analogues; outside	50 %

Again, because many components were chosen with risk and availability in mind, most hardware is off the shelf and the overall vehicle has low management reserves. Application of both reserves can be observed in Table 11.14.

### 11.1.6. Test Flight

In order to make sure the vehicle operates properly, a full mission sequence test flight is performed. Once Hermes is assembled at the ISS, it will rendezvous with the Propellant Depot (PD) and make a full trip to EML1 and back with no payload. To account for the cost of this test flight, one full mission's worth of fuel must be budgeted as outlined in Table 11.9. While no payload is attached at this point, the OTV is still to carry enough fuel to bring a 50,000 lb payload to EML1. This measure is taken so that testing is undergone in an operational flight configuration.

To determine the test flight cost, the total propellant launch cost budget from Table 11.10 is averaged to find the cost to launch fuel per mission. This method is chosen to estimate the test flight cost since it is assumed that the PD can continuously house the fuel being sent up, and the LOX/LH<sub>2</sub> ratio of 7/1 mentioned in Section 11.2.1 is always true, meaning the two can be considered a single propellant entity. The single test flight cost comes out to be \$210 million.

**Table 11.9. Full Mission Test Budget.**

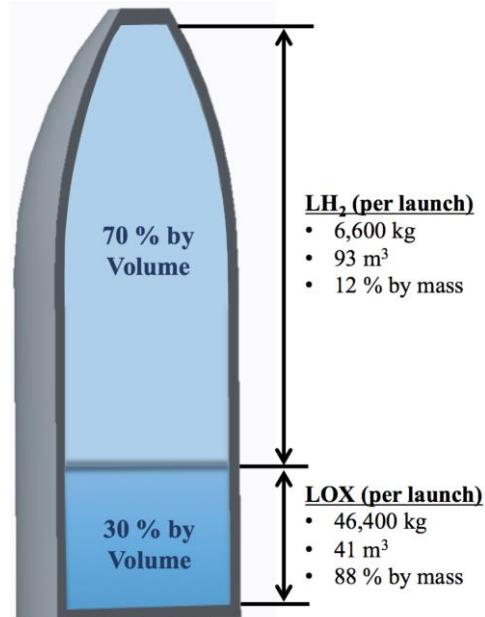
Total Mass of Propellant Required Over Lifetime:	1,342,000 kg
Total Cost to Launch Propellant Over Lifetime:	\$2.31 Billion
Total Number of Missions in Lifetime:	11 (Test + 10 Missions)
<b>One Test Flight Fuel Launch Cost:</b>	<b>\$210 Million</b>

## 11.2. Recurring Costs

Recurring costs account for flight operation, propellant, and the delivery of propellant to the Propellant Depot (PD). The majority of the recurring costs for this mission are from launching the fuel for the missions. It is crucial to understand that although the PD is available for use, WayPoint does not assume that fuel is provided at no cost. If it is indeed the case that the PD will provide unlimited fuel as part of the mission, then the costs outlined in Section 11.2.1 may be disregarded. To clearly differentiate the two costs, Table 11.11 compares the total lifetime mission cost accounting for fuel vs. assuming unlimited fuel at no cost.

### 11.2.1. Launching Fuel to the Propellant Depot

To determine the number of launches needed for the propellant, the mission fuel requirement is established by the Propulsion Subsystem in Section 7.2. For one EML1 round-trip mission, 127,000 kg of total propellant is necessary, with the mass ratio of LOX to LH<sub>2</sub> always being 7/1. Since LH<sub>2</sub> is a light fuel with low density and LOX is a dense fuel, a strategic packing scheme for the Falcon Heavy fairing is developed as shown in Figure 11.2. This arrangement takes full advantage of the launch vehicle as both the available payload mass and volume capabilities are fully occupied at 135 m<sup>3</sup> and 53,000 kg [60].


**Figure 11.2. Propellant Configuration for Falcon Heavy.**

However, since the total amount of fuel needed during Hermes' lifetime does not fit perfectly into the configuration shown, additional launches are required. The Falcon 9 variant can be used instead of the Heavy for these outstanding launches because only LH<sub>2</sub>, the less dense propellant, remains.

Figure 11.3 illustrates a schematic of the propellant launch operation.

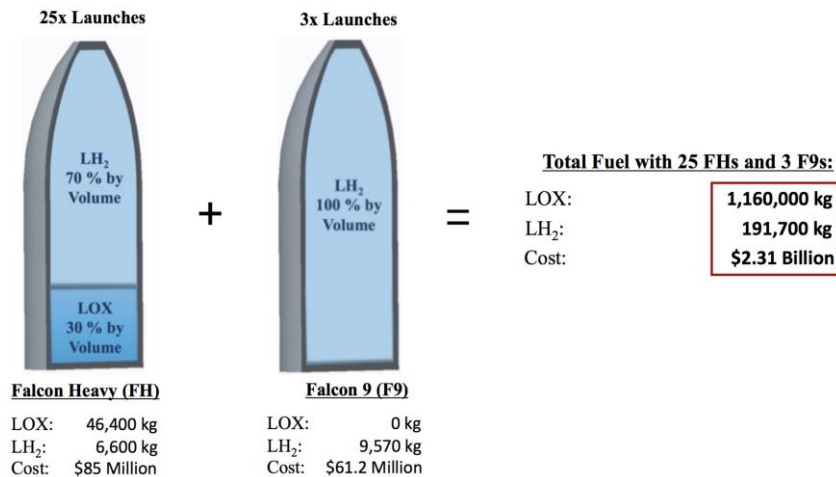


**Figure 11.3. Launching Fuel for Missions.**

As mentioned in Section 11.1.6, the total amount of fuel accounted for includes 10 missions with payload and one test flight. A breakdown of the above representation is shown in Table 11.10. As mentioned in Section 11.2, the \$2.1 billion figure is contingent upon the decision to include fuel launch costs into WayPoint's budget. Table 11.11 shows that the total Hermes lifetime cost without taking fuel costs into account to be only \$969 million.

**Table 11.10. Propellant Launch Cost Breakdown [60].**

Total Mass of LOX Required for 10 Missions and Test Flight:	1,150,300 kg
Total Mass of LH <sub>2</sub> Required for 10 Missions and Test Flight:	191,700 kg
Falcon Heavy/9 Fairing Volume:	135 m <sup>3</sup>
Falcon Heavy/9 Payload to LEO:	53,000 / 13,500 kg
Number of Falcon Heavy Launches for LOX and LH <sub>2</sub> :	25
Number of Falcon 9 Launches for LH <sub>2</sub> :	3
Cost of Falcon 9/Heavy:	\$61.2 / 85 Million
Total Lifetime Launch Cost for Fuel to Depot:	\$2.31 Billion
Cost of Launching Propellant per Mission:	\$210 Million
<b>Total Lifetime Propellant Launch Cost for 10 Missions:</b>	<b>\$2.1 Billion</b>

**Table 11.11. Case Comparison: PD Provides Fuel vs. WayPoint Provides Fuel.**

Case	<b>Total Lifetime Cost</b>
WayPoint takes into account the cost of fuel for all 10 missions:	\$3.28 Billion
Total Lifetime Launch Cost for All Fuel:	\$2.31 Billion
<b>PD provides all fuel during mission lifetime (including test run):</b>	<b>\$969 Million</b>

### 11.2.2. EML2 Contingency

The RFP states that the OTV must be capable of payload transport to EML1 or 2 (Table 1.1, Requirement #3), therefore, WayPoint offers the contingency

**Table 11.12. EML1 vs. EML2 Cost Comparison.**

Average Launch Cost of Fuel per EML 1 Mission:	\$210 Million
Mass of Fuel Needed for EML1 Mission:	127,000 kg
Average Launch Cost per kg of Fuel:	\$1,720 / kg
Mass of Fuel Needed for EML2 Mission:	143,000 kg
Average Launch Cost of Fuel per EML 2 Mission:	\$246 Million
<b>Difference in Cost per Mission:</b>	<b>\$36 Million</b>

of an EML2 passage. As outlined in Section 4.2.4.1, the transfer time to EML2 is roughly 6.2 days. The only difference in vehicle configuration is the fuel carried for the mission. A total of 143,000 kg of propellant is required for the EML2 missions, which leads to an average of \$36 million more per mission than to EML1 (Table 11.12). The service is offered to the customer seeking extend range capability.

### 11.2.3. Operational Costs

Operations costs cover various non-hardware components of the mission including ground facilities, labor, engineering work, and software support. All of these costs are incurred during the operational phase of the mission and are crucial to supporting the mission. Specific personnel and facilities required for this are shown in Table 11.13. Figures for software support are driven by Source Lines of Code (SLOC) from the ADCS and Communications subsections, while communications facility and control tower costs are scaled from previous space exploration missions from *Space Mission Analysis and Design* [10]. The total expenditure for operations comes out to be \$65.34 million.

**Table 11.13. Operations Staff and Facility Costs [10].**

<b>Personnel</b>	<b>Cost/Unit</b>	<b>Units Required</b>	<b>Total Cost</b>
Engineering Support Staff	\$200,000 / FTE	200	\$40,000,000
Software Eng. Support	\$25,000 / Man-month	57	\$1,436,550
Communications Facility	\$2,170/m <sup>2</sup>	474	\$1,028,580
Control Tower	\$8,346/m <sup>2</sup>	465	\$3,880,890

Table 11.14. Non-Recurring Costs.												
Subsystem/Phase	Component	Manufacturer	TFU/Cost per Unit	Unit	Units Required (N)	Unadjusted Cost (TFU)	Learning Curve Factor (S)	Production Cost	Management Reserves	TRL Reserves	Total Cost	% of Total Non-Recurring Budget
R & D	Design Development for Systems Engineering	-	\$200,000	FTE Years	500	\$100,000,000	-	\$100,000,000	-	-	\$100,000,000	8.67%
	Software Development	-	\$25,000	Man-Months	383	\$9,575,000	-	\$9,575,000	-	-	\$9,575,000	0.83%
ADCS/Comms	Tri-Axial External Magnetometer	Rockwell Collins	\$747,252	Magnetometer	1	\$747,252	95%	\$747,252	15%	5%	\$896,702	0.08%
	Deep Space Network X-Band (DSN)	-	\$17,201	Week	260	\$4,472,208	-	\$4,472,208	-	-	\$4,472,208	0.39%
	High Gain Antenna	-	\$4,000	Antenna	1	\$4,000	-	\$4,000	10%	5%	\$4,600	0.00%
	Microstrip Patch Low Gain Antenna	Antenna Development Corp.	\$1,000	Antenna	4	\$4,000	95%	\$3,610	10%	5%	\$4,152	0.00%
	Miniature Inertial Measurement Unit (IMU)	Honeywell	\$50,000	IMU	2	\$100,000	95%	\$95,000	10%	5%	\$109,250	0.01%
	Small Deep Space X-Band Transponder	General Dynamics	\$28,000	Transponder	1	\$28,000	95%	\$28,000	10%	5%	\$32,200	0.00%
	CX5-610 S-Band Transponder	L3	\$30,000	Transponder	1	\$30,000	95%	\$30,000	10%	5%	\$34,500	0.00%
	DragonEye Docking Sensor	Advanced Scientific Concepts	\$12,000	Sensor	6	\$72,000	95%	\$63,059	15%	5%	\$75,671	0.01%
	Proton 400K Computer	Space Micro	\$183,000	Computer	3	\$549,000	95%	\$506,134	15%	5%	\$607,360	0.05%
Propulsion	Vinci Engine	Sneecma	\$24,000,000	Engine	5	\$120,000,000	95%	\$106,526,353	20%	10%	\$138,484,259	12.00%
	Fuel Pump/Cross-Feed System	-	\$20,000	System	1	\$20,000	-	\$20,000	15%	5%	\$24,000	0.00%
	HiPAT RC Thrusters	Aerojet	\$250,000	Thruster	40	\$10,000,000	90%	\$5,707,973	10%	5%	\$6,564,169	0.57%
Power/Thermal	VES-16 Li-ion Batteries	Saft	\$3,600	Battery Pack	5	\$18,000	95%	\$15,979	10%	5%	\$18,376	0.00%
	Ultraflex Solar Array	ATK	\$5,000	Array	2	\$10,000	95%	\$9,500	10%	5%	\$10,925	0.00%
	Electrical Power System (EPS)	-	\$1,000,000	System	1	\$1,000,000	-	\$1,000,000	15%	5%	\$1,200,000	0.10%
	NeXT Triple Junction (XTJ) Solar Cells	Spectrolab	\$1,211	m <sup>2</sup>	4.54	\$5,498	95%	\$4,916	10%	5%	\$5,653	0.00%
	Vapor Cooled Shield	Meyer	\$300,000	Sheild	5	\$1,500,000	95%	\$1,331,579	20%	20%	\$1,864,211	0.16%
Structures	Al-Li Propulsion Tank	-	\$39,423	m <sup>2</sup>	655	\$25,822,065	85%	\$5,645,212	10%	5%	\$6,491,994	0.56%
	Al-Li Main Bus	-	\$39,423	m <sup>2</sup>	20	\$788,460	90%	\$500,057	10%	5%	\$575,065	0.05%
	Trusses	-	\$6,000	kg	75	\$450,000	90%	\$233,452	15%	5%	\$280,142	0.02%
	Coilable Boom	ATK	\$8,382	m	5	\$41,910	95%	\$37,204	10%	5%	\$42,785	0.00%
	Al-Li Connections	-	\$39,423	m <sup>2</sup>	30	\$1,182,690	90%	\$705,251	10%	5%	\$811,039	0.07%
	Inconel Forged Steel Bolts	-	\$500	Bolt	26	\$13,000	90%	\$7,923	10%	5%	\$9,111	0.00%
	Whipple Sheild	Nextel/3M	\$900	m <sup>2</sup>	500	\$450,000	95%	\$284,110	15%	10%	\$355,138	0.03%
Manufacturing	Labor (In-house work)	-	\$95,000	FTE Years	400	\$38,000,000	-	\$38,000,000	-	-	\$38,000,000	3.29%
Assembly/Testing	Assembly of Vehicle at ISS	-	\$250,000,000	Assembly	1	\$250,000,000	-	\$250,000,000	-	-	\$250,000,000	21.66%
	Full Test Run for Design Validation	-	\$210,000,000	Test	1	\$210,000,000	-	\$210,000,000	-	-	\$210,000,000	18.20%
Launch	Falcon Heavy	SpaceX	\$85,000,000	Launch	1	\$85,000,000	-	\$85,000,000	10%	5%	\$97,750,000	8.47%
	Falcon 9	SpaceX	\$61,200,000	Launch	4	\$244,800,000	-	\$244,800,000	10%	5%	\$281,520,000	24.40%
	Custom Payload Fairing	SpaceX	\$500,000	Launch	5	\$2,500,000	-	\$2,500,000	15%	10%	\$3,125,000	0.27%
<b>Total Non-recurring Cost:</b>									<b>\$1,153,975,487</b>			

NON-RECURRING COST BREAKDOWN

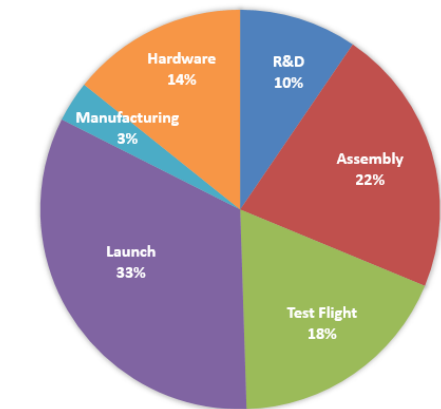


Figure 11.4. Non-Recurring Cost Breakdown.

RECURRING COST BREAKDOWN

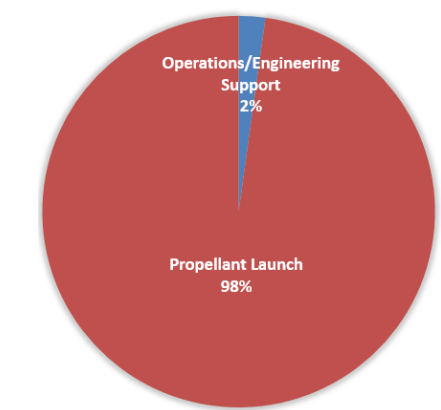


Figure 11.5. Recurring Cost Breakdown.

Table 11.15. Recurring Costs.						
Subsystem/Phase	Component	Cost per Unit	Unit	Units Required	Cost	% of Total Non-Recurring Budget
Operations	Communications Facility	\$2,170	m <sup>2</sup>	474	\$1,028,580	0.05%
	Control Tower	\$8,346	m <sup>2</sup>	465	\$38,80,890	0.18%
	Engineering/Operations Staff	\$200,000	FTE	200	\$40,000,000	1.88%
	Software Engineering Support	\$25,000	Man-Months	57	\$1,425,000	0.07%
Propellant	LH <sub>2</sub>	\$5	kg	212170	\$1,026,903	0.05%
	LOX	\$0.21	kg	1230600	\$254,734	0.01%
	Hydrazine	\$177	kg	2500	\$443,575	0.02%
Propellant Launch	Falcon 9	\$61,200,000	Launch	2	\$122,400,000	5.76%
	Falcon Heavy	\$85,000,000	Launch	23	\$1,955,000,000	91.98%
<b>Total Recurring Cost:</b>				<b>\$2,125,459,682</b>		

**Total Non-recurring Cost:** **\$1,153,975,487**

**Total Recurring Cost:** **\$2,125,459,682**

**Hermes Total Lifetime Cost:** **\$3,279,435,169**

RECURRING VS. NON-RECURRING

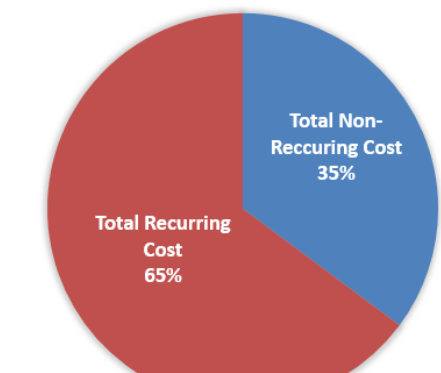
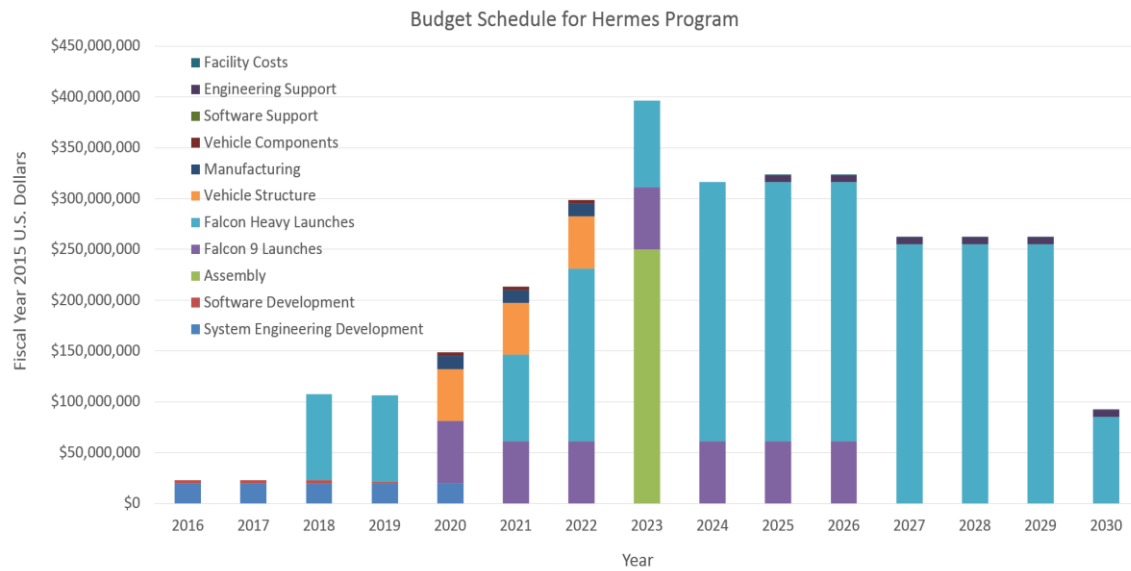


Figure 11.6. Total Lifetime Cost Breakdown.

## 11.3. Cost Schedule

To properly allocate the budget throughout the mission timeline, the program schedule (Figure 2.1) is followed closely to estimate a cost schedule. By combining the technical schedule and cost breakdown, a lifetime budget allocation is estimated in Figure 11.7.



**Figure 11.7. Hermes Cost Schedule.**

The year with the highest cost is 2023 which is when the vehicle will be launched as well as assembled. In order to maintain a level cost schedule and avoid large spikes, WayPoint plans to pay for the launch costs spread out over the mission lifetime. With the large number of launches granted to SpaceX, this assumption is reasonable as payment plans are not an abnormality. The OTV 5-year milestone is met in 2030, however pending vehicle health, Hermes has the ability to continue making EML transfers beyond that mark.

## 12. Risk Analysis and Mitigation

A risk analysis of the entire vehicle is performed for each subsystem. A guideline is defined in Table 12.1 as used by NASA Ames Research Center:

**Table 12.1. Relationship between risk levels and corresponding attributes [61].**

Attribute	Level				
	1	2	3	4	5
Likelihood of Occurrence	$\leq 0.2$	$0.2 - 0.4$	$0.4 - 0.6$	$0.6 - 0.8$	$< 0.8$
Cost (Overrun)	$\leq 5\%$	5% - 10%	10% - 15%	15% - 20%	> 20%
Schedule (Overrun)	$\leq 5\%$	5% - 10%	10% - 15%	15% - 20%	> 20%
Technical (Loss of Success Criteria)	$\leq 5\%$	5% - 10%	10% - 15%	15% - 20%	> 20%
Safety	Negligible injury or partial but negligible loss of spacecraft	Minor injury or partial but minor loss of spacecraft	Moderate injury or partial but moderate loss of spacecraft	Severe injury or partial but significant loss of spacecraft	Loss of life or vehicle

In this relationship matrix, a likelihood level and consequence level is determined for each risk. Four categories are given as consequence options: cost, schedule, technical, and safety. Once a likelihood and consequence level have been identified for a risk, it can be placed on the

**Table 12.2. Risk Assessment Code Matrix [61].**

Likelihood	Level				
	5	1			
5	1	1	1		
4			2	3	
3	1	7	17	8	2
2		2	9	8	2
1	1	2	3	4	5
	Consequence				

Risk Assessment Code (RAC) matrix shown in Table 12.2. Red cells denote high-rated risks, yellow cells denote medium-rated risks, and green cells denote low-rated risks. In each cell are the number of risks WayPoint identifies for Hermes. Table 12.3 shows all the risks identified in each subsystem.

**Table 12.3. Risk Assessment Across All Subsystems.**

Subsystem: Orbital				Subsystem: Docking			
Risk	Likelihood	Consequence	Rating	Risk	Likelihood	Consequence	Rating
Insufficient ΔV for required transfer	1	3	Low	Damage to payload from IDSS interface during flight	1	4	Low
Transfer takes more than 6 days	2	3	Low	Docking structure unable to withstand loads when thrusting	1	4	Low
Prolonged eclipse by the Moon at EML2	1	3	Low	A need to dock with an interface without compatible docking	1	2	Low
Anomalies in transfer trajectory	2	2	Low	Failure during soft docking process	2	3	Low
Missing the optimal launch window	2	2	Low	Failure during hard docking process	2	3	Low
Drifting out of Desired Halo orbit at EML1/2	2	2	Low	Leakage during refueling	3	4	Med
Insufficient staging from ISS during Main Burn	1	3	Low	Subsystem: ADCS/Comms			
Uncontrolled Deorbit/Breakup at end of mission lifetime	1	3	Low	Risk	Likelihood	Consequence	Rating
Rendezvous required during initial assembly	3	3	Med	Critical degradation of momentum wheels	1	4	Low
Low T/W ratio significantly alters Transfer Trajectory	2	3	Low	Failure of flight computer system	2	4	Med
Subsystem: Power/Thermal				Thruster failure	2	4	Med
Risk	Likelihood	Consequence	Rating	Hydrazine leak/fuel line failure	2	3	Low
Less solar array power harvest than expected	2	3	Low	Software bugs/errors	4	3	Med
Not enough battery power capacity	1	3	Low	Failure during antenna boom deployment	2	4	Med
Damage/degradation to solar panels	2	3	Low	Degradation/damage of antennas	2	3	Low
Boiloff of fuel before launch and after pre-launch para-ortho conversion	2	2	Low	Delayed re-orientation of vehicle due to non-optimal weight distribution	2	2	Low
Failure of power distribution to vehicle	1	4	Low	Broken communication to DSN/Earth	2	3	Low
Failure of solar array deployment	2	4	Med	Radiation to computer/hardware systems	2	4	Med
Insufficient thermal regulation	2	3	Low	Error in determining attitude	1	3	Low
Failure of vapor cooled shield	2	4	Med	Transmitter failure/malfunction	1	3	Low
Passive cooling unable to prevent boiloff	3	4	Med	Subsystem: Structural			
Fire in main bus due to electrical components	2	5	Med	Risk	Likelihood	Consequence	Rating
Higher power consumption by vehicle than calculated	2	3	Low	Collisions with MMOD	4	2	Med
Subsystem: Launch and Assembly				Damage to main bus due to compressive loads	2	5	Med
Risk	Likelihood	Consequence	Rating	Failure of connections between propulsion modules	1	5	Med
Falcon Heavy not available for launch	1	2	Low	Damage to propellant tanks due to compressive loads	1	4	Low
SpaceX unable to meet launch volume in time frame	2	3	Low	Material fatigue/creep in propellant tank structure	3	4	Med
Damage to propellant tanks in payload fairing during launch	2	3	Low	Material fatigue/creep in main bus structure	2	3	Low
Not enough fuel to rendezvous	1	3	Low	Subsystem: Propulsion			
Delay of launch due to operational issues	4	1	Low	Risk	Likelihood	Consequence	Rating
Assembly requires more astronauts/time than calculated	2	2	Low	Failure of fuel line	2	3	Low
Missing parts for assembly	2	1	Low	Failure of an engine during flight	2	4	Med
Need more launch operations than originally calculated	2	3	Low	Shortage of propellant on-board	1	4	Low
Damage to propulsion modules with no payload fairing	1	4	Low	Failure of sponge in propellant tank	1	3	Low
Launch delayed due to weather	5	1	Low	Unable to re/start engine	2	3	Low
Damage to ISS/astronauts during assembly	1	4	Low	Vinci engines not ready by launch date	3	3	Med
Damage to vehicle during assembly	2	4	Med	Uneven cycle loading on different engines	2	2	Low
Catastrophic launch failure	1	5	Med				

Once all risks are identified, the mitigation process begins. Strategies are made to lower the likelihood and consequence of all non-Low risks. Below are the mitigation techniques that successfully lowered a risk's rating to Low:

**Table 12.4. Risk Mitigation Techniques.**

Subsystem	Risk	Mitigation	New Likelihood	New Consequence	New Rating
Orbital	Rendezvous required during initial assembly	Stress margin for error on launch vehicle upper stage to vendor to ensure proper orbit insertion	2	3	Low
Power/ Thermal	Failure of solar array deployment	Make extra parts for contingency and thoroughly test units on Earth before launch	2	3	Low
	Failure of vapor cooled shield	Test the shield and ensure proper operation before launch; allocate appropriate amount of time for development by vendor	1	4	Low
	Passive cooling unable to prevent boiloff	Have safety margins on fuel in case of higher boiloff values	2	3	Low
	Fire in main bus due to electrical components	Follow extra safety measures so that there would be close to no chance of flames sparking	1	4	Low
Launch/ Assembly	Damage to vehicle during assembly	Ensure astronauts have enough time to properly train for task; use standardized tools and manufacturing techniques	1	3	Low
Docking	Leakage during refueling	Allow for ample ground testing in space-like environment	1	4	Low
ADCS/ Comms	Failure of flight computer system	Have redundant computer systems and allow for extra safety margins on main bus thermal/radiation protection	1	3	Low
	Thruster failure	Make spare parts for contingency and send up to ISS in the need for replacement/repair	2	2	Low
	Software bugs/errors	Have ground operations constantly updating software and debugging code	2	3	Low
	Failure during antenna boom deployment	Make extra parts for contingency and thoroughly test units on Earth before launch	2	3	Low
	Radiation to computer/hardware systems	Put a large safety margin on radiation capability and test thoroughly on Earth	1	4	Low
Structural	Collisions with MMOD	Incorporate whipple shielding to protect internal components	4	1	Low
	Damage to main bus due to compressive loads	Perform multiple FEA analyses on structure with maximum loads and reinforce areas that undergo high stress with axial trusses.	1	4	Low
	Failure of connections between propulsion modules	Increase strength of connections by welding before launch and reinforce with bolts to lower shear on tanks. Keep safety margins high so partial failure does not mean loss of vehicle or payload	1	4	Low
Propulsion	Failure of engine during flight	Five-engine design for redundancy	1	4	Low



Once all risks are classified as Low, they are accepted as they no longer considered impactful to the mission. Much of the mitigation is handled through contingency back-up parts that can be sent up to the ISS to be used for repairs and maintenance. Component testing before launch and extra safety margins also help diminish risks by lowering their likelihoods.

However, as with any mission, it is unreasonable to expect all risks to be mitigated to a Low rating. Table 12.5 lists the risks that still maintained their Medium rating and were deemed acceptable risks to the mission.

Table 12.5. Accepted Medium Risks.					
Subsystem	Risk	Mitigation	New Likelihood	New Consequence	New Rating
Launch/ Assembly	Catastrophic launch failure	Launch off very reliable Falcon family vehicles	1	5	Med
Structural	Material fatigue/creep in propellant tank structure	Make contingency repair/check- up visits to ISS after every one or two missions	2	4	Med
Propulsion	Vinci engines not ready by launch date	Have a backup ready in the RL- 10 engine	3	2	Med

## 13. Conclusion

WayPoint views this mission as an opportunity to contribute to space exploration and extend its applications. By designing an OTV that is capable of transporting 50,000 lb of payload from Low Earth Orbit (LEO) to a Lagrange point and bringing 15,000 lb of payload back, EML1 and 2 can serve as valuable hosting stations. With total lifetime projected costs merely a fraction of the next nearest technology, Earth-Moon Lagrange Points will become easily accessible to both manned and unmanned payloads.

WayPoint is confident that the proposed design of Hermes will be able to accomplish the tasks stated in the RFP in the most efficient and reliable manner. Tasks that will undoubtedly have great impacts on the future of space exploration. Composed of proven, tested technology and innovative engineering approaches, Hermes will provide efficient and reliable services to customers seeking payload transport.

## 14. References

- [1] R. DaLee, "Space Launch System," 2013. [Online]. Available: [http://www.boeing.com/assets/pdf/despace/space/sls/docs/sls\\_mission\\_booklet\\_jan\\_2014.pdf](http://www.boeing.com/assets/pdf/despace/space/sls/docs/sls_mission_booklet_jan_2014.pdf). [Accessed 20 February 2015].
- [2] "Revisiting SLS/Orion Launch Costs," The Space Review, 15 July 2013. [Online]. Available: <http://www.thespacereview.com/article/2330/1>. [Accessed 28 October 2014].
- [3] J. Foust, "SLS Debut Likely to Slip to 2018," 27 August 2014. [Online]. Available: <http://spacenews.com/41690sls-debut-likely-to-slip-to-2018/>. [Accessed 10 April 2015].
- [4] "SpaceXStats," SpaceX, 2015. [Online]. Available: <http://spacexstats.com/upcoming.php>. [Accessed 1 February 2015].
- [5] "European Space Agency Launch Vehicles," European Space Agency, 14 October 2014. [Online]. Available: [http://www.esa.int/Our\\_Activities/Launchers/Launch\\_vehicles/Adapted\\_Ariane\\_5\\_ME](http://www.esa.int/Our_Activities/Launchers/Launch_vehicles/Adapted_Ariane_5_ME). [Accessed 1 February 2015].
- [6] "JSR Launch Vehicle Database," 2014. [Online]. Available: <http://www.planet4589.org/space/lvdb/list.html>. [Accessed 6 November 2014].
- [7] "With nod to history, SpaceX gets launch pad 39A OK," Florida Today, 2014 April 14. [Online]. Available: <http://www.floridatoday.com/story/tech/science/space/2014/04/15/nod-history-spacex-gets-ok/7721971/>. [Accessed 22 November 2014].
- [8] P. Harding, "NASA Spaceflight," 31 7 2013. [Online]. Available: <http://www.nasaspacesflight.com/2013/07/nasa-planning-module-relocations-future-vehicles/>. [Accessed 2 2 2015].
- [9] H. D. Curtis, "7.2 Relative Motion in Orbit," in *Orbital Mechanics for Engineering Students*, New York: Elsevier, 2014, pp. 368-376.
- [10] J. R. Wertz, D. F. Everett and J. J. Puschell, *Space Mission Engineering: The New SMAD*, Hawthorne, CA: Microcosm Press, 2011.
- [11] J. L. Goodman, "History of Space SHuttle Rendezvous and Proximity Operations," *Journal of Spacecraft and Rockets*, vol. 43, no. 5, pp. 944-959, 2006.
- [12] D. R. Brooks and E. F. Harrison, "Use of Orbit-to-Orbit Shuttles for Hyperbolic Rendezvous with Returning Planetary Spacecraft," NASA, Hampton, VA, 1971.
- [13] M. Jesick, "Abort Options for Human Missions to Earth-Moon Halo Orbits," NASA, Hampton, VA, 2012.
- [14] F. J. Hale, *Introduction to Space Flight*, Eaglewood Cliffs, NJ.: Prentice-Hall, 1994, pp. 48-50.
- [15] J. S. Parker and G. H. Born, "Direct Lunar Halo Orbit Transfers," in *AAS/AIAA Space Flight Mechanics Conference*, Sedona, Arizona, 2007.
- [16] W. W. Mendell, "Strategic Considerations for Cislunar Space Infrastructure," NASA, Houston, TX, 1994.
- [17] R. W. Farquhar, "A Halo-Orbit Lunar Station," NASA, Greenbelt, MD, 1972.
- [18] D. C. Folta, M. A. Woodard and D. Cosgrove, "Stationkeeping of the First Earth-Moon Libration Orbiter The ARTEMIS Mission," in *AAS/AIAA Astrodynamics Specialist Conference*, Girdwood, Alaska, 2011.
- [19] D. Folta, T. Pavlak, A. Haapala, K. Howell and M. Woodard, "Earth-Moon libration Point Orbital Stationkeeping: Theory, Modeling, and Operations," in *IAA Conference on Dynamics and Control of Space Systems*, Porto, Portugal, 2012.
- [20] "Report of the IADC Activities on Space Debris Mitigation Measures," in *United Nations Committee on the Peaceful Uses of Outer Space*, 2004.
- [21] V. A. Chobotov, "6.3 Finite-Duration Burns: Gravity Losses," in *Orbital Mechanics*, Reston, Virginia: AIAA, 2002, pp. 126-129.
- [22] M. R. Reddy, "Effect of low earth orbit atomic oxygen on spacecraft materials," *Journal of Material Science*, vol. 30, pp. 281-307, 1995.
- [23] D. Fraser, H. Kleespies and C. Vasicek, "9 Spacecraft Structures," 2001. [Online]. Available: <https://engineering.purdue.edu/AAE/Academics/Courses/aae450/2007/spring/References/Struct/structures.pdf>. [Accessed 28 January 2015].

- [24] Alcoa, "Alcoa 2090-T83 Sheet," Alcoa, [Online]. Available: [https://www.alcoa.com/mill\\_products/catalog/pdf/alloy2090-t83techsheet.pdf](https://www.alcoa.com/mill_products/catalog/pdf/alloy2090-t83techsheet.pdf). [Accessed 21 February 2015].
- [25] J. R. Davis, Aluminum and Aluminum Alloys, ASM International, 1993.
- [26] E. L. Christiansen, "Handbook for Designing MMOD Protection," NASA, Houston, TX, 2009.
- [27] Orbital ATK, "Helical Quadrifilar Antenna Coilable Boom," Orbital ATK, December 2014. [Online Available: <http://cms.orbitalatk.com/SiteCollectionDocuments/Product%20Data%20Sheets/coilable%20antenna%20ooms%202014.pdf>. [Accessed 21 February 2015].
- [28] Chucking Machine Products, "Aerospace Precision Machined Parts," Chucking Machine Products, [Online Available: <http://www.chucking.com/industries-served/aerospace.html>. [Accessed 21 February 2015].
- [29] NASA, "Extravehicular Activity," NASA, 7 May 2008. [Online]. Available: <http://msis.jsc.nasa.gov/sections/section14.htm>. [Accessed 21 February 2015].
- [30] "NASA Docking System. Interface Definition Document," NASA, November 2010. [Online]. Available: <http://ntrs.nasa.gov/archive/nasa/casi.ntrs.nasa.gov/20110008387.pdf>. [Accessed 2 November 2014].
- [31] Gerstenmaier, "International Docking System Standard Interface Definition Document," 2013.
- [32] C. Mclean, S. Mustafi, L. Walls, B. Pitchford, M. Wollen and J. Schmidt, "Simple, Robust Cryogenic Propellant Depot for near Term Applications," 2011.
- [33] "Robotic Refueling Mission," NASA, [Online]. Available: [http://ssco.gsfc.nasa.gov/rrm\\_refueling\\_task.html](http://ssco.gsfc.nasa.gov/rrm_refueling_task.html). [Accessed 2 April 2015].
- [34] A. Alessandro, "Robotic Refueling Mission," NASA, [Online]. Available: [http://ssco.gsfc.nasa.gov/rrm\\_refueling\\_task.html](http://ssco.gsfc.nasa.gov/rrm_refueling_task.html). [Accessed 10 April 2015].
- [35] W. C. D. Taylor, "Comparing the Results of an Analytical Model of the No-Vent Fill Process wwith the No Vent Fill Test Results for a 4.96 m<sup>3</sup> Tank," 1992.
- [36] D. S. G. A. Scott Rotenberger, "Orbital Express fluid transfer demonstration system," *Sensors and System for Space Applications*, vol. 6958, 2008.
- [37] S. Durteste, "A Transient Model of the VINCI Cryogenic Upper Stage Rocket Engine," in *AIAA/ASME/SAE/ASEE Joint Propulsion Conference and Exhibit*, Cincinnati, 2007.
- [38] S. K. Borowski, D. R. McCurdy and L. M. Burke, "The Nuclear Thermal Propulsion Stage (NTPS): A Key Space Asset for Human Exploration and Commercial Missions to the Moon," in *AIAA SPACE 2011 Conference and Exhibition*, San Diego, 2013.
- [39] D. A. Herman, "NASA's Evolutionary Xenon Thruster (NEXT) Project Qualification Propellant Throughput Milestone Performance, Erosion, and Thruster Service Life Prediction After 450 kg," NASA, Cleveland, 2010.
- [40] "Falcon 9 Launch Vehicle Payload User's Guide," 2009. [Online]. Available: [http://decadal.gsfc.nasa.gov/pace-201206mdl/Launch%20Vehicle%20Information/Falcon9UsersGuide\\_2009.pdf](http://decadal.gsfc.nasa.gov/pace-201206mdl/Launch%20Vehicle%20Information/Falcon9UsersGuide_2009.pdf). [Accessed 18 October 2014].
- [41] "Vinci Space Propulsion," Snecma, [Online]. Available: [http://www.sneecma.com/IMG/files/fiche\\_vinci\\_ang\\_2012\\_modulvoir\\_file\\_fr.pdf](http://www.sneecma.com/IMG/files/fiche_vinci_ang_2012_modulvoir_file_fr.pdf). [Accessed 10 11 2014].
- [42] "Kestrel," Encyclopedia Astronautica, [Online]. Available: <http://www.astronautix.com/engines/kestrel.htm>. [Accessed 10 11 2014].
- [43] "RL-10B-2," Encyclopedia Astronautica, [Online]. Available: <http://www.astronautix.com/engines/r110b2.htm>. [Accessed 10 11 2014].
- [44] "SpaceX - Launch Vehicle Concepts and Designs," Space Flight 101, 5 March 2014. [Online]. Available: <http://www.spaceflight101.com/spacex-launch-vehicle-concepts.html> . [Accessed 20 October 2014].
- [45] G. Lecarrie, "Snecma's fifth Vinci engine, for new versions of Ariane, successfully completes development tests," Snecma, 8 September 2014. [Online]. Available: <http://www.sneecma.com/sneecma-s-fifth-vinci-engine-for.html?lang=en>. [Accessed 10 11 2014].
- [46] P. Alliot, C. Fiorentino and F. Lassoudiere, "Development Status of the VINCI Engine for the Ariane Upper Stage," in *56th International Astronautical Congress*, Fukuoka, Japan, 2005.

- [47] B. Szelinski, H. Lange, C. Rottger, H. Sacher, S. Weiland and D. Zell, "Development of an Innovative Sandwich Common Bulkhead for Cryogenic Upper Stage Propellant Tank," *Acta Astronautica*, no. 81, pp. 200-213, 27 June 2012.
- [48] NASA, "External Tank," [Online]. Available: <http://science.ksc.nasa.gov/shuttle/technology/st:newsref/et.html>. [Accessed 10 February 2015].
- [49] "PMD Technology - Propellant Management Device Design and Analysis," PMD Technology, 2011 [Online]. Available: <http://www.pmdtechnology.com/>. [Accessed 10 February 2015].
- [50] NASA, "Safety Standard for Hydrogen and Hydrogen Systems," NASA, Washington, D.C., 2005.
- [51] "20 N Hydrazine Thruster," Airbus Defense & Space, [Online]. Available: <http://cs.astrium.eads.net/sp/spacecraft-propulsion/hydrazine-thrusters/20n-thruster.html>. [Accessed 10 November 2014].
- [52] "22N Bipropellant Thruster," Airbus Space & Defense, [Online]. Available: <http://cs.astrium.eads.net/sp/spacecraft-propulsion/bipropellant-thrusters/22n-thruster.html>. [Accessed 10 November 2014].
- [53] Aerojet Rocketdyne, *Bipropellant Thruster Fact Sheet*, Redmond, WA: Aerojet Rocketdyne, 2006.
- [54] B. Aerospace, "CT-602 Star Tracker".
- [55] Ball Aerospace, "CT-633 Stellar Attitude Sensor".
- [56] Sinclair Interplanetary, "ST-16 Star Tracker".
- [57] Terma Space, "Star Tracker HE-5AS".
- [58] Space Micro, " $\mu$ STAR-200H".
- [59] SSBV Aerospace, "Cubesat Sun Sensor".
- [60] Bradford Engineering, "Fine & Coarse Sun Sensor," 2006.
- [61] Airbus, "Linear Accurate Sun Sensor - LIASS," Airbus. [Online]. [Accessed 2015].
- [62] Airbus, "Coarse Bi-Axis Sun Sensor," Airbus, [Online]. Available: <http://www.space.airbusds.com/en/equipment/bass.html>. [Accessed 2015].
- [63] Space Micro, "MSS-01,02 Medium Sun Sensors," 2013.
- [64] SSBV Aerospace, "Magnetometer".
- [65] Honeywell, "Smart Digital Magnetometer HMR2300".
- [66] Honeywell, "Three-Axis Magnetic Sensor".
- [67] Rockwell Colling, "Tri-Axial External Magnetometer," 2008.
- [68] K. Crabtree, *Honeywell Delivers 250th Miniature Inertial Measurement Unit For Space Missions*, 31 December 2009.
- [69] Honeywell, "MIMU Miniature Inertial Measurement Unit," 2003.
- [70] Northrop Grumman, "LN-200S Inertial Measurement Unit (IMU)," 2013.
- [71] Honeywell, "HG1700 Inertial Measurement Unit".
- [72] Maxwell Technologies, "Single Board Computer For Space".
- [73] BAE Systems, "RAD750 6U CompactPCI extended single-board computer".
- [74] Space Micro, "Proton 400k- Single Board Computer".
- [75] L3, "Eyesafe Laser Rangefinder (ELRF)," 2012.
- [76] L3, "Diode-Pumped Laser Rangefinder (LRF)," 2012.
- [77] Advanced Scientific Concepts, "GoldenEye 3D Flash LIDAR™ Space Camera," Advanced Scientific Concepts, 2013. [Online]. Available: <http://www.advancedscientificconcepts.com/products/portable.html>.
- [78] A. S. Concepts, "DragonEye 3D Flash LIDAR Space Camera™," Advanced Scientific Concepts, 2011 [Online]. Available: <http://www.advancedscientificconcepts.com/products/older-products/dragoneye.html>
- [79] J. H. Brown, "Spacecraft Guidance, Navigation and Control Systems," in *Encyclopedia of Space Science and Technology*, 2003.
- [80] "VECTRONIC Aerospace GmbH," 2014. [Online]. Available: <http://www.vectronic-aerospace.com/space.php?p=starsensor>. [Accessed 21 November 2014].
- [81] "NASA's Mission Operations and Communications Services," NASA, January 2009.

- [82] NASA JPL, "Mission Introduction to the DSN," NASA, Pasadena, 2015.
- [83] Surrey Satellite Technology, S-Band Patch Antenna.
- [84] Clyde Space, CubeSat S-Band TX and Patch Antenna, 2011.
- [85] Antenna Development Corporation, Microstrip Patch Antennas, 2013.
- [86] General Dynamics, "Small Deep-Space Transponder (SDST)".
- [87] L3, "CXS-610 STDN/USB/DSN Transponder," 2012.
- [88] L3, "MSX-765 Miniature L-/S-Band T&C Transceiver," 2012.
- [89] M. R. Patel, Spacecraft Power Systems, CRC Press, 2004.
- [90] The Astronautics Community, Space Mission Engineering: The New SMAD, J. R. Wertz, D. F. Everett and J. J. Puschell, Eds., Space Technology Library, 2011.
- [91] Spectrolab, "Spectrolab NeXt Triple Junction (XTJ) Solar Cells," Spectrolab, Sylmar, 2010.
- [92] ATK, "UltraFlex Solar Array Systems," ATK-Goleta, Goleta.
- [93] Saft, "Saft batteries... powering outer space for half a century," Saft, Bagnolet, 2013.
- [94] 3M, "Thermal Conductivity of Nextel Woven Fabric," 3M.
- [95] J. Lewis, "NASA Docking System (NDS) Interface Definitions Document (IDD)," National Aeronautics and Space Administration, Houston, 2010.
- [96] F. Rossini, "A Report of the International Practical Temperature Scale of 1968," 1968.
- [97] J. F. LeBar and E. C. Cady, "The Advanced Cryogenic Evolved Stage (ACES) - A Low-Cost, Low-Risk Approach to Space Exploration Launch," AIAA, Huntington Beach.
- [98] S. A. Dye, W. L. Johnson, D. W. Plachta, G. L. Mills, L. Buchanan and A. B. Kopelove, "Design, fabrication and test of Load Beearing multilayer insulation to support a broad area cooled shield," vol. 64, 2014.
- [99] D. H. Weitzel, W. V. Bloebenstein, J. W. Draper and O. E. Park, "Ortho-Para Catalysis in Liquid-Hydrogen Production," vol. 60, no. 3, 1958.
- [100] D. B. Kanipe, "Estimating the Cost of Space Systems," Texas A & M Engineering, 25 September 2014 [Online]. Available: [http://engineering.tamu.edu/media/1832106/Estimating-the-Cost-of-Space-Systems\\_2014.pdf](http://engineering.tamu.edu/media/1832106/Estimating-the-Cost-of-Space-Systems_2014.pdf). [Accessed 20 February 2015].
- [101] "Mission to Hubble," NASA, 15 September 2008. [Online]. Available: [http://www.nasa.gov/mission\\_pages/hubble/servicing/SM4/main/SM4\\_Essentials.html](http://www.nasa.gov/mission_pages/hubble/servicing/SM4/main/SM4_Essentials.html). [Accessed 1 February 2015].
- [102] W. Harwood, "Final Servicing Mission Begins to Extend Hubble's life," Spaceflight Now, 11 May 2009 [Online]. Available: <http://spaceflightnow.com/shuttle/sts125/090511launch/>. [Accessed 10 February 2015].
- [103] "NASA Ames Research Center Health and Safety Procedural Requirements," NASA Ames Research Center, 29 May 2012. [Online]. Available: <http://procure.arc.nasa.gov/assets/docs/APR17001R/APR8715.1C51.html#toc>. [Accessed 26 November 2014].